

NASA CR-167870

R81AEG700



National Aeronautics and  
Space Administration

# ENERGY EFFICIENT ENGINE ICLS NACELLE DETAIL DESIGN REPORT

N85-10993

Unclass  
24803

G3/07

by

R.R. Eskridge  
A.P. Kuchar  
C.L. Stotler

GENERAL ELECTRIC COMPANY

LIBRARY COPY

AUG 26 1982

LANGLEY RESEARCH CENTER  
LIBRARY, NASA  
HAMPTON, VIRGINIA

Prepared for

National Aeronautics and Space Administration

(NASA-CR-167870) ENERGY EFFICIENT ENGINE  
ICLS NACELLE DETAIL DESIGN REPORT (General  
Electric Co.) 125 P HC AC6/NF A01 CSCL 21E

NASA Lewis Research Center  
Contract NAS3-20643

1. Report No. CR-167870		2. Government Accession No.		3. Recipient's Catalog No.	
4. Title and Subtitle Energy Efficient Engine ICLS Nacelle Detail Design Report				5. Report Date July 1982	
				6. Performing Organization Code	
7. Author(s) K.R. Eskridge A.P. Kuchar C.L. Stotler				8. Performing Organization Report No. R81AEG700	
9. Performing Organization Name and Address General Electric Company Aircraft Engine Business Group Cincinnati, Ohio 45215				10. Work Unit No.	
				11. Contract or Grant No. NAS3-20643	
12. Sponsoring Agency Name and Address NASA-Lewis Research Center 21000 Brookpark Road Cleveland, Ohio 44135				13. Type of Report and Period Covered Topical Report	
				14. Sponsoring Agency Code	
15. Supplementary Notes NASA Project Manager - Carl C. Ciepluch NASA Engineer - Tom Strom GE Project Manager - Ray W. Bucy					
16. Abstract <p>This report summarizes the results of the detail design of the Nacelle for the General Electric Energy Efficient Engine (E<sup>3</sup>) Integrated Core Low Spool (ICLS) test vehicle. An oral version of this report was presented at the NASA Lewis Research Center on July 9, 1981.</p> <p>The objective of this effort was to design a slave nacelle for the ICLS test. Cost and reliability were the important factors considered. The slave nacelle simulates the internal flow lines of the actual Flight Propulsion System (FPS) but has no external fairing.</p> <p>The report presents the aerodynamic differences between the ICLS and FPS nacelles followed by the structural description and analysis of the various nacelle components.</p> <p style="text-align: center;"><b>ORIGINAL PAGE IS OF POOR QUALITY</b></p>					
17. Key Words (Suggested by Author(s)) Energy Efficient Engine Nacelle Bellmouth Exhaust Nozzle			18. Distribution Statement		
19. Security Classif. (of this report) Unclassified		20. Security Classif. (of this page) Unclassified		21. No. of Pages	22. Price*

## PREFACE

This report presents the results of the ICLS Nacelle aerodynamic and mechanical design performed by the General Electric Company for the National Aeronautics and Space Administration, Lewis Research Center, under Contract NAS3-70643. This work was performed as part of the Aircraft Energy Efficiency (ACEE) Program, Energy Efficient Engine (E<sup>3</sup>) Project. Mr. Carl C. Ciepluch is the NASA Project Manager. The NASA Project Engineer responsible for this effort is Mr. Tom Strom. This report was prepared by Messrs. R.R. Eskridge, A.P. Kuchar and C.L. Stotler of the General Electric Company, Evendale, Ohio.

PRECEDING PAGE BLANK NOT FILMED

TABLE OF CONTENTS

<u>Section</u>	<u>Page</u>
I Introduction	1
II Overview	3
III Aerodynamic Design	8
A. NASA Langley Wind Tunnel Test	25
IV Component Detail Design	42
A. Aero-Acoustic Inlet	42
B. Core Cowl	56
C. Fan Cowl	56
D. Aft Outer Exhaust Nozzle	74
E. Pylon	91
V Assembly and Trial Fit	109
VI Instrumentation	111
VII Summary	113
VIII References	115

PRECEDING PAGE BLANK NOT FILMED

LIST OF ILLUSTRATIONS

<u>Figure</u>		<u>Page</u>
1.	Nacelle Structures Plan.	2
2.	ICLS Cross Section.	4
3.	ICLS Inlet Configurations.	9
4.	ICLS Performance Bellmouth.	10
5.	ICLS Aero-Acoustic Inlet Bellmouth.	12
6.	ICLS Aero-Acoustic Inlet - STC Analysis of Mach Number Along Diffuser Wall.	13
7.	ICLS Aero-Acoustic Inlet - STC Analysis of Mach Number Across Inlet Throat.	14
8.	ICLS Fan Duct STC Analysis (Altitude Cruise Condition).	17
9.	Mixer Scale Model Test Results - Pylon and Mount Link Effects.	19
10.	ICLS Exhaust Nozzle Aero Design.	20
11.	ICLS Versus FPS Fan Exhaust Duct Comparison.	22
12.	FPS Flared Turbine Flowpath.	23
13.	Pressure Loss Items.	24
14.	Typical Fan Powered Nacelle Model.	29
15.	Nacelle Configurations - Phase I.	30
16.	E <sup>3</sup> Nacelle Positions.	31
17.	E <sup>3</sup> Tailpipe Variations.	32
18.	Aircraft/Nacelle Installed Performance.	34
19.	Nacelle Installation Drag - Phase I.	35
20.	Nacelle Installation Drag - Phase II.	36
21.	Isolated Nacelle External Drag - Phase II.	38

LIST OF ILLUSTRATIONS (Continued)

<u>Figure</u>		<u>Page</u>
22.	Nacelle Interference Drag - Phase I.	39
23.	Nacelle Interference Drag - Phase II.	40
24.	Aero-Acoustic Inlet.	42
25.	ICLS Aero-Acoustic Bellmouth Estimated Static Pressure Distribution.	44
26.	Inlet Axial Load.	46
27.	Inlet Bellmouth Assembly.	48
28.	Inlet Lip Assembly.	49
29.	Bellmouth Interface Ring Assembly.	50
30.	Inlet Diffuser Assembly.	52
31.	Inlet Diffuser Assembly - 9 Panels Total.	53
32.	Typical Diffuser Panel Connection.	54
33.	Interface Bellmouth to Diffuser.	55
34.	Interface Diffuser to E <sup>3</sup> Fan Case.	57
35.	Core Cowl.	58
36.	ICLS Core Cowl Door - Estimated Static Pressure Distribution.	59
37.	ICLS Cowl Doors Estimated Maximum Static Pressure Distribution (Performance Nozzle Exit Station 348.3).	60
38.	Inner Cowl Doors.	63
39.	Cowl Door Structure.	64
40.	Zee Flanges.	65
41.	Front Flange.	66
42.	Rear Flange.	67

LIST OF ILLUSTRATIONS (Continued)

<u>Figure</u>		<u>Page</u>
43.	Inner Cowl - Bottom View.	68
44.	Inner Cowl Doors - Latch Installation.	69
45.	Hinge and Upper Longeron Assembly.	70
46.	Apron Seal.	71
47.	Panel.	72
48.	Fan Cowl.	73
49.	ICLS Fan Cowl Doors - Estimated Static Pressure Distribution.	75
50.	Forward Interface Ring.	78
51.	Aft Interface Ring.	78
52.	Fan Cowl Hinge (Typical 6 Places).	79
53.	Outer Cowl Doors Bottom Centerline.	80
54.	Fan Cowl Latch (Aft 4).	81
55.	Fan Cowl Latch - Fwd Only.	82
56.	Shell and Acoustic Panels.	83
57.	Aft Outer Exhaust Nozzle.	84
58.	ICLS Aft Outer Exhaust Nozzle - Estimated Static Pressure Distribution.	85
59.	Typical Cross Section of Midfan Cowl.	88
60.	Orientation Midfan Cowl Assembly.	89
61.	Midfan Cowl Upper Attachment to Mount Beam.	90
62.	Aft Fan Cowl.	93
63.	Forward Interface Aft Fan Cowl.	94

LIST OF ILLUSTRATIONS (Concluded)

<u>Figure</u>		<u>Page</u>
64.	Aft Interface Aft Fan Cowl.	94
65.	Station Cut of Aft Fan Cowl.	95
66.	Nozzle Assembly Version No. 1 and Version No. 2.	96
67.	Interface Ring.	97
68.	Typical Top and Bottom Vertical Centerline Splice.	97
69.	Pylon.	98
70.	Scoop and Plenum.	101
71.	Scoop - Top View.	102
72.	Pylon Plenum Chamber and Airscoop Inlet.	103
73.	Pylon Leading Edge Section.	104
74.	Sidewall Panels - Removable Section.	106
75.	Pylon - Seal Cross Section.	106
76.	Pylon - Trailing Edge Section.	107
77.	Pylon - Typical Pylon to Beam Support.	107
78.	Aft Mount Link Penetration.	108
79.	Mount Structure - Assembly and Trial Fit.	110
80.	ICLS Nacelle Cross Section.	114



LIST OF TABLES

<u>Table</u>		<u>Page</u>
I	ICLS Nacelle Program Objectives.	1
II	ICLS Nacelle Components.	5
III	Differences Between FPS and ICLS Nacelle.	6
IV	Method of Operation.	7
V	Acoustic Configuration.	7
VI	ICLS Aero-Acoustic Inlet/Bellmouth Aero Design.	11
VII	Adjustment for Soft-Mounted Inlet.	16
VIII	ICLS Fan Exhaust Duct Aero Design.	16
IX	ICLS Fan Exhaust Duct Aero Design - Differences From FPS.	21
X	Fan Duct/Exhaust Nozzle Aero Design - Performance Adjustment Procedures, ICLS Versus FPS.	26
XI	EET/E <sup>3</sup> Nasa-Langley Wind Tunnel Test.	27
XII	Inlet Stresses.	45
XIII	Bellmouth Lip - Basic Design Features and Materials.	47
XIV	Inlet Diffuser - Basic Design Features and Materials.	51
XV	Core Cowl Doors and Inner Apron.	61
XVI	Core Cowl Doors and Inner Apron Attach Loads.	61
XVII	Core Cowl Doors - Basic Design Features and Materials.	62
XVIII	Fan Cowl Doors and Outer Apron.	76
XIX	Latch and Hinge Loads.	76
XX	Fan Cowl Doors - Basic Design Features and Materials.	77
XXI	Aft Outer Exhaust Nozzle Loads.	86
XXII	Midfan Cowl - Basic Design Features and Materials.	87
XXIII	Aft Fan Cowl - Basic Design Features and Materials.	92

LIST OF TABLES (Concluded)

<u>Table</u>		<u>Page</u>
XXIV	Nozzle Assembly - Basic Design Features and Materials.	92
XXV	Pylon Loads.	99
XXVI	Pylon - Basic Design Features and Materials.	100
XXVII	Instrumentation.	112
XXVIII	Summary.	113

## I INTRODUCTION

This report summarizes the results of the detail design of the nacelle for the General Electric Energy Efficient Engine (E<sup>3</sup>) Integrated Core Low Spool (ICLS) test vehicle. The results of the detail design effort were presented in a Detail Design Review (DDR) delivered at the NASA-Lewis Research Center on July 9, 1981. The DDR included an aerodynamic and mechanical design review of the ICLS nacelle.

The objectives of the ICLS nacelle program are shown in Table I and the program plan to achieve these objectives is shown in Figure 1.

Table I. ICLS Nacelle Program Objectives.

### Aerodynamic

- Duplicate FPS Internal Flow Lines as Close as Possible

### Mechanical

- Provide Slave Nacelle Hardware for ICLS Test
  - Low Cost
  - Functional
  - Reliable



## II OVERVIEW

A cross section of the overall ICLS test vehicle is shown in Figure 2. The major nacelle components consist of an inlet, core cowl, fan cowl, aft outer exhaust nozzle, and pylon assembly as outlined in Table II. The design of the ICLS nacelle was based on the Flight Propulsion System (FPS) nacelle described in Reference 1. There are several differences between the ICLS nacelle and the FPS nacelle. The major differences are that the ICLS nacelle has no outer flowpath, is of boilerplate (not flight weight) construction, and has no fan thrust reverser. All of the differences are summarized in Table III.

The basic nacelle design and analysis was performed by the General Electric design engineers at Evendale, Ohio. The detail design drawings, the tooling, and component fabrication are the responsibility of General Electric's Edwards Flight Test Center (EFTC) at Mojave, California. The method of operation between these two organizations is shown in Table IV.

The acoustic treatment for the nacelle is all of the bulk absorber type using one inch thick Kevlar felt and a 30% open area face sheet. Some of this treatment is in the form of replaceable panels and some is built into the basic structure as defined in Table V. The acoustic treatment will be taped to obtain the acoustic baseline data.

ORIGINAL PAGE IS  
OF POOR QUALITY

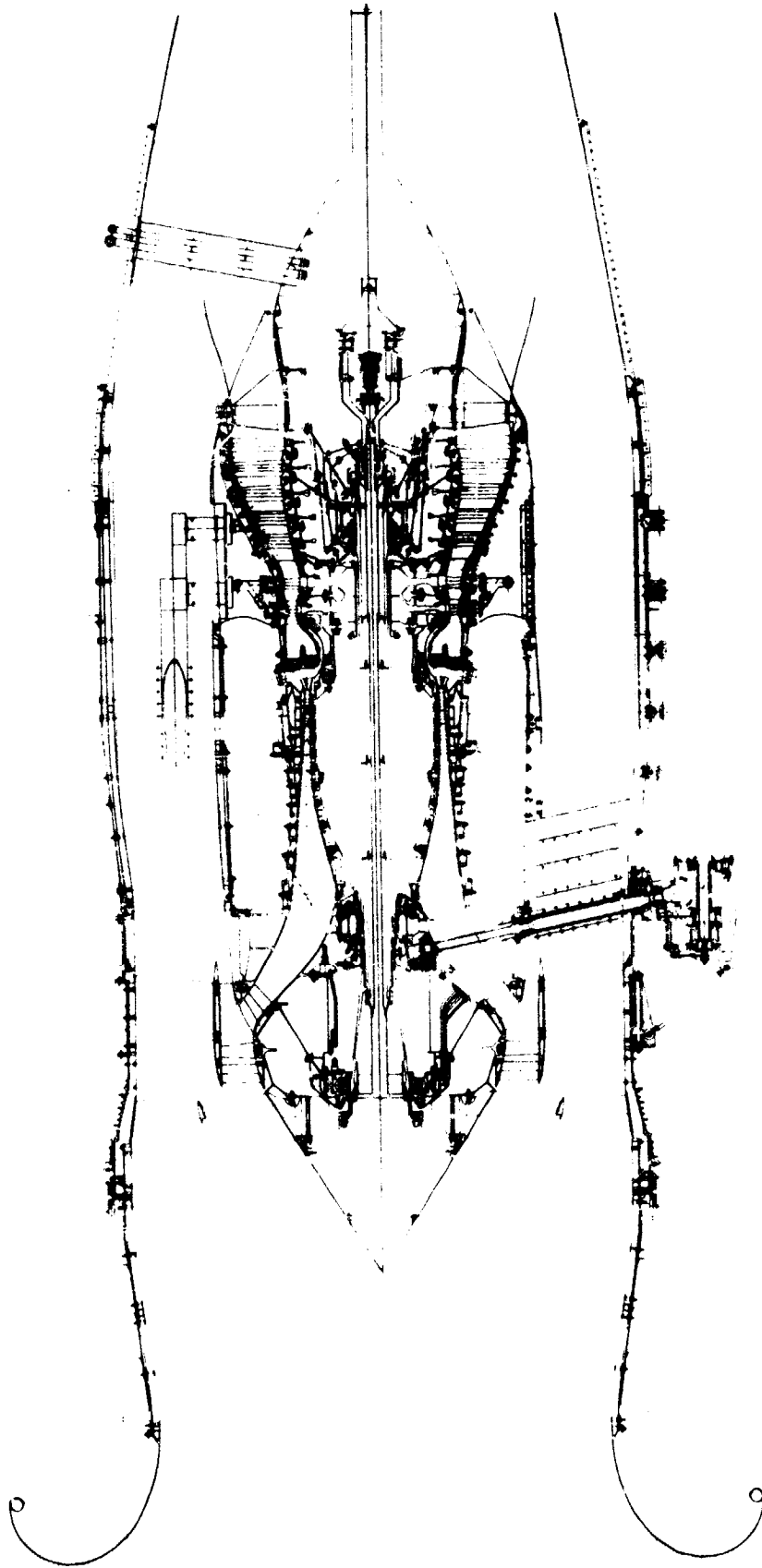


Figure 2. ICLS Cross Section.

ORIGINAL PAGE IS  
OF POOR QUALITY

Table II. ICLS Nacelle Components.

- Aero-Acoustic Inlet
  - Bellmouth Lip
  - Diffuser Assembly
- Core Cowling
  - Core Cowl Doors
  - Inner Apron Assembly
- Fan Cowling
  - Fan Cowl Doors
  - Outer Apron Assembly
- Aft Outer Exhaust Nozzle
  - Midfan Cowling
  - Aft Fan Cowling
  - Performance Nozzle
  - Survey Nozzle
- Pylon Assembly
  - Pylon Sidewalls
  - Pylon Scoop and Plenum

**ORIGINAL PAGE IS  
OF POOR QUALITY**

Table III. Differences Between FPS and ICLS Nacelle.

- No Outer Flowpath
- All Slave Hardware
  - Aluminum
  - Steel
  - Fiber Glass
- No Reverser
  - Blocker Door/Fixed Structure Interface Smoothed Out
- Inlet Has Aero Bellmouth Forward of Throat
  - Not Drooped
  - Supported From Facility
- ICLS Has Two Fan Exit Nozzles
- ICLS Has Some Replaceable Acoustic Panels
- ICLS Has Lower Pylon
- ICLS Has Aft Instrumentation Strut
- Outer Fan Cowling/Nozzle is Supported From Facility Mount Str.
- Instrumentation Provisions
- No 5th Stage Or CDP Bleed Lines Installed
  - Provisions for Later Installation
- External Mounted Gearbox
  - Proper FPS Core Cowl Flow Lines



ORIGINAL PAGE IS  
OF POOR QUALITY

Table IV. Method of Operation.

Evendale Design

- Establishes Design Intent
- Coordinates all Interfaces
- Performs Structural Analysis
- Issues Layout Drawings

Mojave

- Detail Part Design
  - Can Alter Initial Approach - Evendale Approval
- Final Assembly Drawings
- Tool Design/Fab/Procurement
- Fabrication
- Trial Assembly and Fit

All Drawings Issued by Evendale

Table V. Acoustic Configuration.

Basic Treatment

- Bulk Absorber
  - 2.54 cm (1 in.) Deep
  - 30% Porous Face Sheet
  - No Wire Mesh

Build-In Treatment

- Inlet
- Forward Portion of Fixed Fan Nozzle

Replaceable Panels

- Outer Cowl Doors
- Inner Cowl Doors

No Hardwall Panels -- Tape Acoustic Treatment

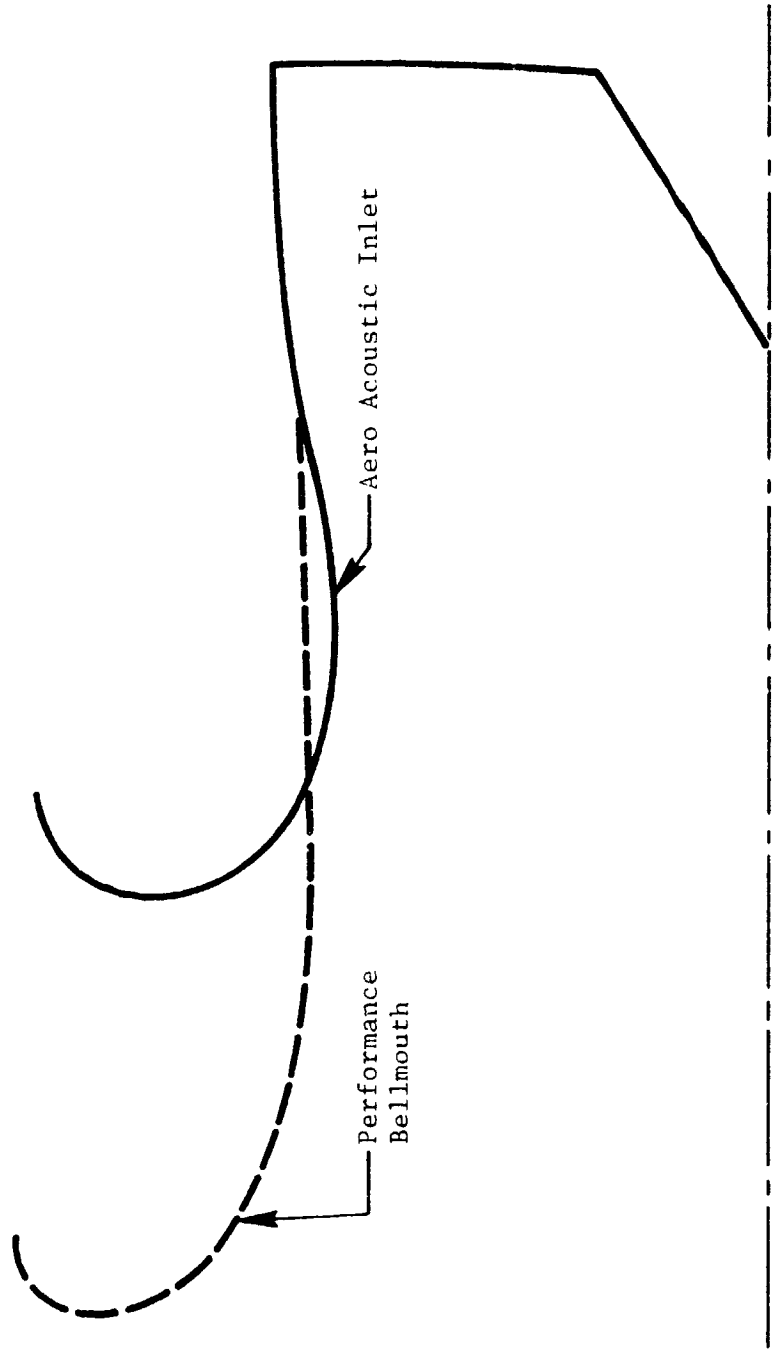
### III AERODYNAMIC DESIGN

In the current E<sup>3</sup> Program, the ICLS engine will be tested at the Peebles Test Facility with two different inlet bellmouths: the performance bellmouth and the aero-acoustic inlet/bellmouth. A schematic of the two inlets is presented in Figure 3. The performance bellmouth is the same hardware that will have been used for the full scale fan component test and will also be installed on the engine for all ICLS performance tests. The performance bellmouth has been designed to provide high flow measurement accuracy and to be compatible with the full scale fan test facility and test requirements. The inlet lip and contraction section has been designed based on CF6 engine bellmouth experience. A 16.5 inch, low Mach number cylindrical section provides a high accuracy flow measurement station. A schematic of the bellmouth and several key dimensions are shown in Figure 4. The aero-acoustic inlet will be used exclusively during ICLS engine noise measurement tests.

The aero design of the aero-acoustic inlet was established primarily by the acoustic testing requirements as summarized in Table VI. To ensure the proper acoustic environment, the inlet was designed to provide the same diffuser wall and throat Mach number distribution at SLS max power operating conditions as the real FPS inlet at the T/O noise rating point. To achieve this requirement, the inlet diffuser flowpath was made identical to the FPS inlet undrooped. This provides the same inlet acoustic treatment area and meets the same inlet diffusion criteria. The bellmouth/lip contour was defined using CF6 bellmouth design experience to provide a uniform flow field acceleration to the throat with no flow separation. Figure 5 summarizes the aero-acoustic inlet bellmouth description.

Following the flowpath design definition, an analytical study of the inlet was conducted using the GE Streamtube Curvature (STC) potential flow program. The bellmouth was analyzed at SLS max power conditions and compared to the FPS inlet analysis at the T/O noise rating point. Results shown in Figures 6 and 7 show that the wall and throat Mach number distributions are nearly identical for each inlet, particularly the important wall Mach number

ORIGINAL PAGE IS  
OF POOR QUALITY



- Performance Bellmouth Used for Fan Component Test and all ICLS Performance Tests; High Flow Measurement Accuracy.
- Aero-Acoustic Inlet Used for ICLS Noise Tests.

Figure 3. ICLS Inlet Configurations.

ORIGINAL PAGE IS  
OF POOR QUALITY

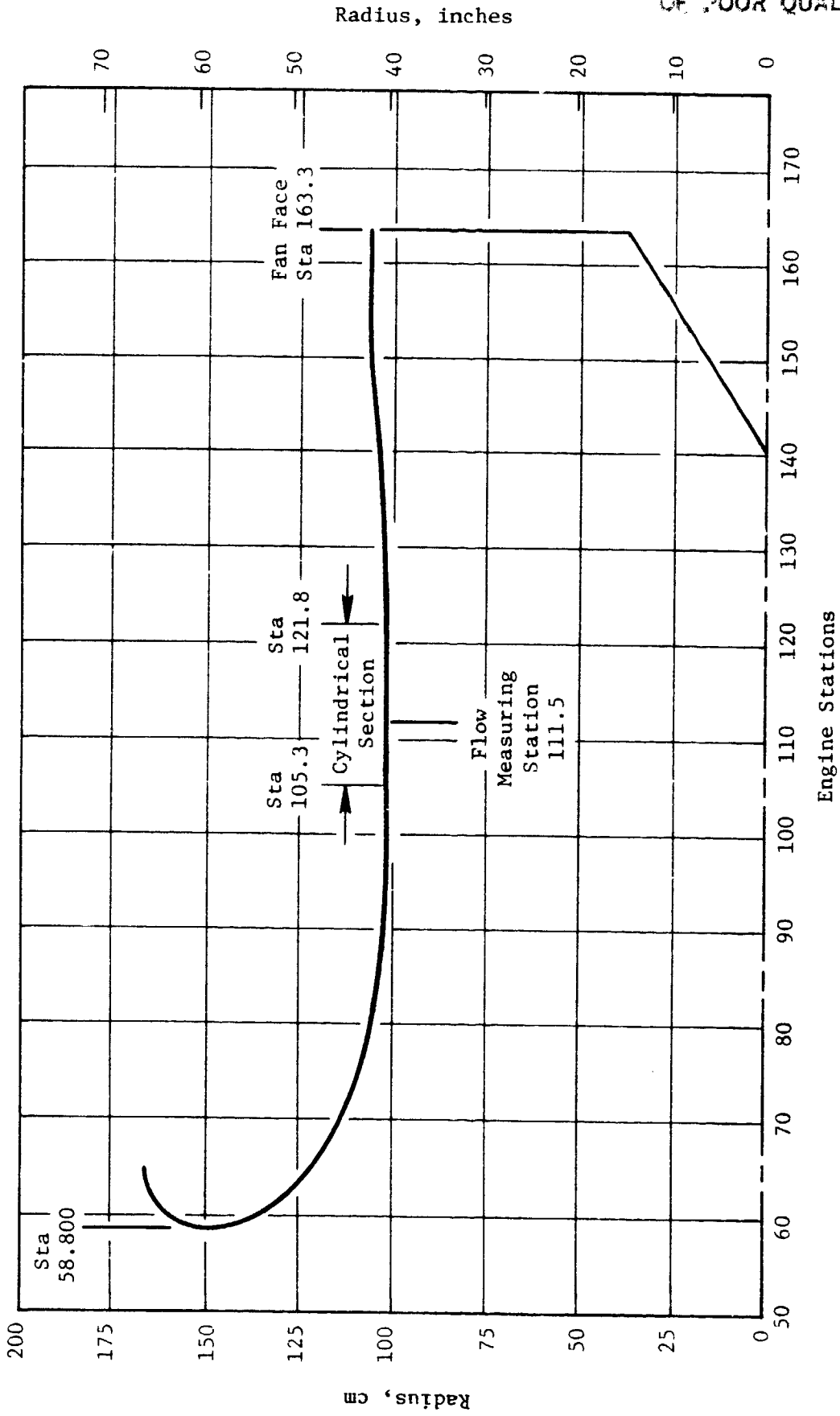


Figure 4. ICLS Performance Bellmouth.

Table VI. ICLS Aero-Acoustic Inlet/Bellmouth Aero Design.

- Inlet Defined to Achieve Acoustic Testing Requirements; Provide Same Wall and Throat Mach Numbers at SLS Max Power as FPS Inlet at M 0.3/304.8 m (1000 ft.); Max Power (T/O Noise Rating PT)
  - Diffuser Flowpath Identical to FPS Inlet (Undrooped); Consistent with Required Acoustic Treatment and Inlet Diffusion Design Criteria
  - Bellmouth/Lip Contour Defined for Uniform Flow Acceleration and No Flow Separation; Uses CF6 Bellmouth Design Experience.
  
- STC Analysis Conducted; Flow Field Matches FPS Inlet
  - Same Wall Mach Number
  - Same Throat Radial Mach Number Distribution

ORIGINAL PAGE IS  
OF POOR QUALITY

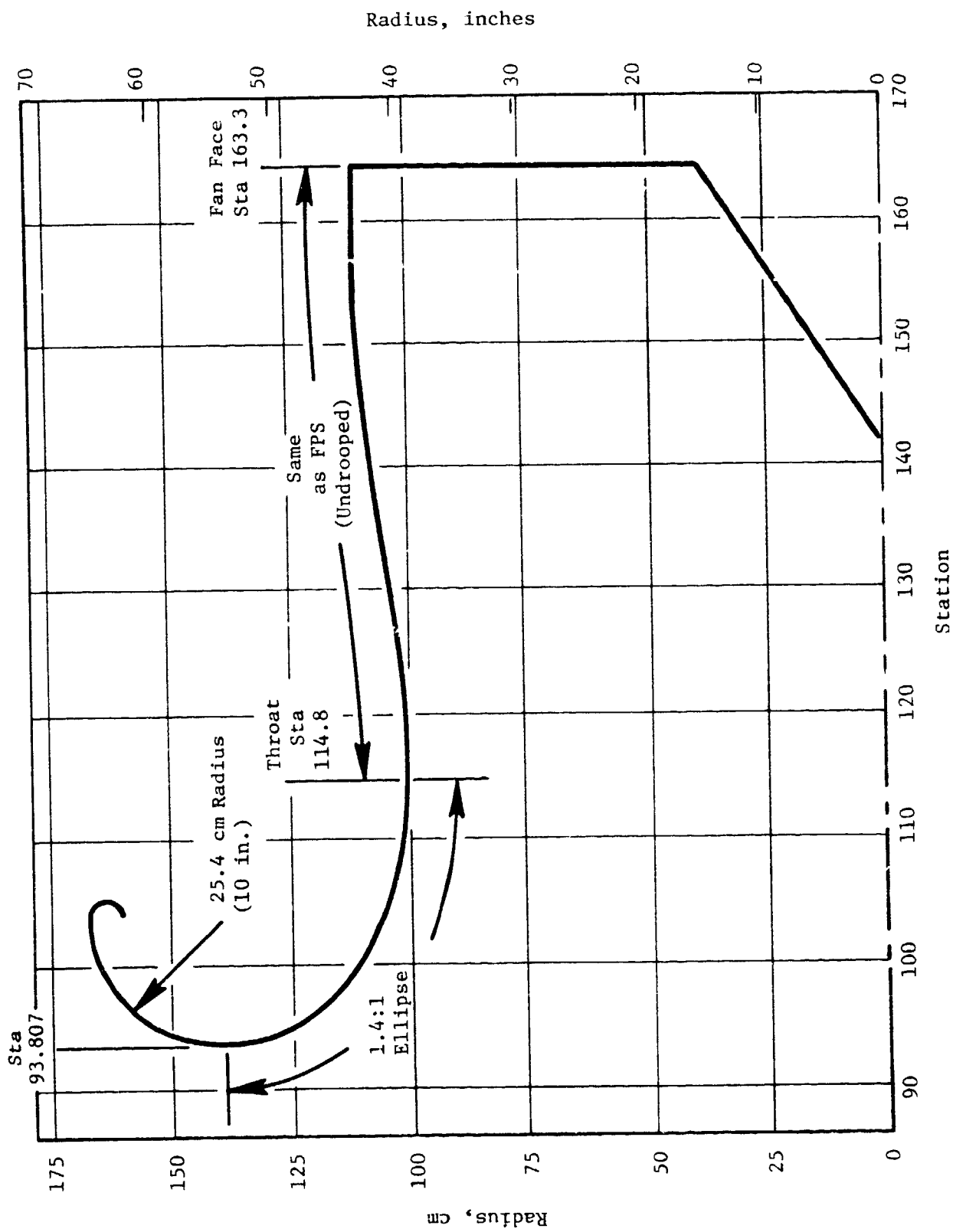


Figure 5. ICLS Aero-Acoustic Inlet Bellmouth.

ORIGINAL PAGE IS  
OF POOR QUALITY

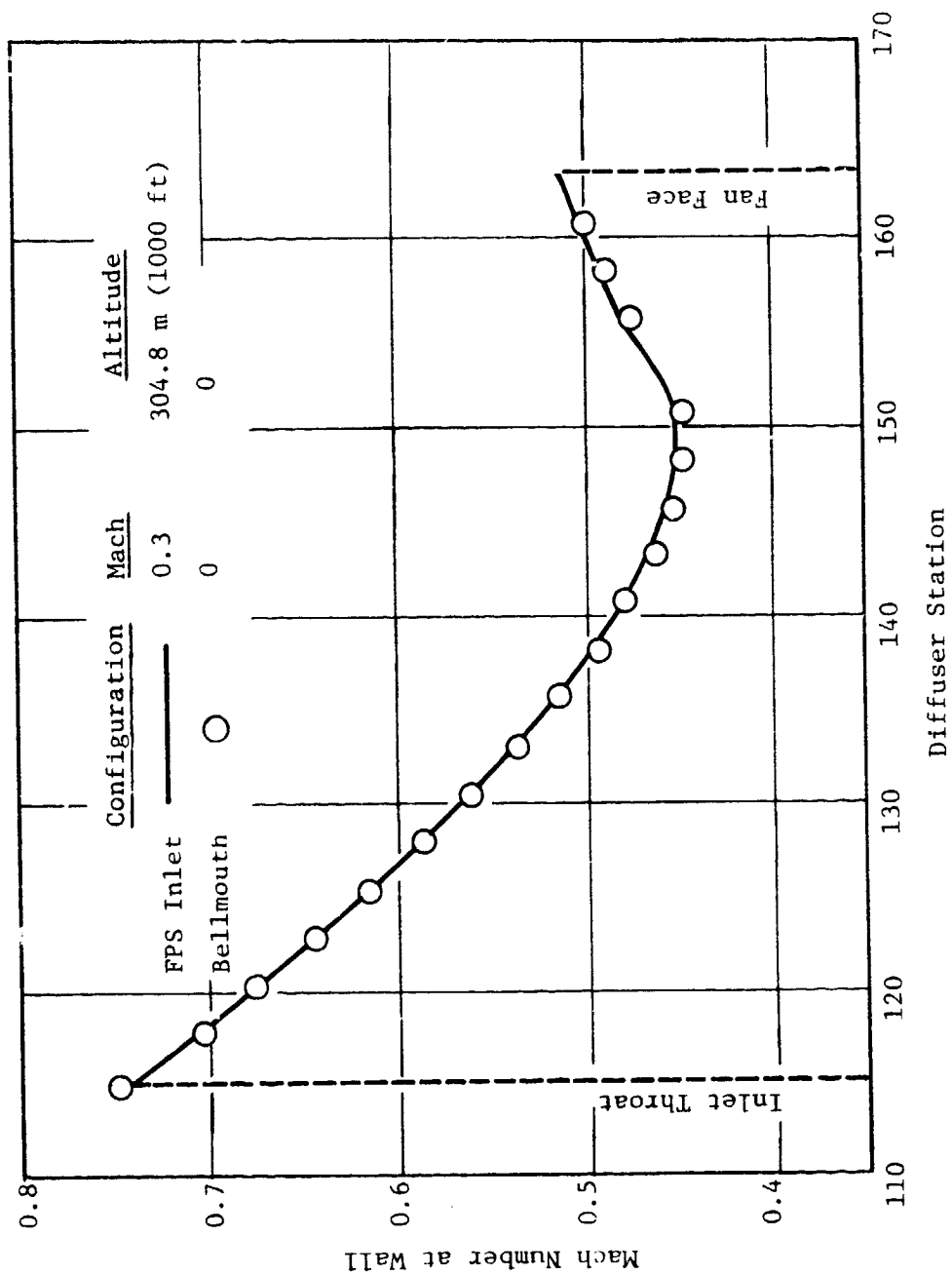


Figure 6. ICLS Aero-Acoustic Inlet - STC Analysis of Mach Number Along Diffuser Wall.

ORIGINAL PAGE IS  
OF POOR QUALITY

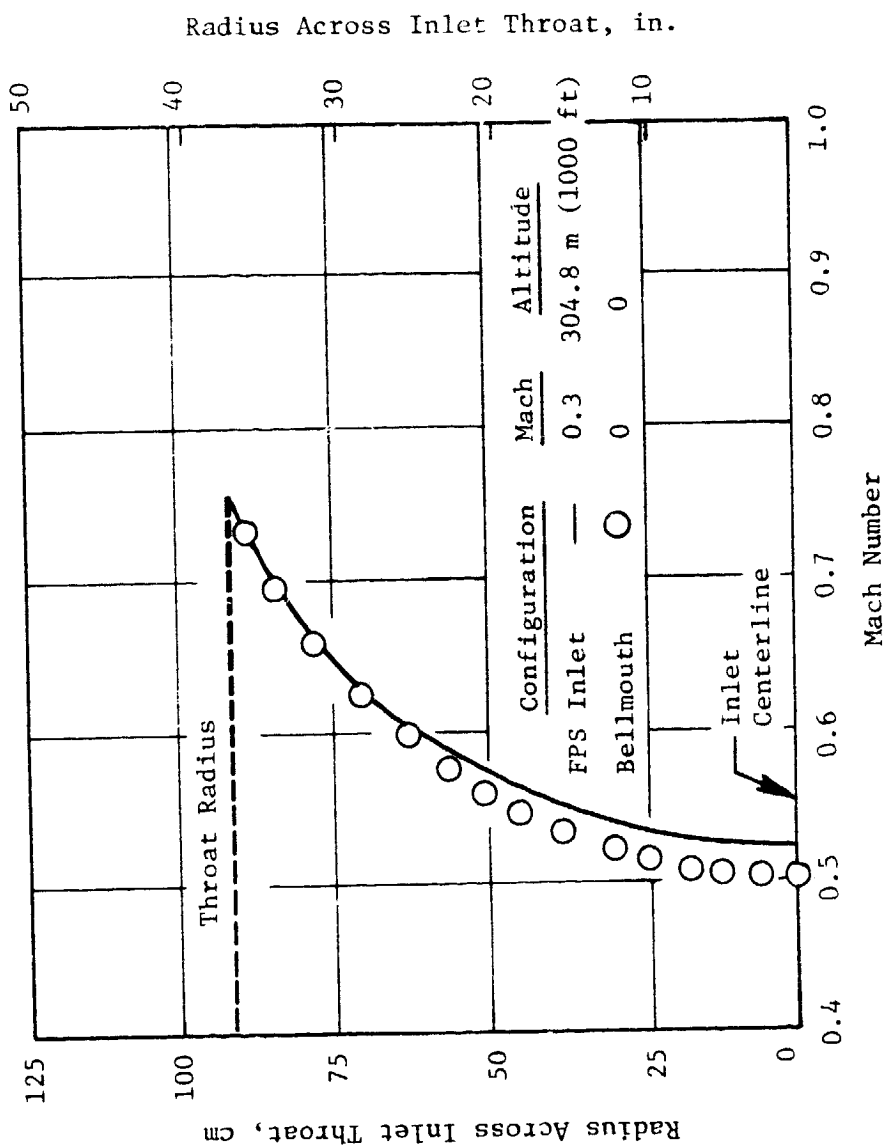


Figure 7. ICLS Aero-Acoustic Inlet - STC Analysis of Mach Number Across Inlet Throat.



where the noise attenuation is achieved. These results were reviewed with the E<sup>3</sup> acoustic personnel and were found completely satisfactory.

The ICLS slave inlet will not be directly mounted to the engine/fan casing. Rather, it will be "soft-mounted" with a flexible seal between the inlet and engine. At high power settings, relative motion will occur between the engine and inlet, and it is planned to measure this relative displacement with potentiometers. This measurement will be used to determine the magnitude of the displacement and to thus identify any discrete aeolian tones which are normally associated with flow separation. Identification of the source of the tones will thus provide substantiation for editing the tones out of the data (Table VII).

The rationale for the ICLS fan exhaust duct aero design is summarized in Table VIII. The duct has been designed for low Mach numbers to minimize duct pressure losses and at the same time be compatible with (1) a thrust reverser for an FPS low drag nacelle, (2) a core mounted gearbox for FPS and (3) the mixer flowpath. An STC analysis of the duct at cruise operating conditions indicates that low Mach numbers were achieved as shown in Figure 8. Typical Mach numbers for separate flow nacelle fan ducts range from 0.45 to 0.50 whereas the E<sup>3</sup> fan duct ranges from below 0.40 to 0.45 for most of the duct. The fan duct flowpath has been included in all the scale model mixer performance tests and results have verified a low pressure loss, therefore a good aero design. Measured nozzle thrust coefficients come within 0.1% of prediction which includes the duct losses.

The pylon cross section flowpath has been designed with two major considerations. The forward, or nose, portion of the pylon was designed by the fan aero designers to assure compatibility with the fan. The aft portion of the pylon from the maximum width to the trailing edge was designed to be aerodynamically compatible with the mixer and to provide low pressure loss. The pylon has been simulated in the scale model mixer development tests, and back-to-back testing with and without the pylon verify pressure losses even lower than predicted. The engine aft mount links positioned over the turbine frame have been designed for minimum drag and no interaction/impact on the mixer. These links were also tested in the scale model mixer development

Table VII. Adjustment for Soft-Mounted Inlet.

- Aero-Acoustic Inlet Soft-Mounted Due to Structural Inadequacy of ICLS Slave Hardware
- Relative Motion Between Bellmouth and Engine Will be Measured With Potentiometers
- Discrete Aeolian Tones Associated With Flow Separation Can be Edited Out of Noise Data

Table VIII. ICLS Fan Exhaust Duct Aero Design.

- Fan Duct Flowpath Designed for Low Mach Numbers and Compatibility with:
  - Low Drag Nacelle With Thrust Reverser for FPS
  - Core Mounted Gearbox for FPS
  - Mixer Flowpath
- STC Analysis Indicates Low Mach Number Levels
- Scale Model Mixer Test Substantiates Good Aero Design; Thrust Coefficients Match Prediction
- Pylon Cross Section Flowpath Designed for:
  - Compatibility With Design Criteria for No Interaction With Fan
  - Integration With Mixer and Closure Half Angle  $<7^\circ$  for Low Drag; Mixer Scale Model Test Verified Low Pressure Loss
- Aft Mount Links Contoured and Aligned With Fan Flow; Mixer Scale Model Test Verified Low Pressure Loss.

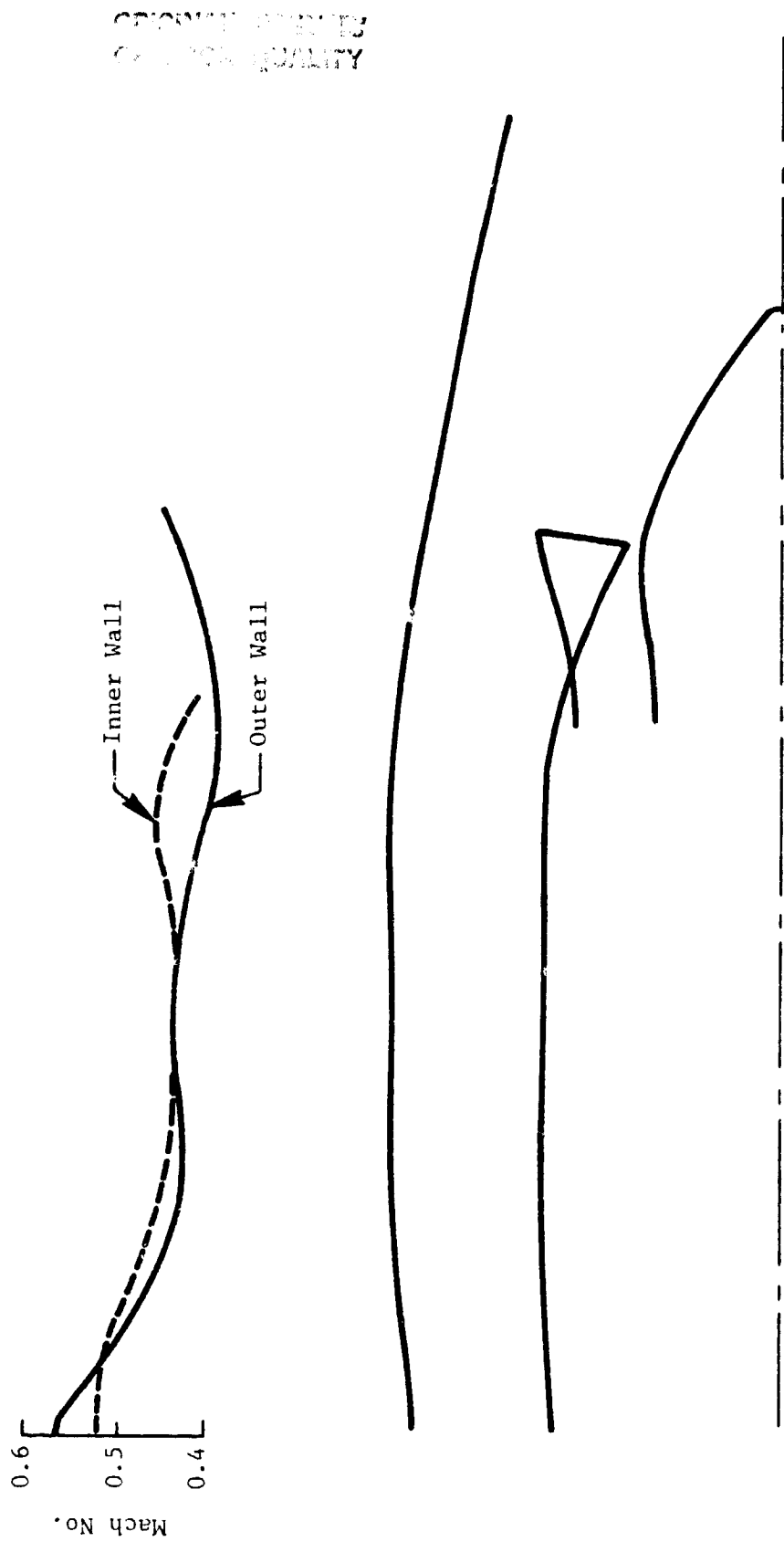


Figure 8. ICLS Fan Duct STC Analysis (Altitude Cruise Condition).

ORIGINAL PAGE IS  
OF POOR QUALITY

program and were shown to have low drag/pressure loss. The pylon and mount link test results are shown in Figure 9.

The ICLS engine will be tested with two exhaust nozzles as shown in Figure 10. The basic performance nozzle is a conical nozzle designed to provide area trim capability for optimizing the engine cycle area match. The exit survey nozzle will be used during the exhaust nozzle exit survey tests and has been opened up by 5% in exit area to account for estimated exit survey rake blockage.

The differences between the ICLS fan exhaust duct aero design and the FPS flowpath are summarized in Table IX. For the ICLS engine, the basic flowpath is consistent with the ICLS LPT and mixer designs. The FPS flowpath differs from the ICLS due to the LPT and mixer flared flowpath designs. An overall comparison of the exhaust ducts is shown in Figure 11. Forward of the turbine frame, the two flowpaths are identical. Aft of the turbine frame, the ICLS exhaust nozzle geometry differs from the FPS to match the ICLS mixer flowpath as previously noted. The FPS design has a larger centerbody and a mixer which is larger in diameter; consequently, the FPS exhaust nozzle diameter must be increased at the mixing plane to maintain mixing plane areas and Mach numbers. This change in the FPS design was incorporated to improve performance as noted in Figure 12. Based on scale model mixer tests, it was concluded that the flared turbine/mixer flowpath would improve mixing effectiveness and reduce mixer pressure loss resulting in an sfc improvement of 0.2% at max cruise. Additionally, the increased diameter of the last LPT stages was estimated to improve LPT efficiency resulting in a 0.16% sfc gain. These analyses and conclusions were completed in mid-1980; this was too late to incorporate these changes into the ICLS hardware.

In addition to the basic flowpath difference in the exhaust nozzle region, there are several differences in flowpath pressure loss between ICLS and FPS. These differences are listed in Table IX along with an estimate of the change in duct pressure loss. Figure 13 shows the location of several of these items.

Finally, the exhaust nozzle shape is different between FPS and ICLS. The FPS has a CD nozzle for desired takeoff-to-cruise nozzle flow coefficient

ORIGINAL PAGE IS  
OF POOR QUALITY

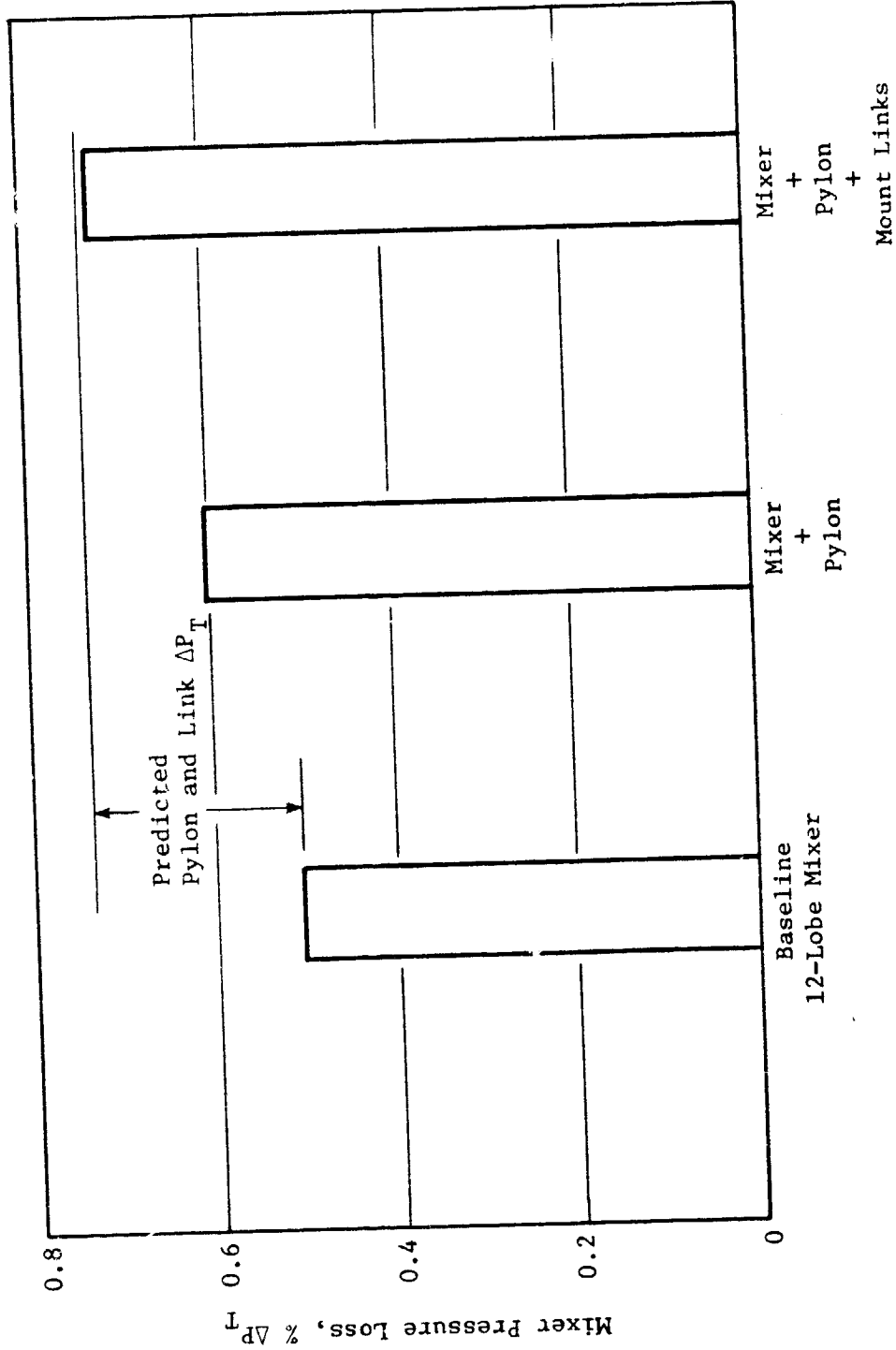
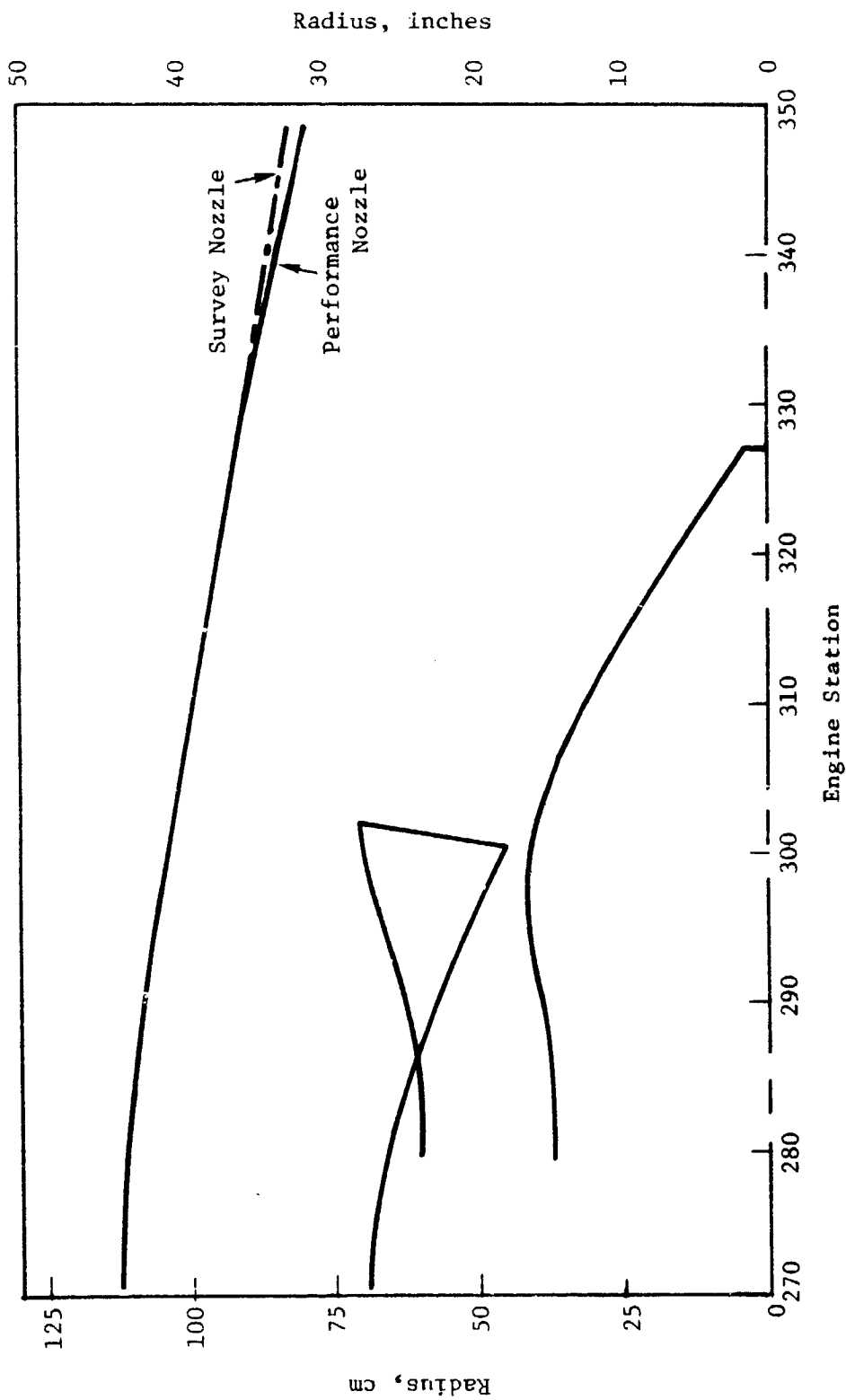


Figure 9. Mixer Scale Model Test Results - Pylon and Mount Link Effects.



ICLS has Two Nozzles:

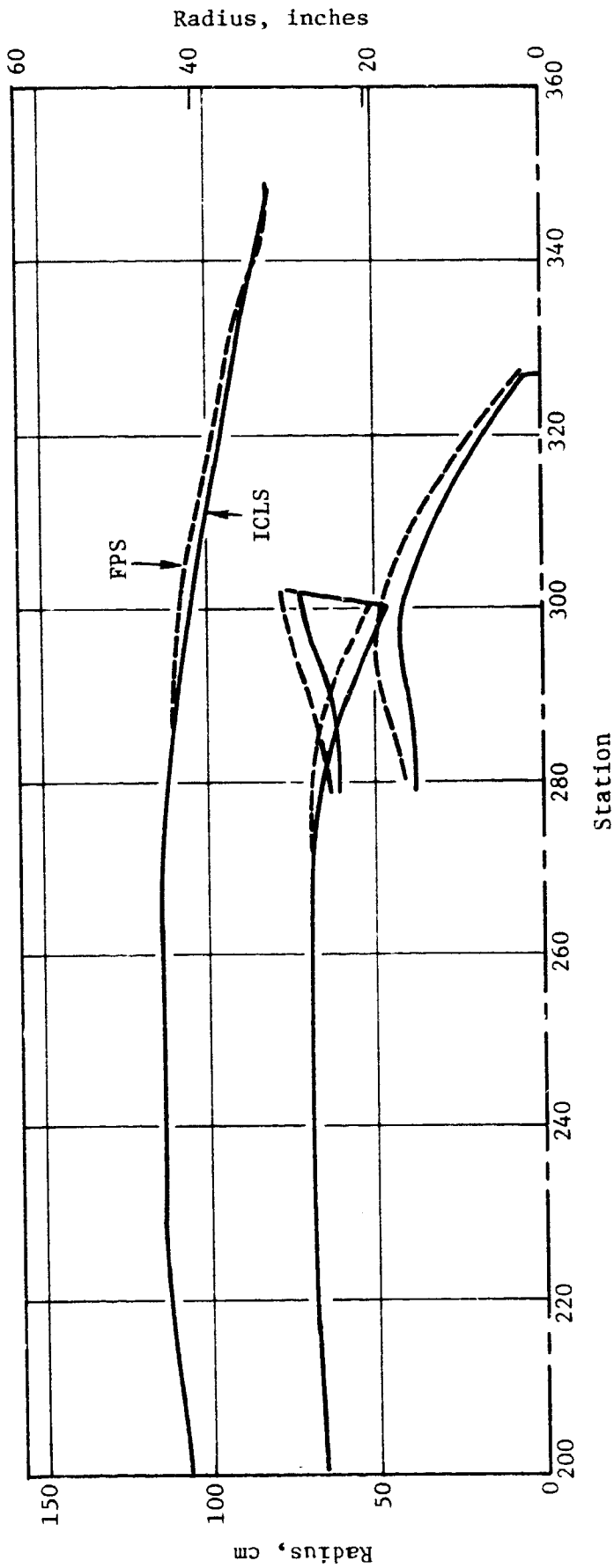
- Conical Performance Nozzle to Provide Area Trim Capability to Match Engine Cycle
- Conical Exit Survey Nozzle with Increased Area to Account for Survey Rake Blockage

Figure 10. ICLS Exhaust Nozzle Aero Design.

Table IX. ICLS Fan Exhaust Duct Aero Design.

Differences from FPS

- Fan Exhaust Duct Basic Flowpath Consistent with ICLS LPT and Mixer Design; FPS Has Flared LPT/Mixer Flowpath
- Differences in Flowpath Pressure Loss Items include:
  - No Steps and Gaps Associated With Reverser (+0.12%  $\Delta P_T$ )
  - No Drain Mast at Bottom Centerline (+ 0.01%  $\Delta P_T$ )
  - No Precooler Scoop (+ 0.05%  $\Delta P_T$ )
  - Instrumentation Strut at 75° in Exhaust Nozzle (-0.10%  $\Delta P_T$ )
  - Lower Pylon Behind Fan Frame for ICLS Gearbox (-0.05%  $\Delta P_T$ )
- FPS Has CD Nozzle for Desired Takeoff-to-Cruise Nozzle Flow Coefficient Characteristics

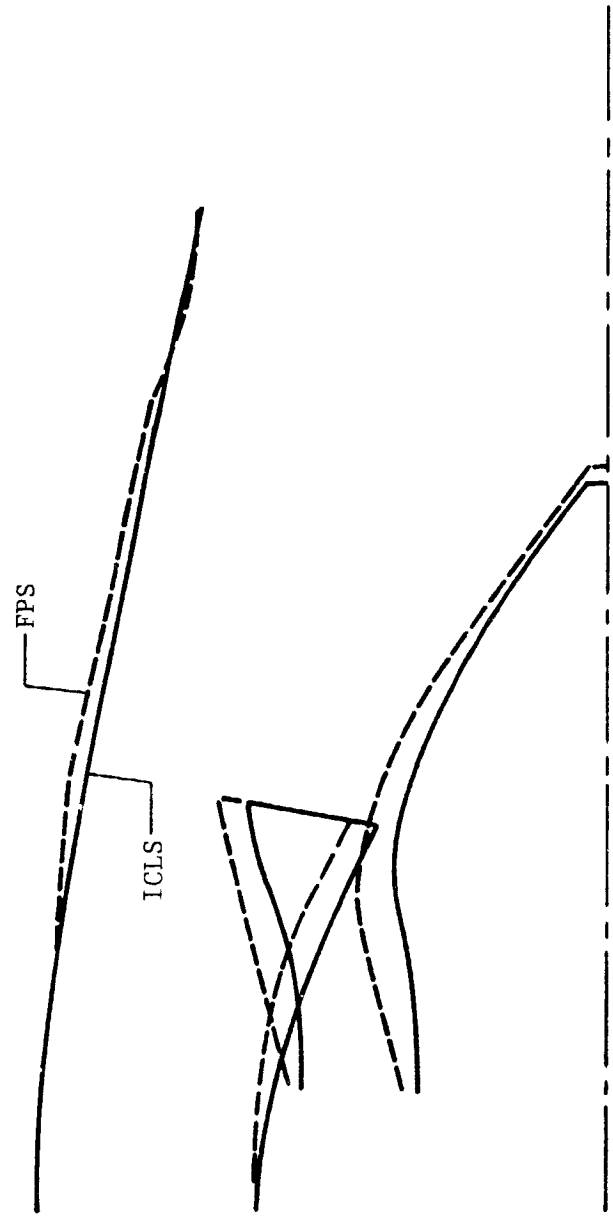


ORIGINAL PAGE IS  
OF POOR QUALITY

Figure 11. ICLS Versus FPS Fan Exhaust Duct Comparison.



ORIGINAL PAGE IS  
OF POOR QUALITY



- Flared Turbine Flowpath Provides:
    - Improved Mixing Effectiveness
    - Potential for Reduced Mixer Pressure Loss
    - Improved LPT Efficiency
  - Analysis and Conclusions too Late (June 1980) for Incorporation into ICLS
- } 0.2% SFC Estimated  
0.16% SFC Estimated

Figure 12. FPS Flared Turbine Flowpath.

ORIGINAL PAGE IS  
OF POOR QUALITY

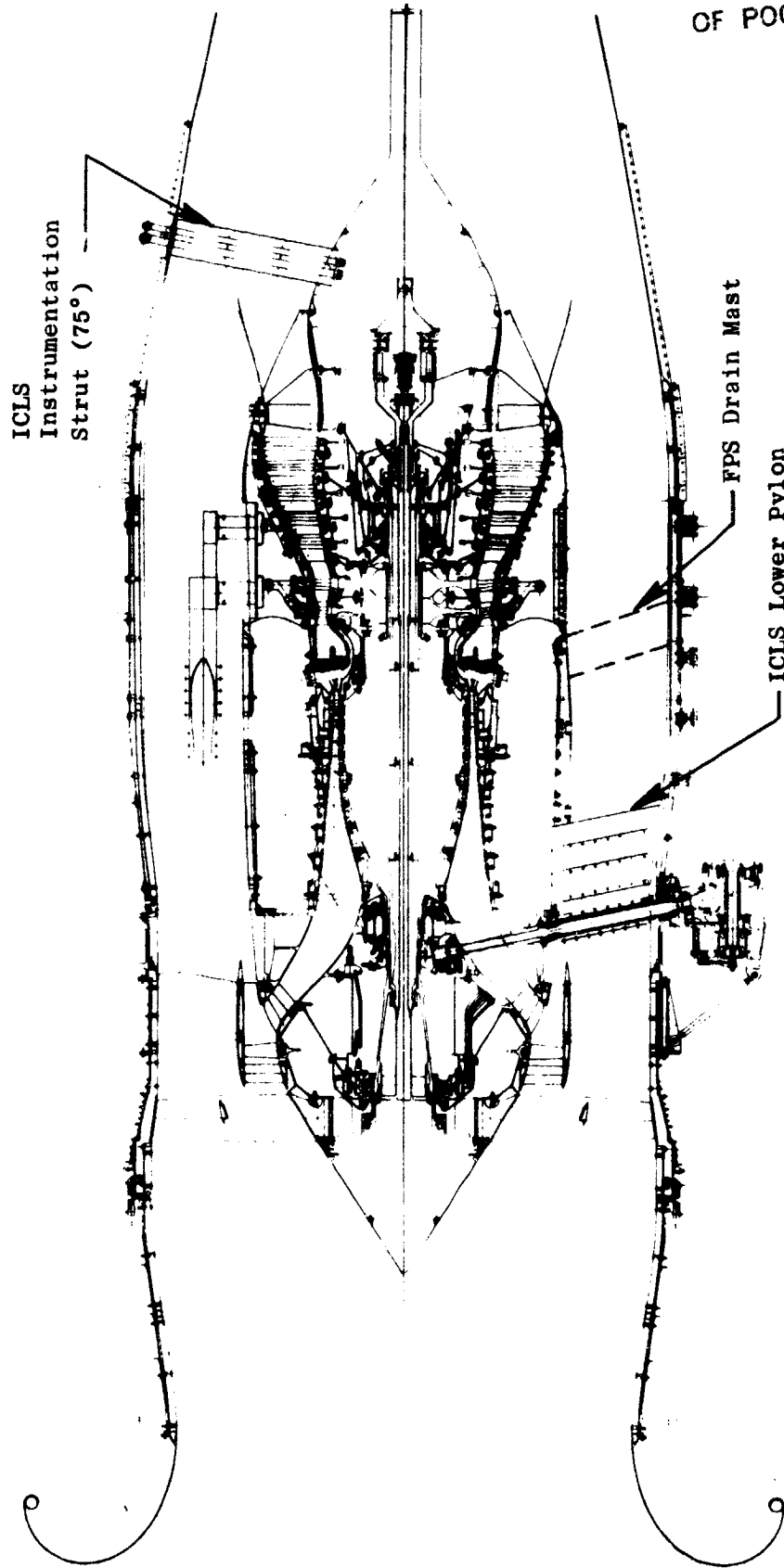


Figure 13. Pressure Loss Items.

characteristics. This type of nozzle is not amenable to area trimming and would, for a typical engine development program, be sized for production based on substantial engine development testing. Since the ICLS engine is a single engine technology program and will only be tested at SLS conditions, it was concluded that the exhaust nozzle be a simple, conical/convergent nozzle to provide area trim capability as previously discussed. This nozzle difference can be seen in both Figures 11 and 12.

Because of the differences between the ICLS and FPS flowpaths, adjustments to the ICLS engine test data will be required to adjust performance to the FPS design. These adjustments will be conducted using both analytical calculations and experimental data as noted in Table X. The basic duct flowpath friction differences and pressure loss items will be calculated analytically using standard duct friction loss and component drag methodology. Both the ICLS and FPS exhaust nozzles were tested in the Phase III scale model mixer test; thus, the differences in nozzle exit flow and velocity coefficients between the CD and converging nozzles will be determined by test.

#### A. NASA LANGLEY WIND TUNNEL TEST

One of the differences between the ICLS and FPS nacelles is in the external flowpath. Because the ICLS engine is strictly a ground test demonstrator engine, there is no need to include a flight propulsion system external nacelle. This difference does not affect the ICLS engine test performance adjustment. Details of the FPS nacelle design were presented in the Nacelle Preliminary Analysis and Design Report. The following discussion briefly summarizes preliminary results of a wind tunnel test of the E<sup>3</sup> nacelle conducted at NASA Langley.

The NASA Langley wind tunnel test evaluation of the E<sup>3</sup> nacelle was an add-on to a previously planned Energy Efficient Transport (EET) wind tunnel test program. The purpose of the test is outlined in Table XI. The major objective of the Langley EET program was to evaluate the effects of nacelle configuration, nacelle placement, and pylon configurations on nacelle interference drag. By agreement with NASA Langley, the E<sup>3</sup> nacelle was added to

Table X. Fan Duct/Exhaust Nozzle Aero Design Performance Adjustment Procedures, ICLS Versus FPS.

- Exhaust Duct/Nozzle Friction Loss Differences (ICLS Versus FPS Flared Turbine) Determined Analytically
- Flowpath Pressure Loss Items to be Adjusted Analytically
  - Reverser Steps and Gaps
  - Struts
  - Precooler Scoop
- Phase III Scale Model Mixer Test Will Define ICLS and FPS Exhaust Nozzle Exit Flow and Velocity Coefficients

Table XI

EET/E<sup>3</sup> NASA-Langley Wind Tunnel Test

- Evaluate E<sup>3</sup> Isolated Nacelle Drag - Compare with Reference CF6-50C
- Evaluate Installation Effects of E<sup>3</sup> Long Duct Mixed Flow Nacelle
- Semispan Wind Tunnel Model with Turbopowered Simulators
- Phase I Test March - July 1979, Follow-on Test Feb. - April 1980

the test program. All nacelles evaluated were tested both isolated and installed on the airplane model. Since one of the three nacelles which Langley planned to evaluate in the EET program was the CF6-50C reference nacelle, testing of the E<sup>3</sup> isolated nacelle not only provided the opportunity to evaluate the E<sup>3</sup> isolated nacelle drag, but allowed a direct isolated drag comparison to be made with the CF6-50 reference nacelle.

The wind tunnel model was a 6% scale semispan model designed by NASA Langley. The wing was an advanced technology supercritical design with one engine per wing. Turbopowered simulators (TPS) as depicted in Figure 14, were used for nacelle inlet and exhaust airflow simulation. High pressure air is used to drive a turbine in the simulator which in turn drives a two-stage fan. The turbine discharge air provides the primary or core discharge flow, and the fan provides both the nacelle inlet flow and the fan nozzle discharge. The TPS units thus provide simultaneous simulation of both the inlet and exhaust system flow conditions. The test was conducted in the NASA Langley 8-foot Transonic Wind Tunnel in two phases; Phase I extended from March to July, 1979 and the follow-on Phase II test was conducted in February - March, 1980.

Figure 15 shows the four nacelles tested in Phase I, two were mixed flow and two were separate flow. The two separate flow nacelles were the CF6-50 long core exhaust system (E<sup>3</sup> reference) and the short core engine. The mixed flow nacelles included a long duct nacelle version of the CF6-50 and the E<sup>3</sup> nacelle. The two separate flow nacelles and the -50 long duct nacelle were part of the original EET program. The CF6-50 short core and long duct nacelles were tested in two positions, forward and rear, and the -50 long core was tested in the rear position only. Although five pylons were fabricated for the E<sup>3</sup> nacelle to evaluate five nacelle positions, only two were tested in Phase I due to a lack of test time. Two additional positions (Figure 16) were tested in Phase II. The fifth position was not tested due to hardware interface problems. In addition to the basic E<sup>3</sup> nacelle tested in Phase I, in Phase II an E<sup>3</sup> nacelle with a longer nacelle afterbody and a shallower boattail angle was tested (Figure 17). This configuration

ORIGINAL PAGE IS  
OF POOR QUALITY

ORIGINAL PAGE IS  
OF POOR QUALITY

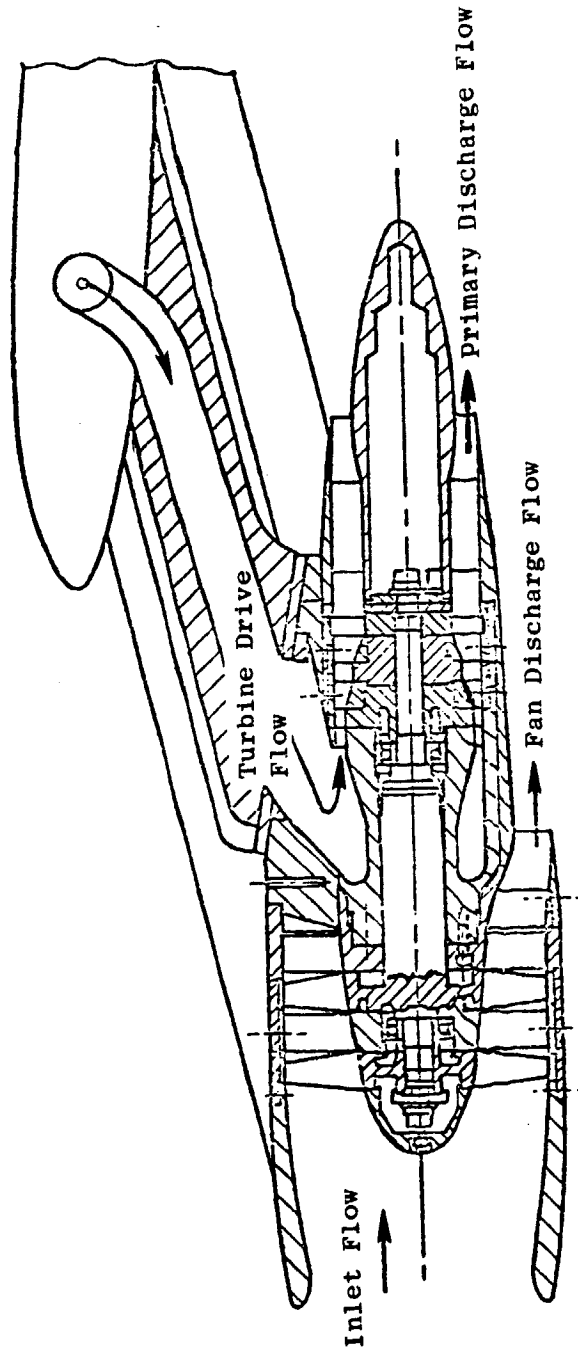
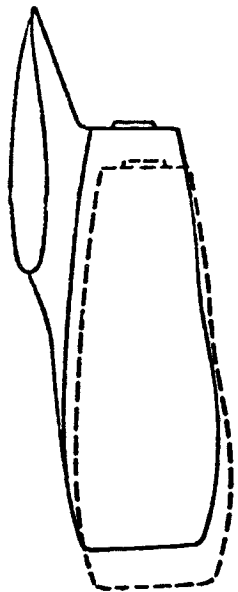


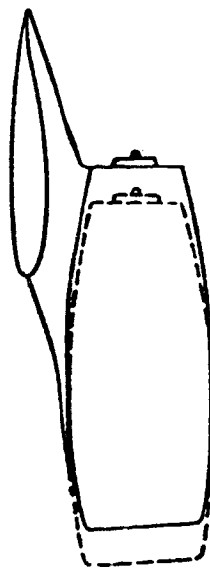
Figure 14. Typical Fan Powered Nacelle Model.

ORIGINAL PAGE IS  
OF POOR QUALITY

Mixed Flow Nacelles

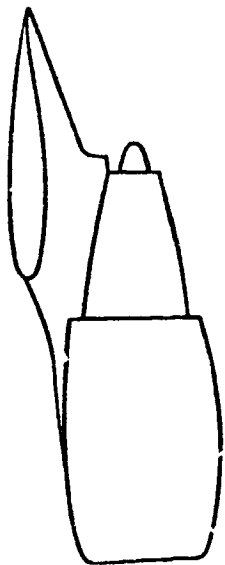


Long Duct Nacelle

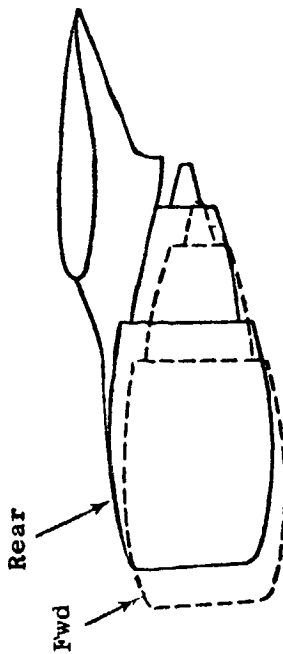


Advance E<sup>3</sup> Nacelle

Separate Flow Nacelles



Long Core Nacelle

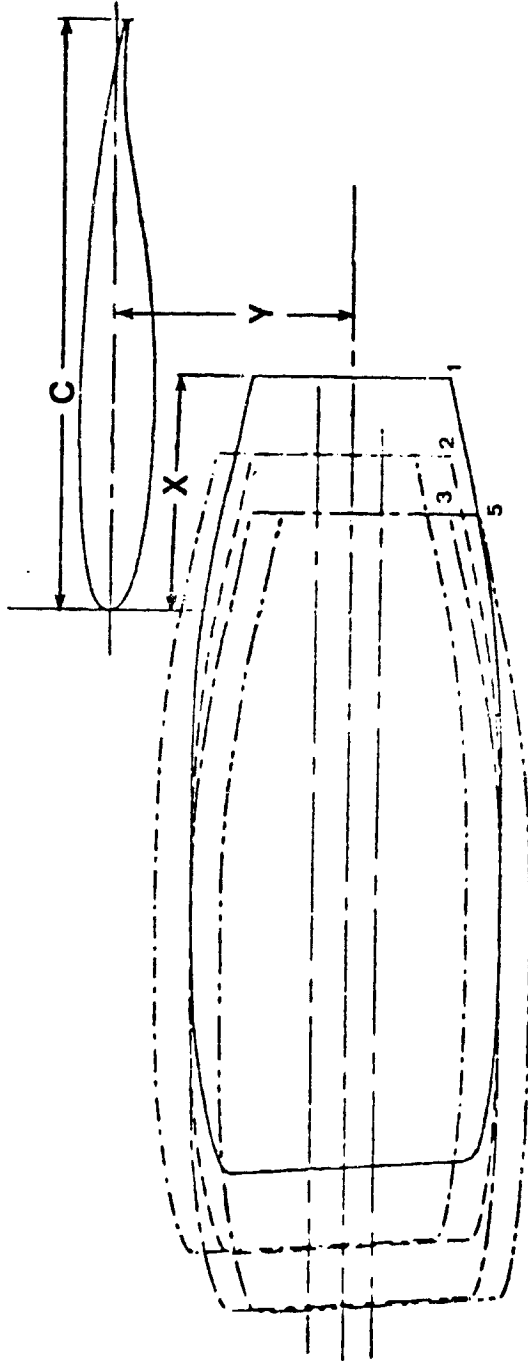


Short Core Nacelle  
(Primary Reverser Removed)

Figure 15. Nacelle Configurations - Phase I.



ORIGINAL PAGE IS  
OF POOR QUALITY



<u>Pylon No.</u>	<u>X/C</u>	<u>Y/C</u>	<u>Phase I</u>	<u>Phase II</u>
1	0.40	0.40	X	
2	0.27	0.40	X	X
3	0.17	0.40		X
4	0.27	0.34	Not Tested Due to Hardware Incompatibility	
5	0.17	0.45		X

Figure 16. E<sup>3</sup> Nacelle Positions.

ALTIMETRY  
QUALITY

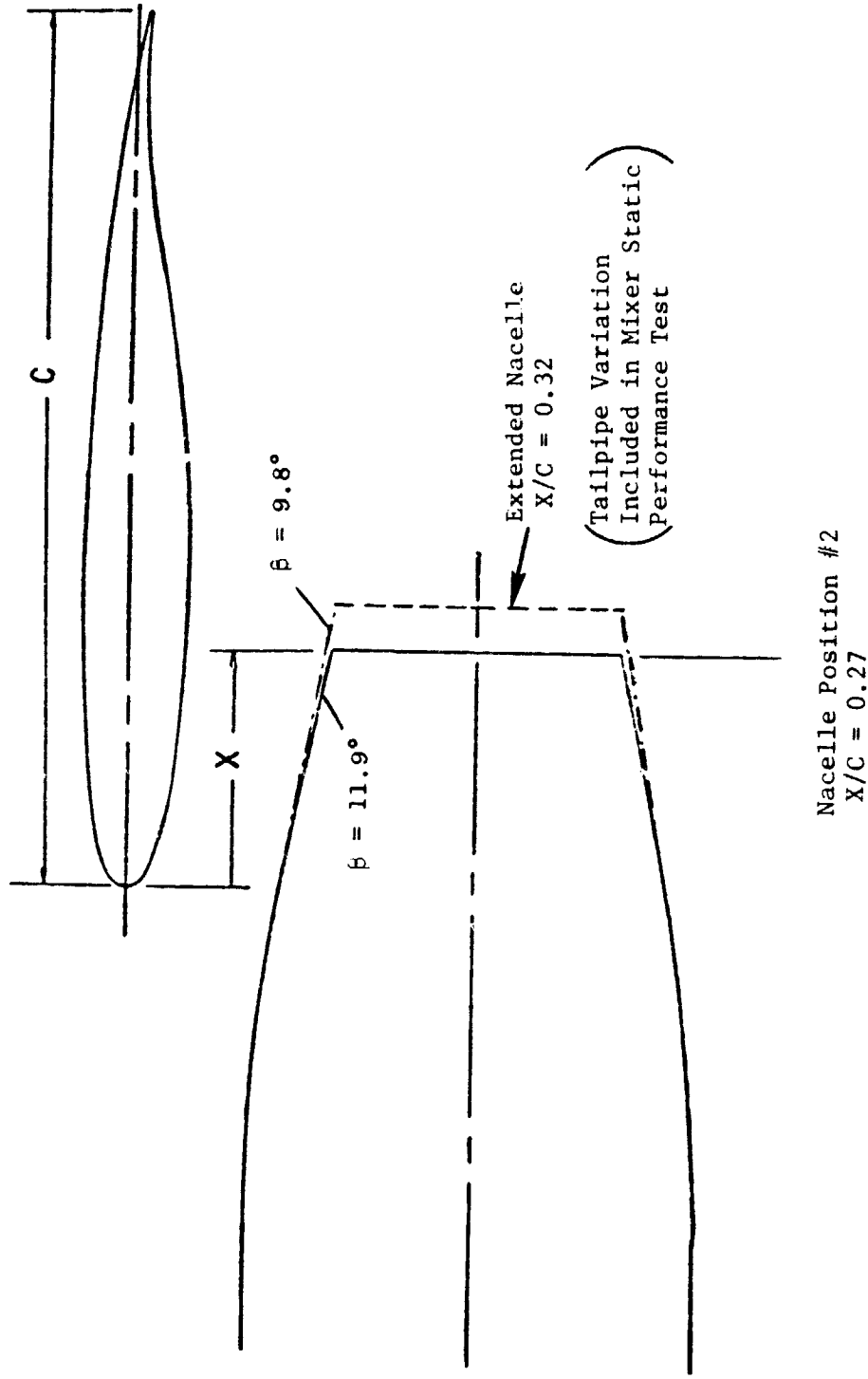


Figure 17. E<sup>3</sup> Tailpipe Variations.

represented one of the tailpipe variations included in the mixer scale model performance tests. All pylons were cambered and individually area ruled by Dr. R.T. Whitcomb of NASA Langley.

Each nacelle configuration was tested on an isolated strut and on the airplane model. Figure 18 conceptually illustrates test results of the two setups which, combined with the basic aircraft test without nacelles (clean wing), allowed an evaluation of aircraft/nacelle installed performance which included the determination of isolated nacelle drag, total nacelle drag, and interference drag. The total nacelle installation drag is presented in Figures 19 and 20 for Phase I and II respectively at the supercritical wing design point of Mach 0.82 and wing lift coefficient,  $C_L$ , of 0.55. Drag is presented in terms of aircraft drag counts where 3.5 counts is equivalent to approximately 1% aircraft drag (or 1%  $F_n$ ) for the Langley model.

Important conclusions resulting from Phase I and Phase II testing are as follows. For each nacelle which was tested in two positions, the forward position gave the lowest drag as expected. The drag difference between forward and rear ranged from as little as 0.5% for the short core nacelle to 4% for the E<sup>3</sup> nacelle. The total installed drag of the long core nacelle is less than the short core nacelle; this is consistent with similar tests conducted on current aircraft applications. The CF6-50 long duct nacelle drag is considerably higher than the two separate flow nacelles. A good portion of this drag increase is due to the significant increase in nacelle surface area and, thus, friction drag. In Phase I the E<sup>3</sup> nacelle in the forward position exhibited the lowest total drag of all configurations tested. In Phase II, however, a repeat run gave a more realistic value for the E<sup>3</sup> drag in the forward position which is slightly higher than the reference -50 long core nacelle. However, the wing design was changed between Phase I and II; more twist was added to the wing and surface recontouring was performed in the vicinity of the nacelles. This modification could have had an adverse effect on the long duct nacelle installed drag. It must be kept in mind that a direct comparison of the E<sup>3</sup> nacelle installed drag with the -50 nacelles is not entirely valid due to different scaling effects. Since one common simulator was used, the two engines could not be scaled by the same amount to give the same full scale thrust on a given wing. The E<sup>3</sup> nacelle would have to

ORIGINAL PAGE IS  
OF POOR QUALITY

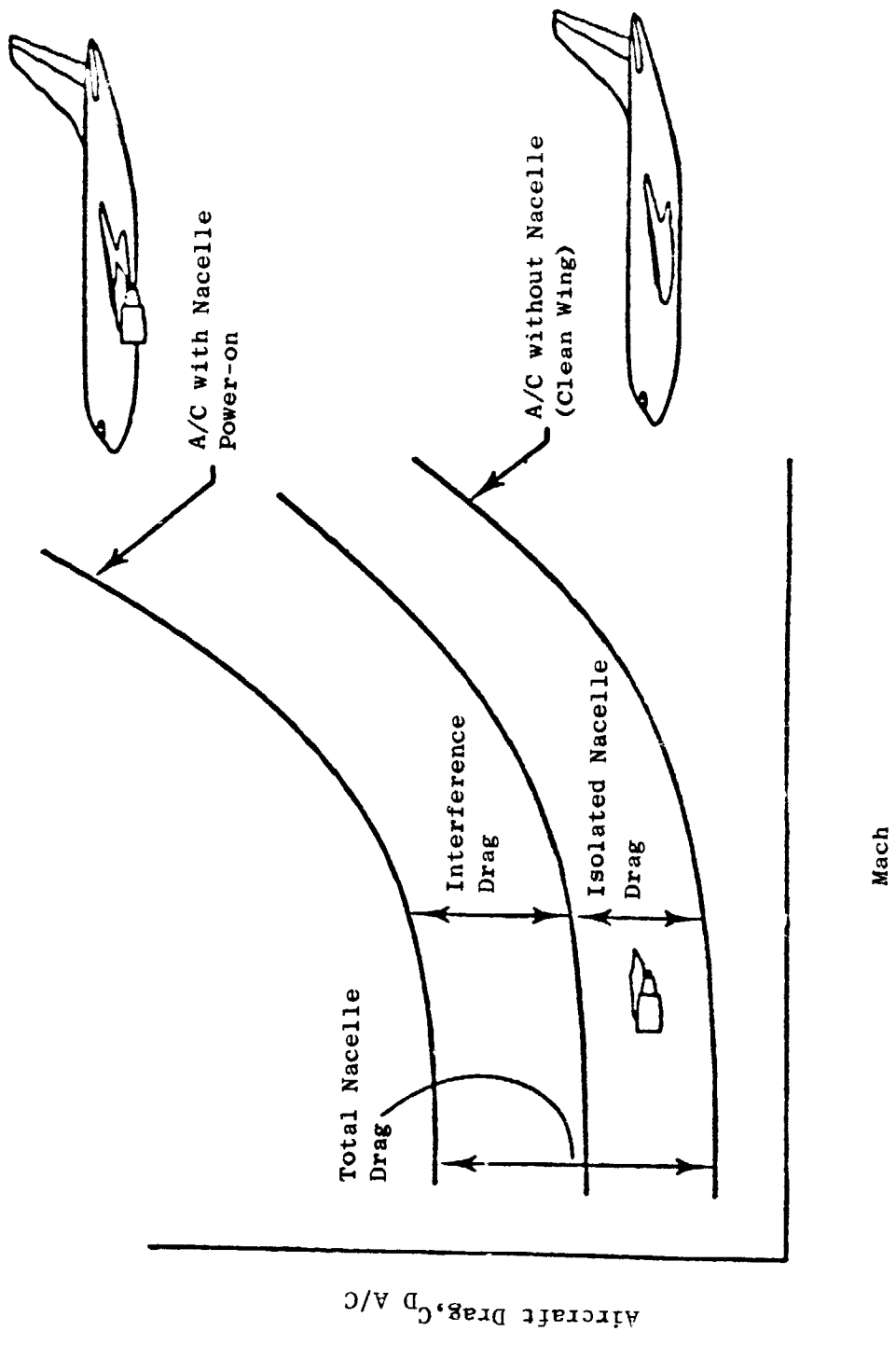
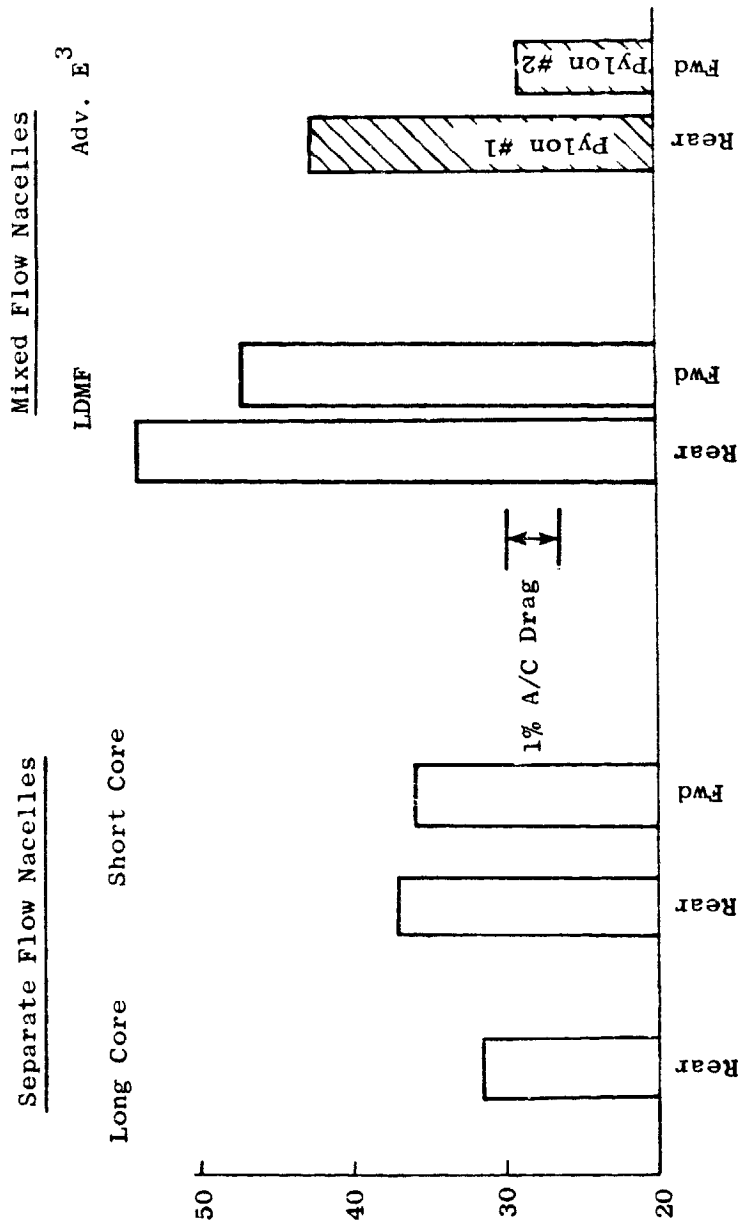


Figure 18. Aircraft/Nacelle Installed Performance.

ORIGINAL PAGE IS  
OF POOR QUALITY

Mach 0.82,  $C_L = 0.55$



$C_D$  Installed -  $C_D$  Wing/Body, Cnts

Installed Nacelle Drag,  $\Delta C_D =$

Figure 19. Nacelle Installation Drag - Phase I.

ORIGINAL PAGE IS  
OF POOR QUALITY

Mach = 0.82,  $C_L = 0.55$

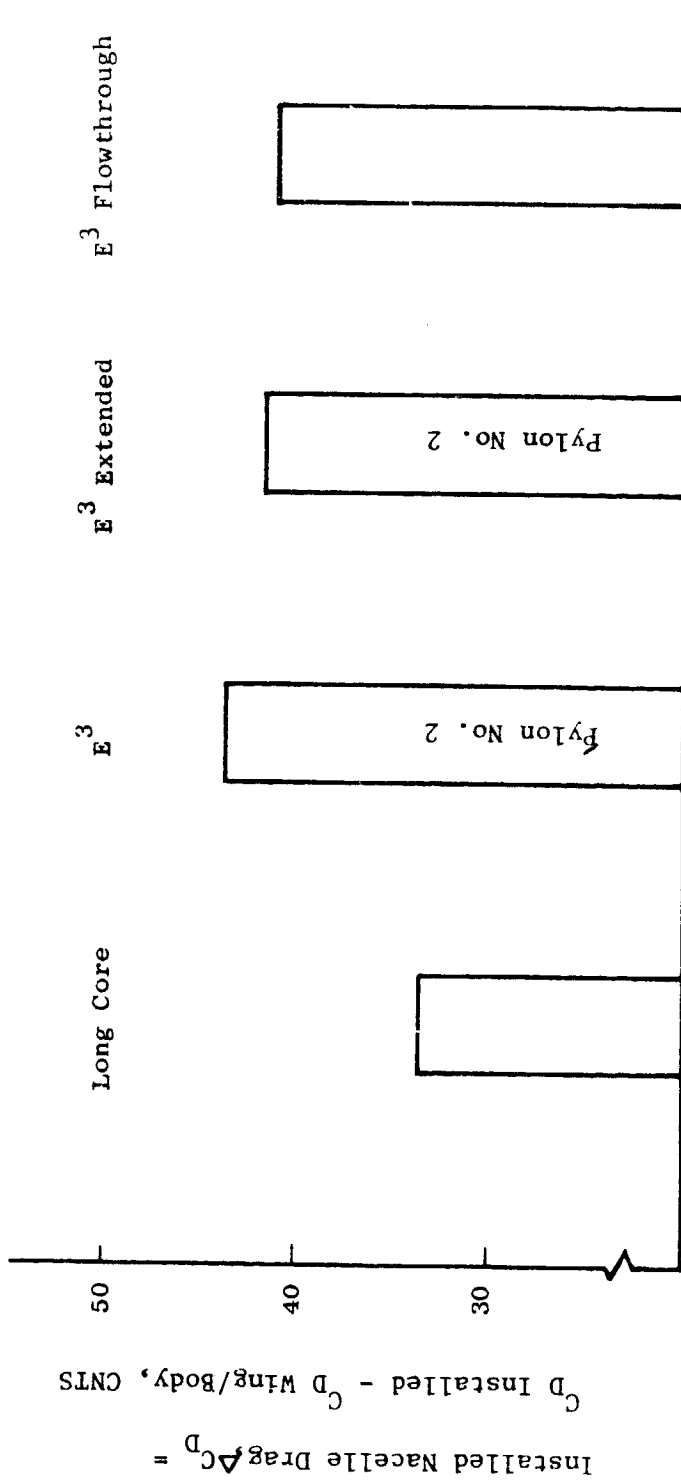


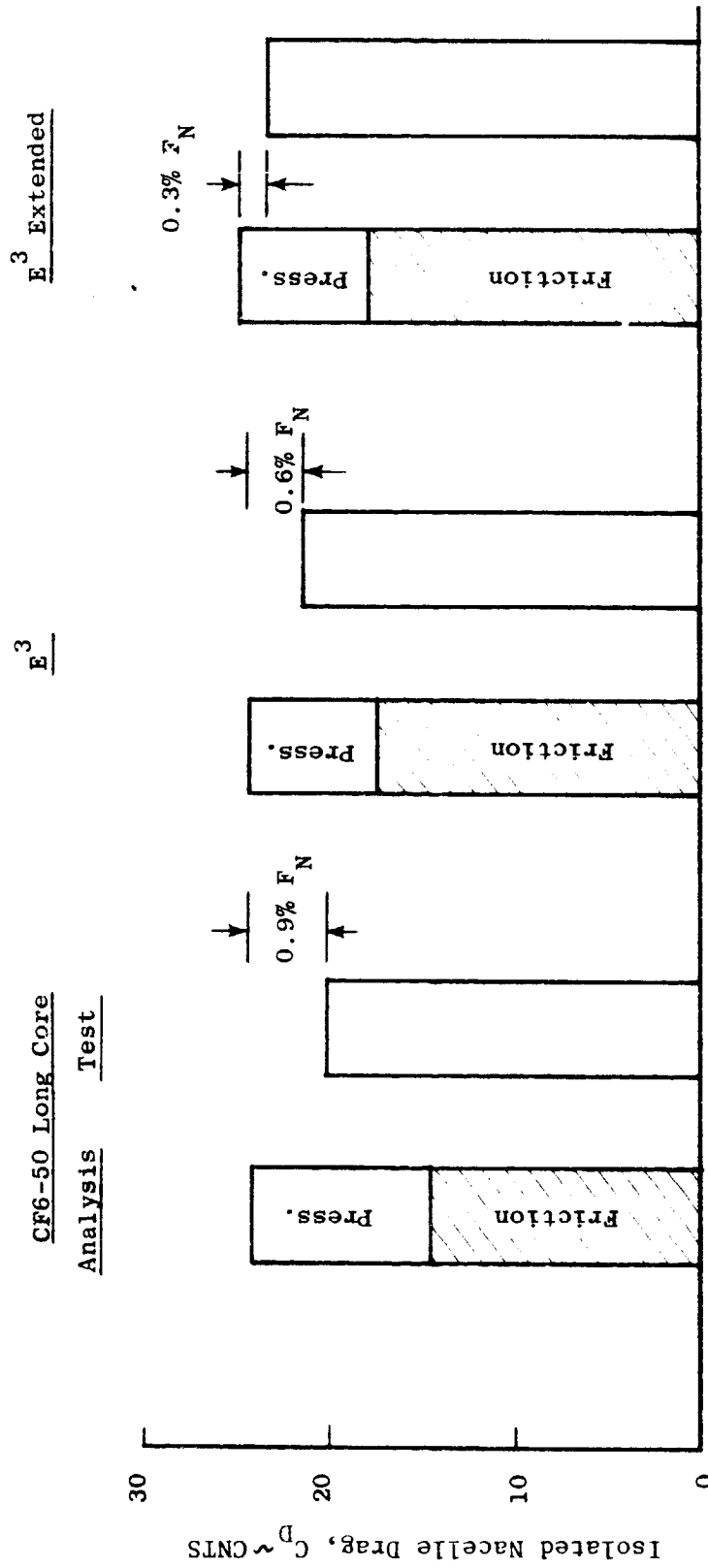
Figure 20. Nacelle Installation Drag - Phase II.

have been approximately 5% larger for a direct E<sup>3</sup> versus -50 cycle comparison. However, the E<sup>3</sup> nacelle technology versus the -50 nacelle technology (long duct, core mounted gearbox, slim line nacelle versus fan mounted gearbox, separate flow nacelle) is a valid direct comparison and results show that the advanced E<sup>3</sup> type long duct nacelle can be installed under an advanced technology wing with comparable total installed drag.

Isolated nacelle drags from Phase II for the CF6-50 long core reference nacelle, the E<sup>3</sup> nacelle, and the E<sup>3</sup> extended nacelle are presented in Figure 21 in terms of aircraft drag counts at Mach 0.82. Two values are presented for the scale models: an analytically derived prediction and the measured test values. For all the nacelles the test results were lower than predicted. If the differences between the analytical and test values were applied to the M 0.8/0.67 km (35,000 ft) max cruise design point for E<sup>3</sup>, the change in net thrust (or sfc) for the CF6-50 reference and the E<sup>3</sup> would be 0.9% and 0.6% respectively.

Nacelle interference drag is presented in Figures 22 and 23 for Phases I and II, respectively, at the supercritical wing design point of M 0.82 and  $C_L = 0.55$ . The interference drag is the difference between the  $\Delta C_D$  of the nacelle installation and the isolated nacelle drag. Since the isolated nacelle drag can be determined experimentally and analytically, two values of interference drag are shown. A test value of interference drag for the CF6-50 LDMF is not shown due to problems encountered in the Phase I isolated test. In fact, the test values of isolated drags for the CF6-50 long core reference and the E<sup>3</sup> nacelles were obtained from Phase II isolated tests, and the CF6-50 short core isolated drag was obtained from tests run at NASA Ames of the exact same nacelle. Again, it is important to note that, because of slightly different scaling factors, the E<sup>3</sup> nacelle interference drag cannot be directly compared with the CF6-50 nacelles. However, as with the total nacelle installation drag, the E<sup>3</sup> technology nacelle is directly comparable, and these results show that the E<sup>3</sup> nacelle can be installed on an advanced technology supercritical wing with interference drag penalties which are comparable to current technology separate flow nacelles. Data analysis is still in progress, and a final report will be issued in 1982.

M = 0.82



ORIGINAL PAGE IS  
OF POOR QUALITY

Figure 21. Isolated Nacelle External Drag - Phase II.



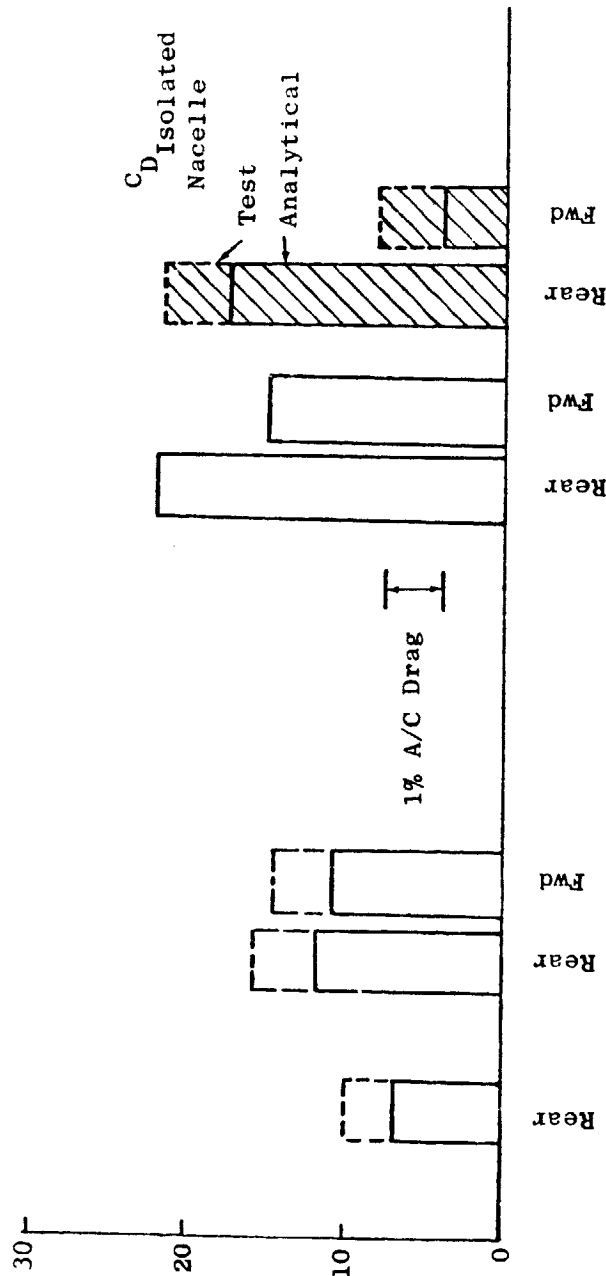
Mach 0.82

$C_L = 0.55$

Separate Flow Nacelles  
 Long Core      Short Core

Mixed Flow Nacelles  
 LDMF      Adv. E<sup>3</sup>

$$\Delta C_D \text{ Interference} = C_D \text{ Installed} - \left( C_D \text{ Clean} + C_D \text{ Wing} \text{ Nacelle} \right), \text{CNTS}$$



Nacelle Interference Drag,

ORIGINAL PAGE IS  
 OF POOR QUALITY

Figure 22. Nacelle Interference Drag - Phase I.

Mach = 0.82  $C_L = 0.55$

Pylon = 0° Engine = -2°

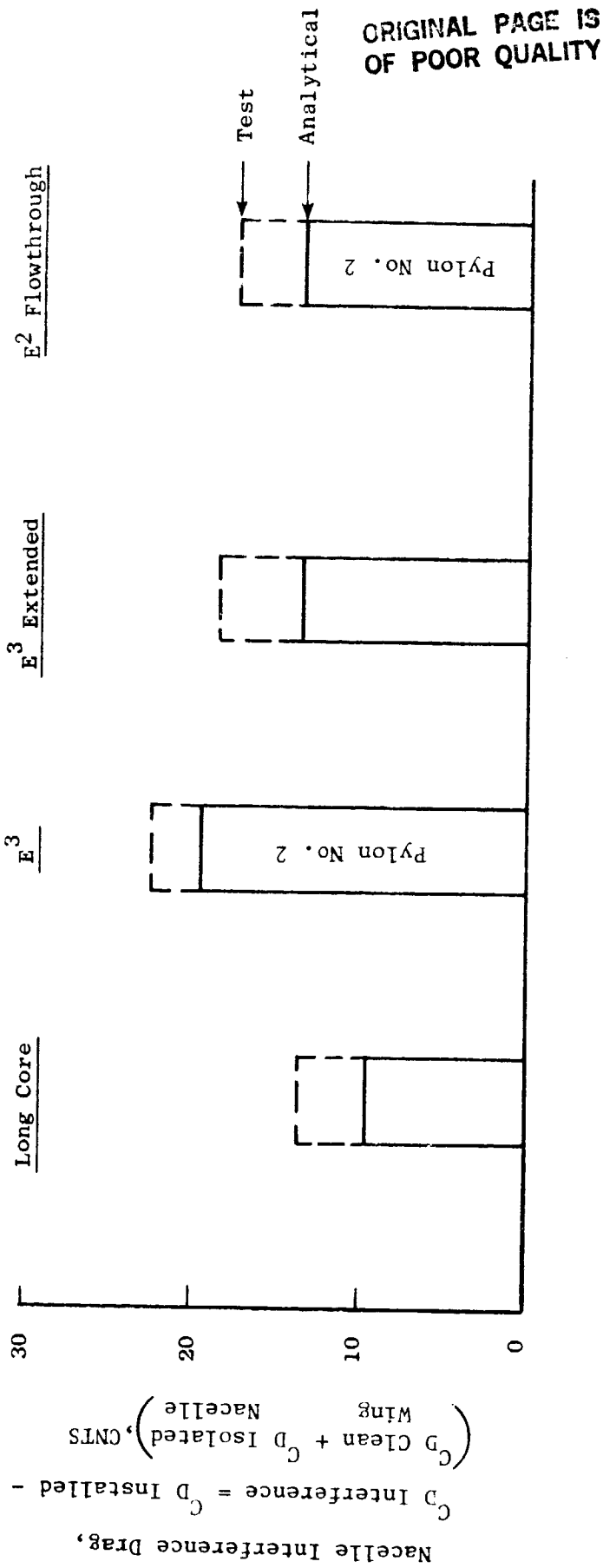


Figure 23. Nacelle Interference Drag - Phase II.

The Langley wind tunnel test results have been very encouraging. The isolated nacelle drag data indicates that the low drag nacelle design intent was achieved. Additionally, the installed test results indicate that the E<sup>3</sup> long duct slim nacelle can be installed under an advanced technology wing with relatively low installation drag penalty.

#### IV COMPONENT DETAIL DESIGN

The objective of the ICLS nacelle mechanical design was to provide slave nacelle hardware for the ICLS test that is functional, reliable, and low cost. The internal flow lines were maintained consistent with the FPS design but no external flow lines were provided; and safety and costs were prime objectives, not weight. The design and analysis of the individual components are discussed below.

A. Aero-Acoustic Inlet - The aero-acoustic inlet (Figure 24) consists of a diffuser section, with a flowpath identical to the undrooped FPS inlet, and a bellmouth/lip structure to provide uniform flow acceleration. The estimated static pressure distribution for the inlet is shown in Figure 25. Based on this pressure curve, the maximum  $\Delta P$  across the wall was determined. The loads thus produced were compared to the structures allowable loads and the margins of safety were determined as shown in Table XII. Since the inlet is supported from the facility instead of the engine it was necessary to calculate the net axial loading on the inlet for incorporation into the overall engine thrust balance used to obtain the mount loads. The results of this analysis are shown in Figure 26.

The inlet bellmouth is a one-piece separable assembly with the basic design features shown in Table XIII. The materials used in the construction of the bellmouth are also listed in Table XIII and a cross section is shown in Figure 27. Details of the lip assembly and diffuser interface assembly are shown in Figures 28 and 29.

The inlet diffuser is primarily a fiber glass face sheet/honeycomb core structure with integrated acoustic treatment. The basic design features and materials are listed in Table XIV. A cross section of the diffuser, showing the basic construction features is shown in Figure 30. In order to reduce tooling costs, the diffuser is made in nine circumferential sections as shown in Figure 31. The method of connecting these sections is shown in Figure 32. The attachment of the diffuser to the bellmouth and to the facility interface ring is shown in Figure 33. The inlet has a soft seal at its interface with

ORIGINAL PAGE IS  
OF POOR QUALITY

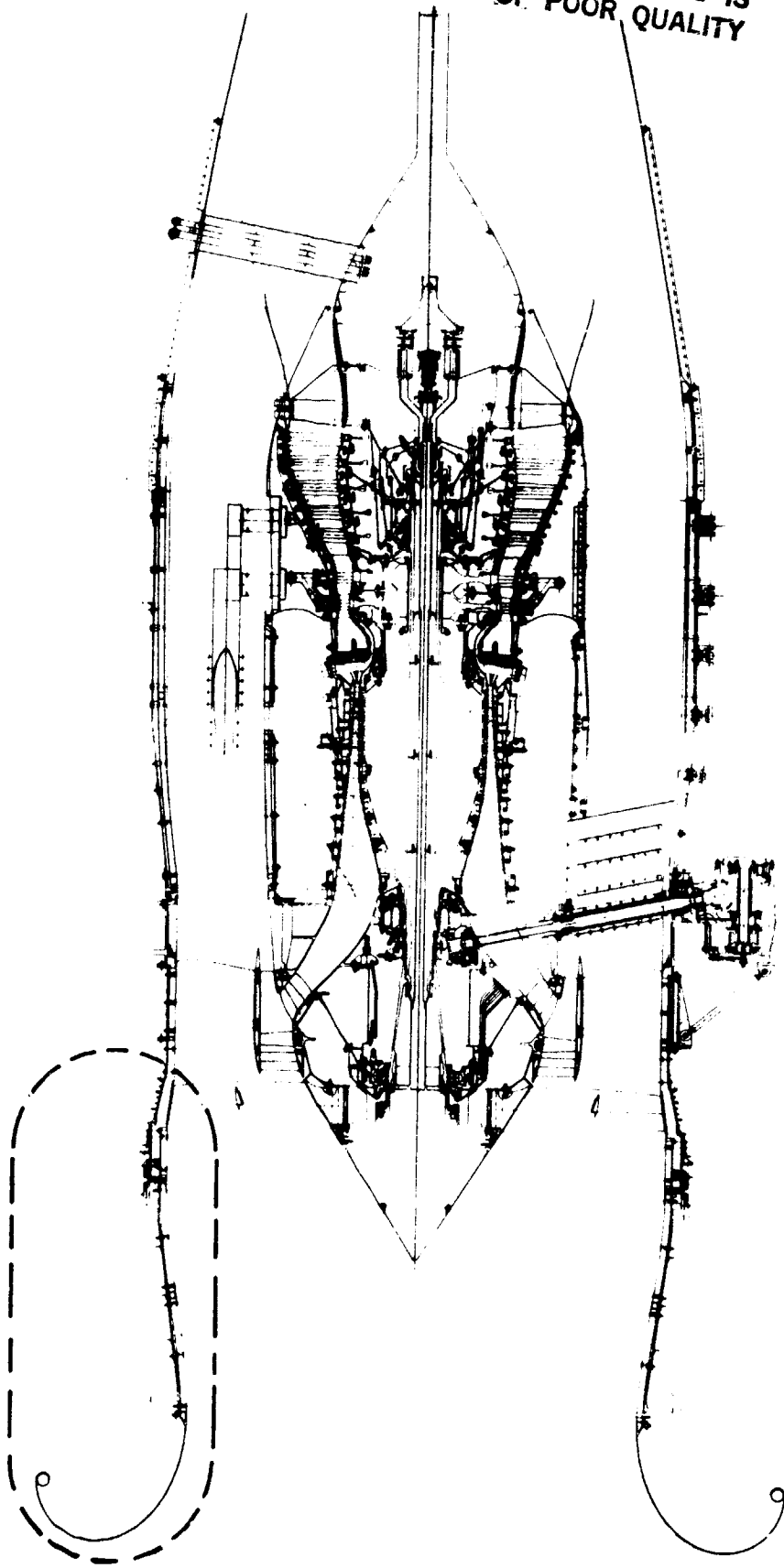


Figure 24. Aero-Acoustic Inlet.

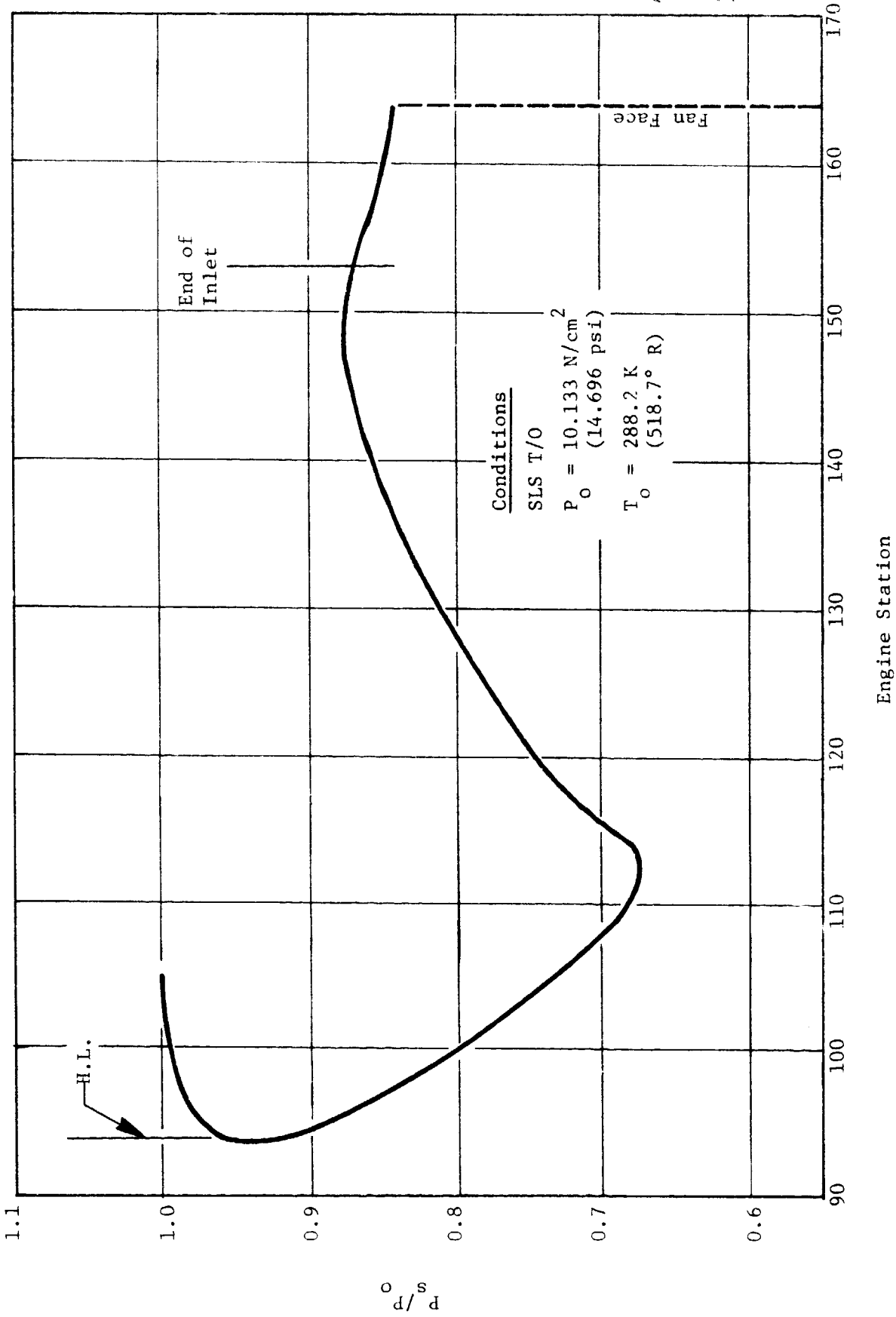
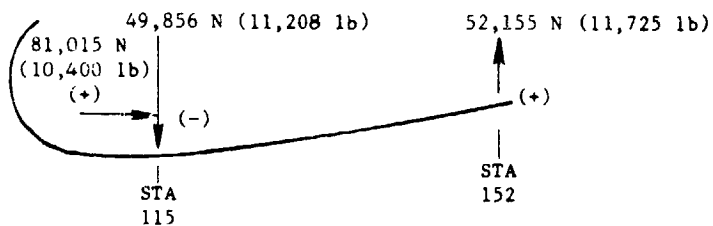


Figure 25. ICLS Aero-Acoustic Bellmouth Estimated Static Pressure Distribution.

ORIGINAL PAGE IS  
OF POOR QUALITY

Table XII. Inlet Stresses.

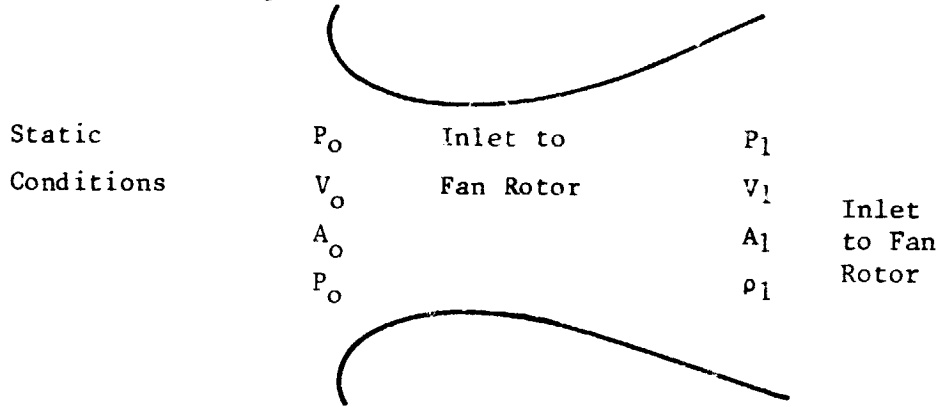
- Max Temperature Environment
  - $T_{max} = 323.1 \text{ K (121.7}^\circ \text{ F)}$   
(SLS Hot Day T/O:  $M_o = 0$ ;  $\Delta T = 63$ )  
 $\Delta T = 35 \text{ K (63}^\circ \text{ F)}$
- Loading
  - Max  $\Delta P$  (External Loading) Across Structure  
 $\Delta P = 3.48 \text{ N/cm}^2 \text{ (5 psi)}$ 
    - Hoop Stress  
 $\sigma_{Hoop} = 1166 \text{ N/cm}^2 \text{ (1692 psi); MS = 16.1}$
    - Meridional Stress  
 $\sigma_M = 585 \text{ N/cm}^2 \text{ (846 psi); MS = 33.1}$
    - Critical Buckling Pressure
      - Material: NARMCO 3203;  
 $E = 2,378,691 \text{ N/cm}^2 \text{ (3.45 x 10}^6 \text{ psi)}$   
 $\mu = 0.14$   
 $F_{tu} = 39.989 \text{ N/cm}^2 \text{ (58,000 psi)}$
    - $P_{CR}^i = 18.1 \text{ N/cm}^2 \text{ (26.2 psi); MS = 2.5}$
- Resultant Loading



- STA 115
  - Bolt Loads
    - Shear Load  
 $P_s = 1219 \text{ N (274 lb)/Bolt}$
    - Tension Load  
 $P_{ten} = 1130 \text{ N (254 lb)/Bolt}$
- STA 152
  - Bolt Load  
 $P = 5218 \text{ N (1173 lb)/Bolt; MS = 1.8}$

ORIGINAL PAGE IS  
OF POOR QUALITY

• Net Axial Loading



$$A_0 = 28484 \text{ cm}^2 (4415 \text{ in.}^2)$$

$$A_1 = 34910 \text{ cm}^2 (5411 \text{ in.}^2)$$

(-)

(+)

(-)

$F_{net} \Rightarrow$  Rate of Change of Linear Momentum + Pressure/Area Change

$$F_{net} = (\dot{m}V_0 + P_0 A_0) - (\dot{m}V_1 + P_1 A_1) - P_0 (A_0 - A_1)$$

or (-)

$$F_{net} = \dot{M} (V_1 - V_0) - A_1 (P_0 - P_1)$$

$$\dot{M}_{max} = 600 \text{ kg/sec (4% Adder for Pressure and Temperature Variations Due to Overspeed)}$$

$$600 \text{ kg/sec (1322 lb/sec)}$$

(-)

$$F_{net} = 46,261 \text{ N (10,400 lb)}$$

Figure 26. Inlet Axial Load.



Table XIII. Bellmouth Lip.

Basic Design Features

- 1-Piece Separable Assy
- Supported from Inlet Diffuser by Mounting Flange
- Ring Lip Stiffened by Circular Metal Tubing
- Composite Bellmouth Walls
- No Acoustic Treatment

Materials

- Lip Support Tube - 1018 Steel
- Interface Mounting Flange - 6061-T651 Al Alloy
- Flexcore - 5052 Al
- Face Sheets - 3203/1581 Cloth Prepreg Fiber Glass
- Attach Fasteners - AN4 Bolts

ORIGINAL PAGE IS  
OF POOR QUALITY

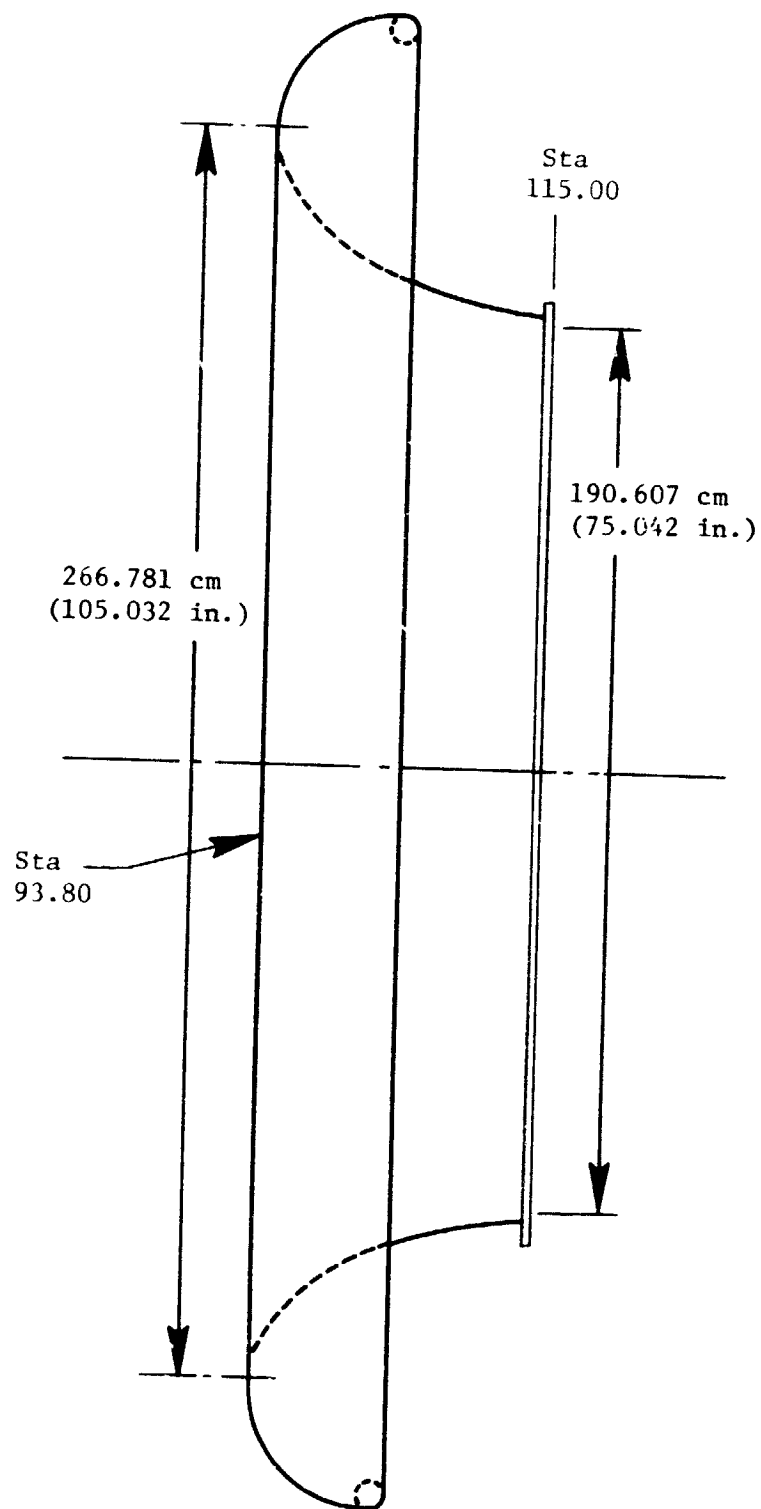


Figure 27. Inlet Bellmouth Assembly.

ORIGINAL PAGE IS  
OF POOR QUALITY

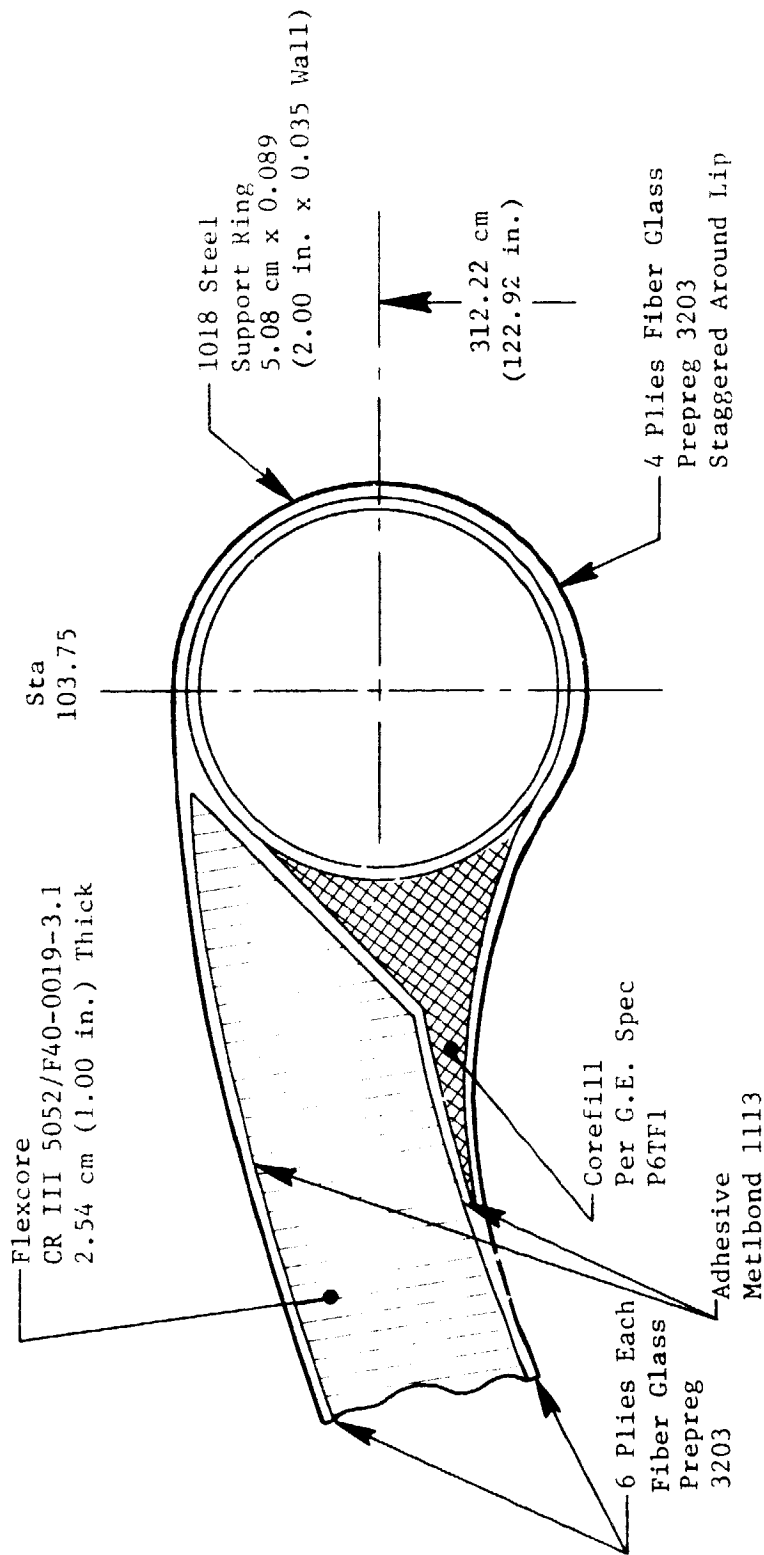


Figure 28. Inlet Lip Assembly.

ORIGINAL PAGE IS  
OF POOR QUALITY

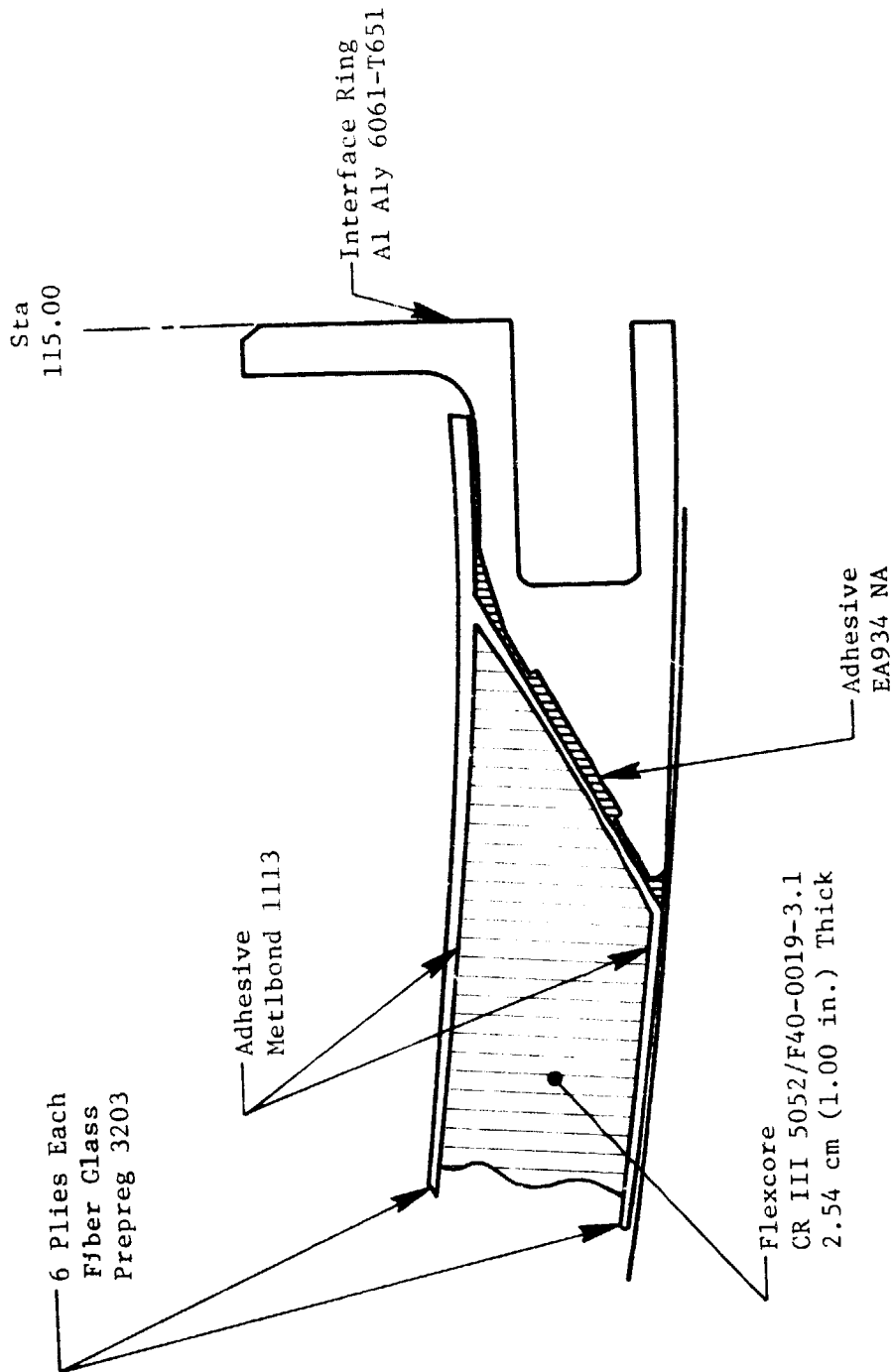


Figure 29. Bellmouth Interface Ring Assembly.

Table XIV. Inlet Diffuser.

Basic Design Features

- Supported From Facility
- Soft Seal Interface to Fan Casing
- Integral Acoustic Treatment
- Integral Acoustic/Structural Panels
  - Nine Panels Circumferential, Mounted to Interface Rings at Each End
  - Panels are Bolted together Longitudinally Along Sides

Materials

- Perforated Face Sheet - 6061-T4 Al Alloy
- Interface Rings - 6061-T651 Al Alloy
- Support Structures - 3203 Prepreg Fiber Glass
- Flex Core - 5052 Al Alloy
- Acoustic Treatment - Kevlar 29 Felt
- Facility Interface Rings - 1018 Steel

ORIGINAL PAGE IS  
OF POOR QUALITY

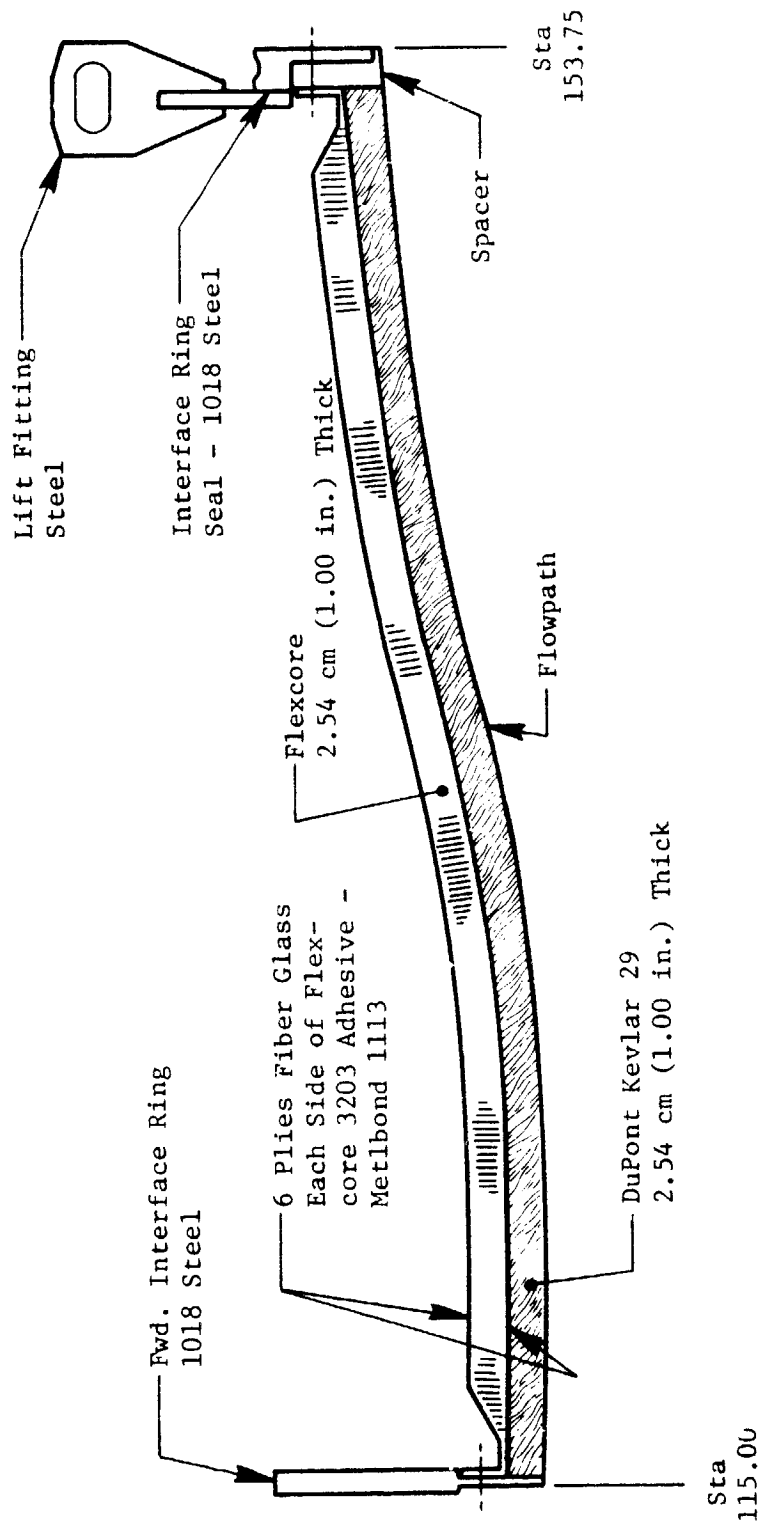


Figure 30. Inlet Diffuser Assembly.

ORIGINAL PAGE IS  
OF POOR QUALITY

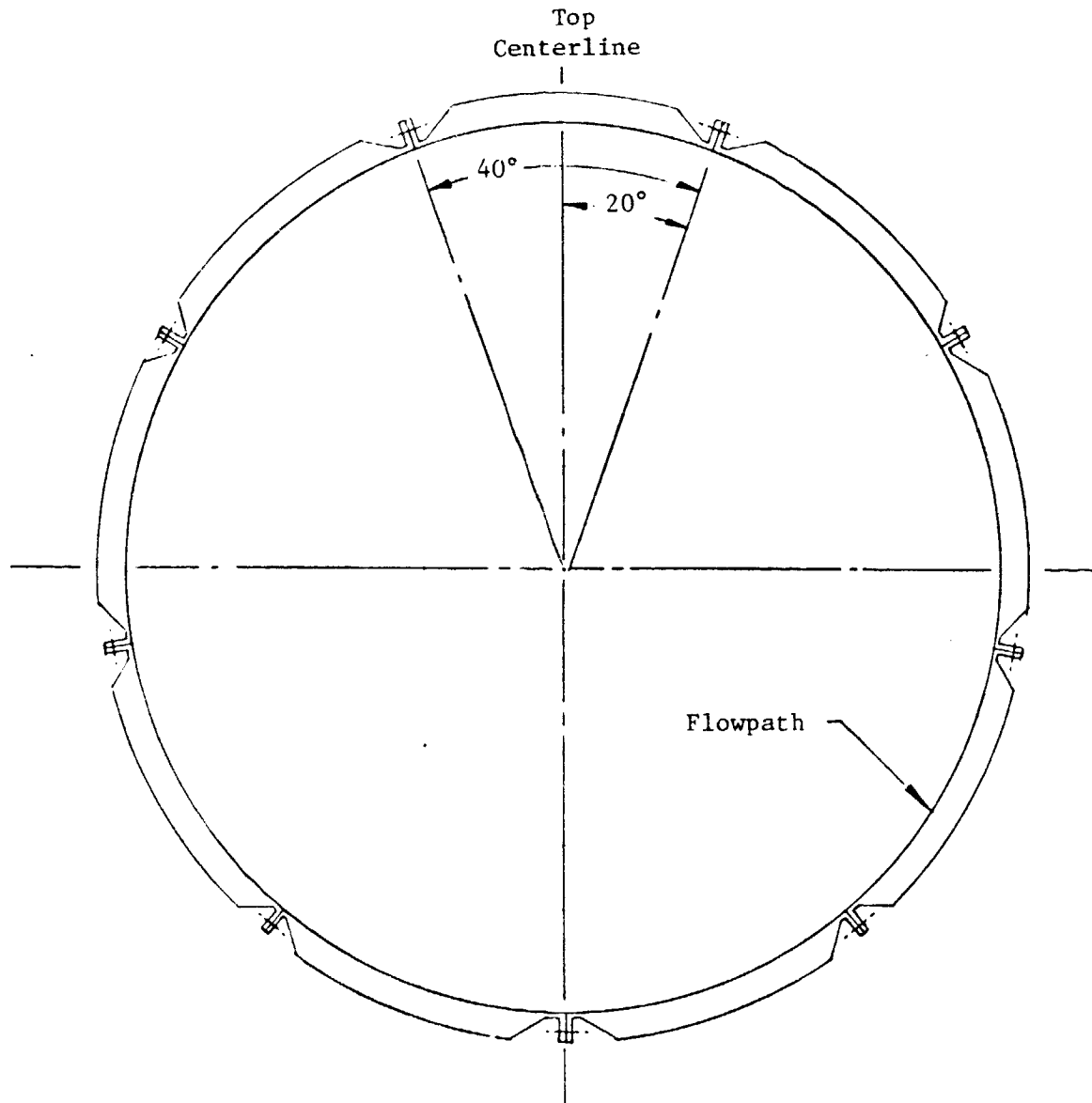


Figure 31. Inlet Diffuser Assembly (9 Panels Total).

ORIGINAL PAGE IS  
OF POOR QUALITY

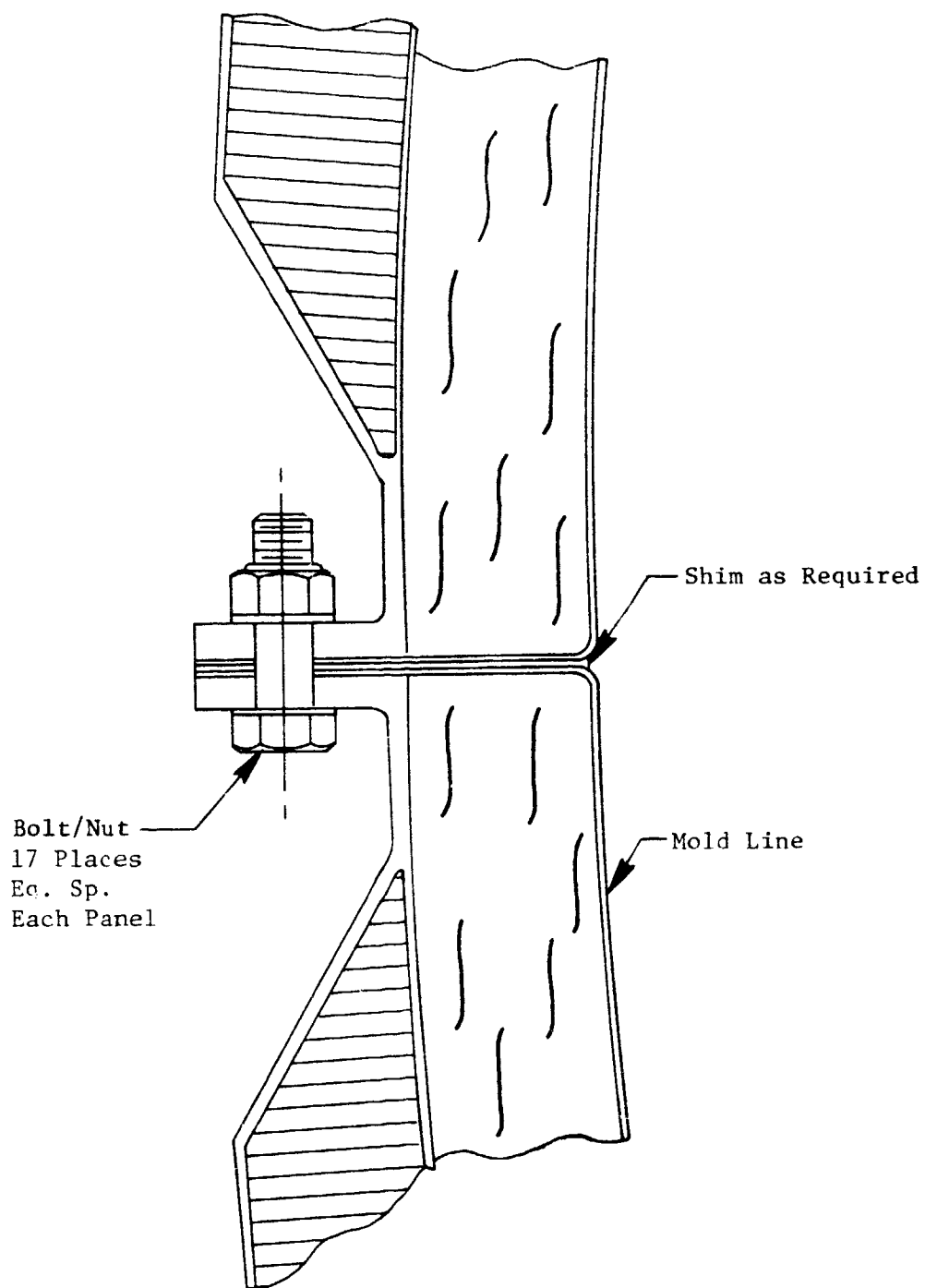


Figure 32. Typical Diffuser Panel Connection (9 Panels Total).



ORIGINAL PAGE IS  
OF POOR QUALITY

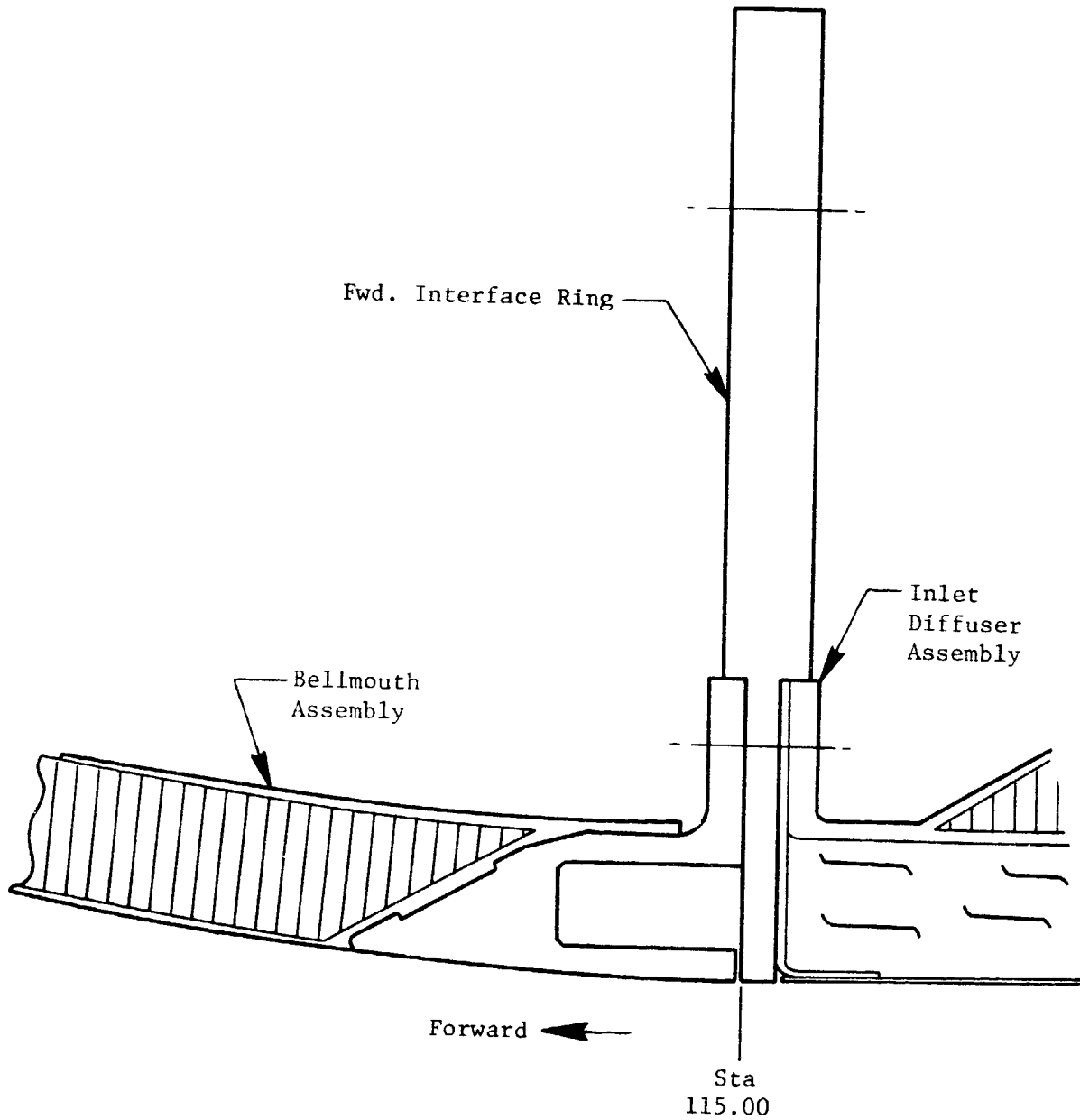


Figure 33. Interface Bellmouth to Diffuser.

the fan casing. This seal must be able to absorb a relatively large differential deflection since the two structures are not physically attached. This seal is shown in Figure 34.

B. Core Cowl - The core cowl is located as shown in Figure 35. It consists of two doors which are hinged to a floating apron structure at the top and latched at the bottom. The static pressure distribution in the fan stream is shown in Figures 36 and 37. The skin stress and margins of safety for the cowl doors and apron structure are shown in Table XV. The analysis of the latch and hinge loads is given in Table XVI. As can be seen from these figures, adequate margins of safety exist for the core cowl structure.

The basic design features and the materials of the core cowl doors are shown in Table XVII. The primary structure of the core cowl is shown in Figures 38 and 39. It consists primarily of a steel structural shell to which are attached acoustic panels which form the flowpath. Even though the ICLS will utilize a fan mounted gearbox, the expanded flow lines in the lower portion of the core cowl necessary to accommodate a core mounted gearbox were incorporated in the ICLS design. The stiffeners used to form this expansion in the flow lines are fastened with corner tie plates as shown in Figure 40. The forward flange contains a tongue, Figure 41, which engages a groove in the fan frame to provide an axial load path for the core cowl. The aft end of the cowl, Figure 42, provides a slip joint on the aft cowling.

The door is latched together at the bottom centerline as shown in Figure 43. At the forward edge, the doors are latched to the fan frame to provide circumferential continuity in the area of the ICLS lower pylon. A detail view of a typical latch installation is shown in Figure 44. The doors are hinged from, and sealed to, the apron structure at four axial locations. A typical hinge is shown in Figure 45 and the seal is shown in Figure 46. The acoustic panels are attached to the basic structure through stand-offs as shown in Figure 47.

C. Fan Cowl - The fan cowl is located as shown in Figure 48. It consists of two doors which are hinged to the facility engine mount beam structure at the top and latched together at the bottom. For the ICLS these doors do not contain the reverser structure that would be included in an FPS design. The

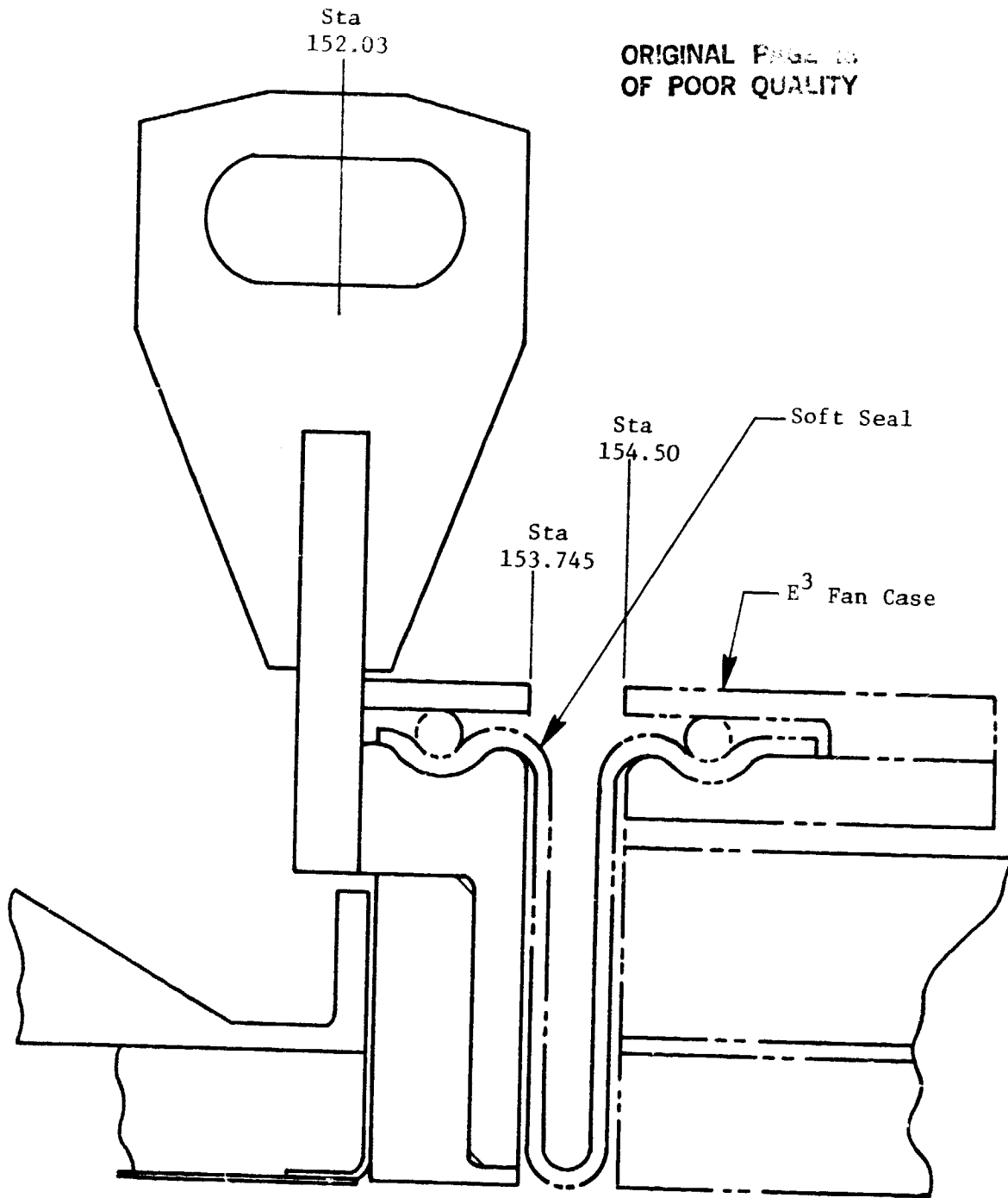
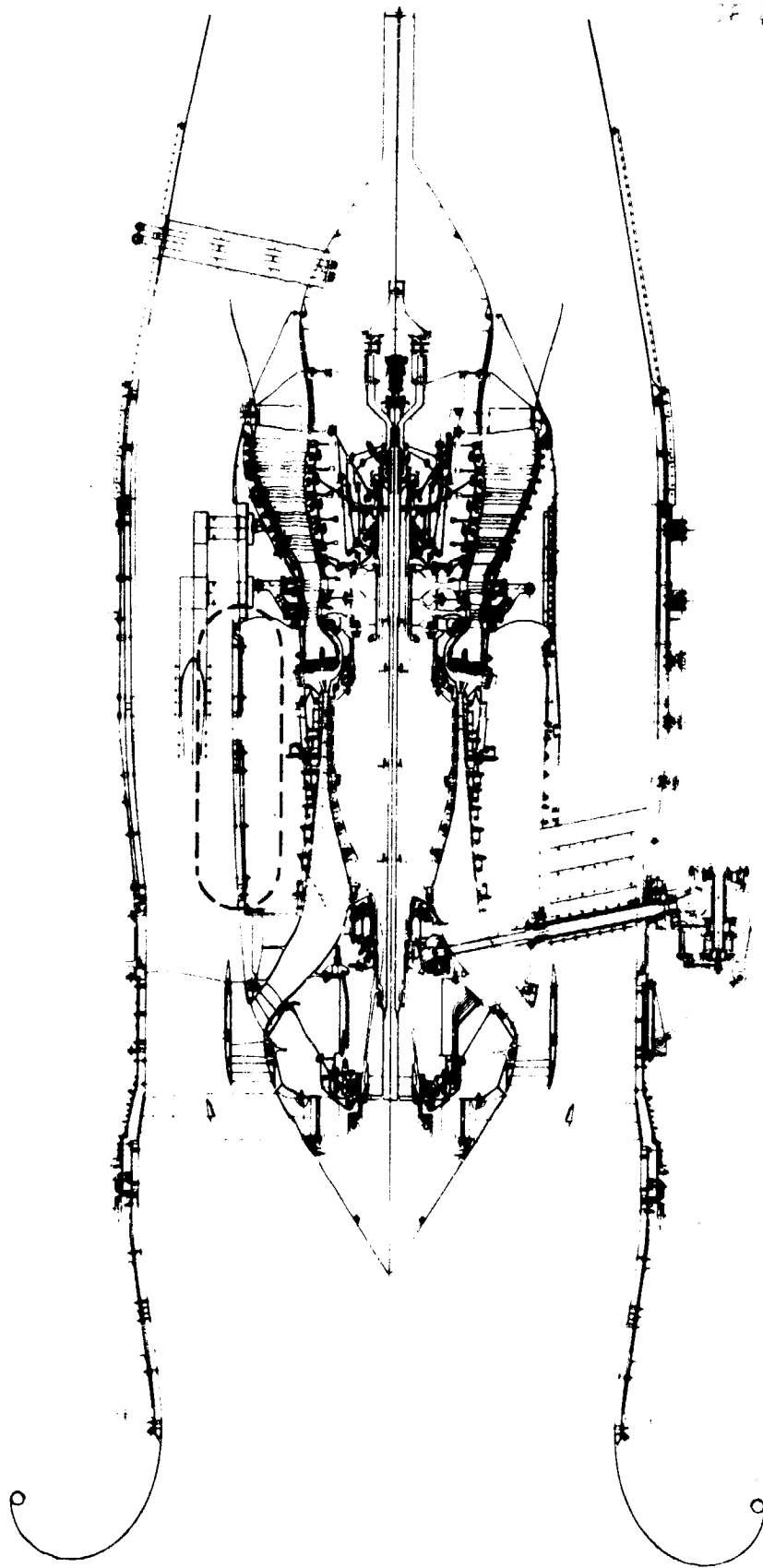


Figure 34. Interface Diffuser to E<sup>3</sup> Fan Case.



CONSTRUCTION  
OF POOL COWLING

Figure 35. Core Cowl.

ORIGINAL PAGE IS  
OF POOR QUALITY

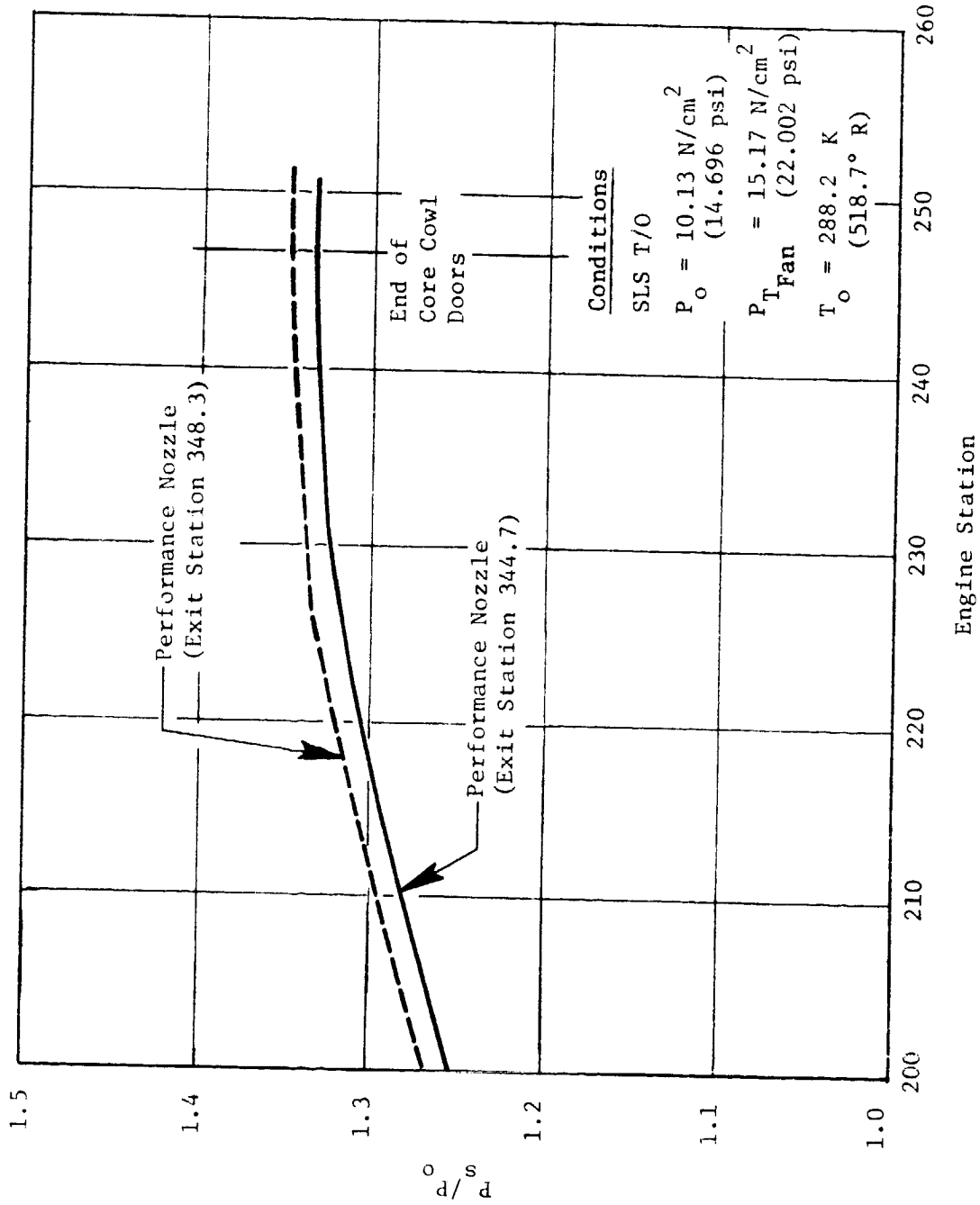


Figure 36. ICLS Core Cowl Door - Estimated Static Pressure Distribution.

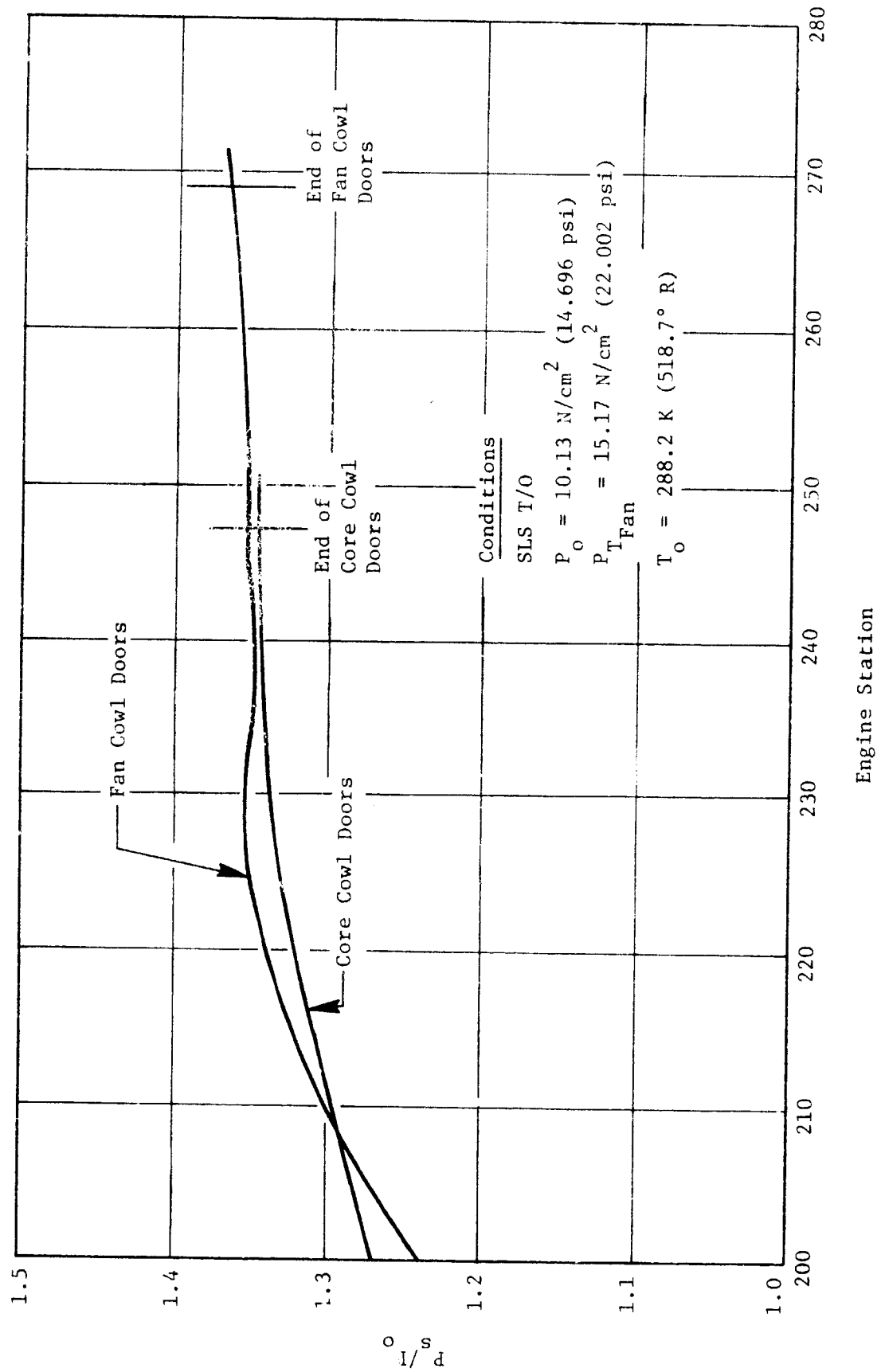


Figure 37. ICLS Cowl Doors Estimated Max Static Pressure Distribution (Performance Nozzle Exit Station 348.3).

ORIGINAL PAGE IS  
OF POOR QUALITY

Table XV. Core Cowl Doors and Inner Apron.

- Max Temperature Environment
  - Tmax (Outer Surface) = 327.3 K (129.4° F)  
(SLS Hot Day T/O; Mo = 0; ΔT = 35 K (63° F))
  - Tmax (Inner Surface) = 561 K (550° F) ~ Assumed
- Loading
  - Max ΔP (Internal Loading) Across Door Structure  
ΔP = 2.06 N/cm<sup>2</sup> (3 psi)
    - Hoop Stress  
σ = 269 N/cm<sup>2</sup> (390 psi); MS = 209
    - Meridional Stress  
σ<sub>m</sub> = 134.4 N/cm<sup>2</sup> (195 psi); MS = 419
  - Max ΔP (Internal Loading) Across Inner Apron Structure  
ΔP = 5.17 N/cm<sup>2</sup> (7.5 psi)
    - Max Bending Stress in Panel  
σ<sub>max</sub> = 18,088 N/cm<sup>2</sup> (26,234 psi); MS = 2.1

Table XVI. Core Cowl Doors and Inner Apron Attach Loads.

- Latch Loads

<u>Latch No.</u>	<u>Max Load N/cm (lbs)</u>	<u>Safety Margin</u>
1-2	1334 (300/Latch)	14.5/Latch
3	4973 (1118)	3.17
4	4848 (1090)	3.28
5	3527 (793)	4.88

- Hinge Loads

<u>Hinge No.</u>	<u>Max Load (lbs)</u>	<u>Safety Margin</u>
1	2976 (669)	14.3
2	4732 (1064)	8.65
3	4732 (1064)	8.65
4	2976 (669)	14.3

Table XVII. Core Cowl Door.

Basic Design Features

Inner Shell

- Supported From Apron
- Basic Flow Path is Elliptical in Cross Section, Composed of a Different Radius at Top and Bottom Joined by Tangent Lines
- Machined Tongue and Groove Front Flange - Incorporates a Portion of the Forward Latch
- Machined Slip Joint Rear Flange - Incorporates the Aft Latch
- 4 Hinges With Uniballs Attached to Upper Longerons
- 4 Latches at Lower Split Line With Alignment Pins
- Metallic Finger Seal at Door Hinge Split Line
- Inner Shell Houses the Panels, Lower Segment is Not Symmetrical With Upper Segment

Acoustic Panels

- Solid Back Skin, Perforated Face Sheet 30% Open
- Rolled "C" Section End Rings
- Formed Solid Longerons Ribs
- Panels are 80° Segments With 4 Ribs Equally Spaced
- 2 Forward Panels and 2 Aft Panels Per Door
- Mounted to the Inner Shell by Special Inserts, Bolted to Stand Offs That are Welded to the Inner Shell

Materials

Inner Shell

- Flanges, Longerons, Alignment Pins, and Hard Wall - 321 Stainless Steel
- Hinges - 17-4PH (HT-TR H1050)
- Bulb Seal - Hercules 7701 (HAVEG IND.) Etched Teflon With Inconel Wire Mesh Embedded in Fluorocarbon Rubber

Acoustic Panels

- 0.1016 cm (0.040 in.) Thick Aluminum Outer Sheet - Perforated 6061-T6
- Acoustic Treatment - Kevlar 29 Felt
- Support Structure 6061-T6
- 0.1016 cm (0.040 in.) Thick 6061-T6 Aluminum Backup Sheet



ORIGINAL FILED BY  
OF POOR QUALITY

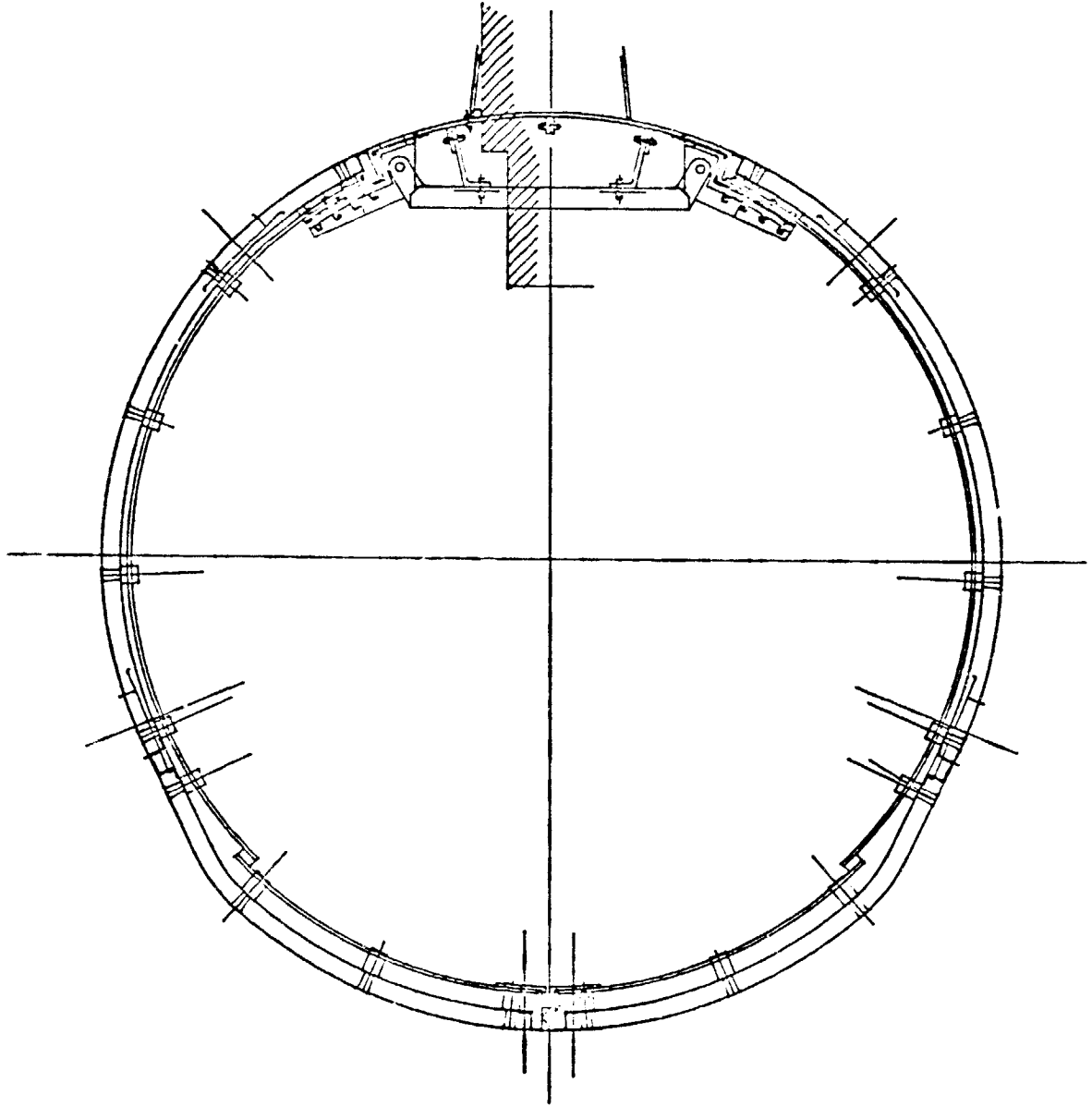


Figure 38. Inner Cowl Doors.

ORIGINAL PRICE 18  
 12 POOR QUALITY

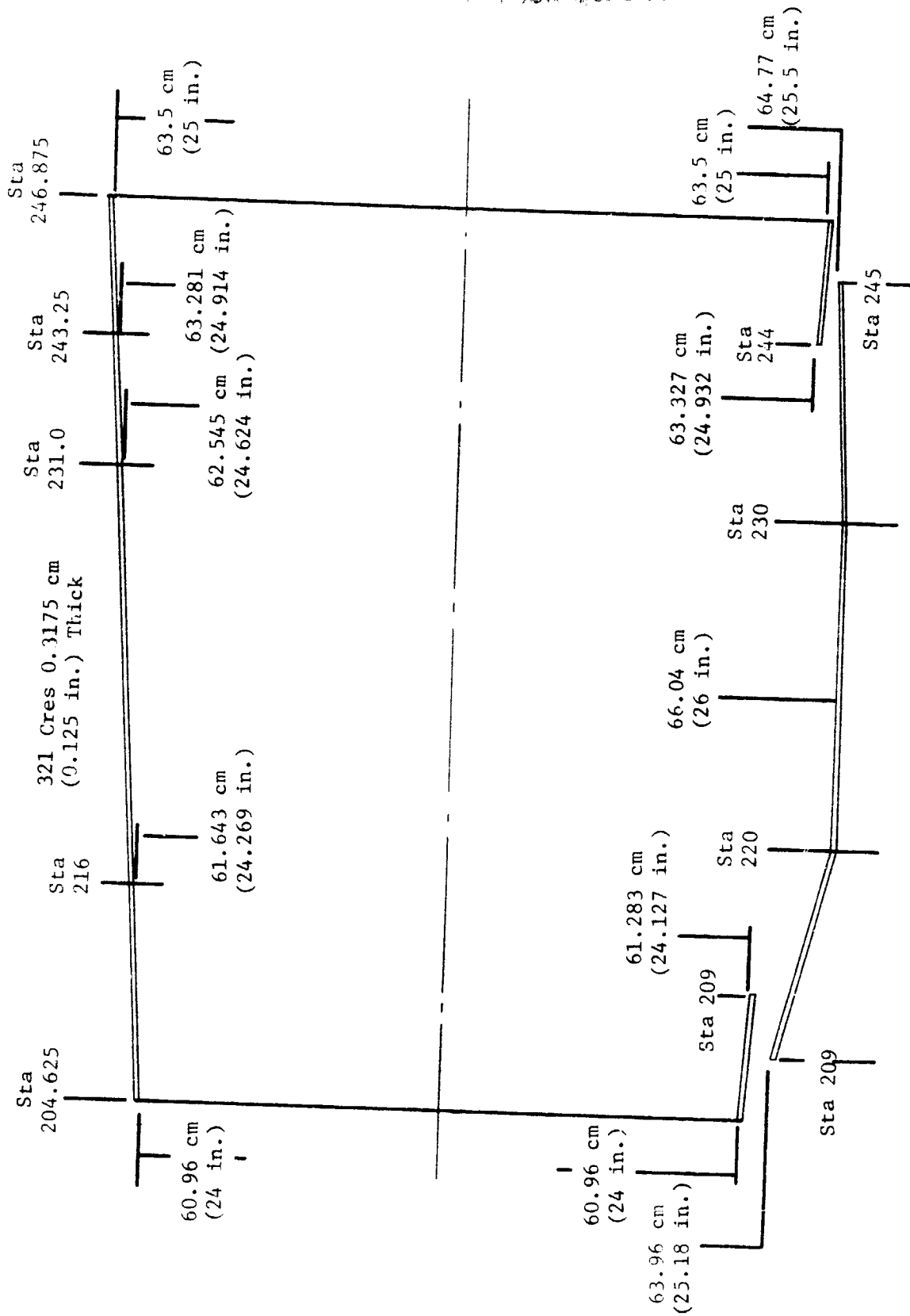


Figure 39. Cowl Door Structure.

ORIGINAL PAGE IS  
OF POOR QUALITY

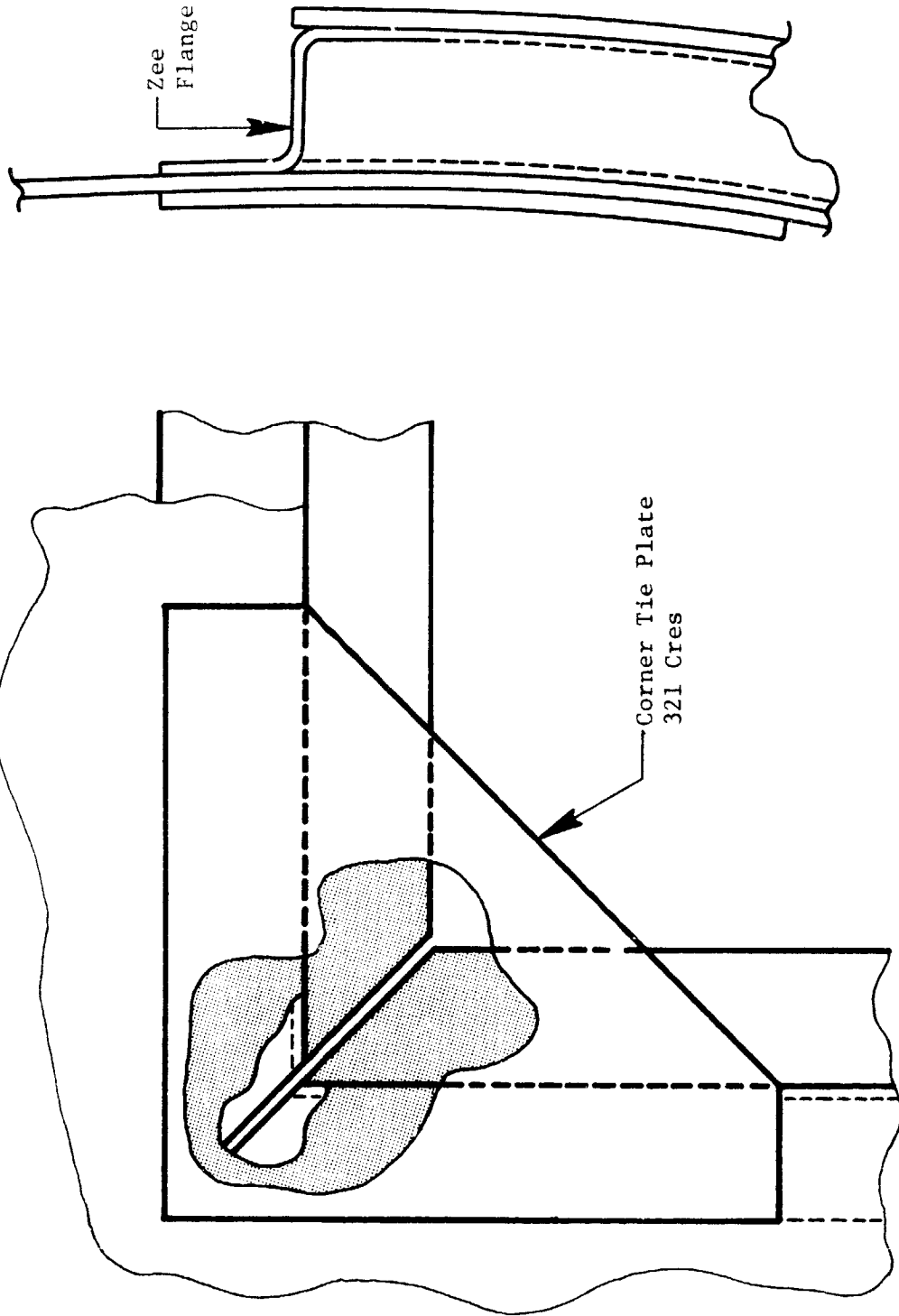


Figure 40. Zee Flanges.

ORIGINAL PAGE IS  
OF POOR QUALITY

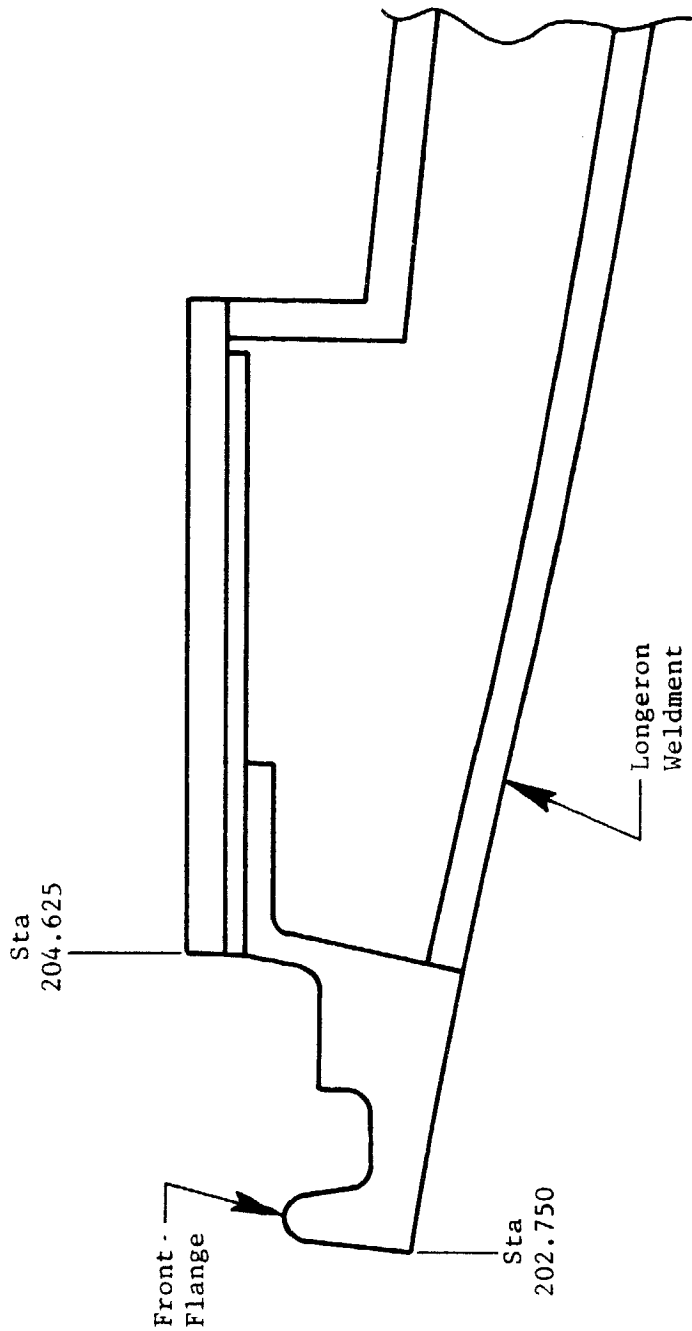


Figure 41. Front Flange.

ORIGINAL PAINTED  
CE. FOR C. 17

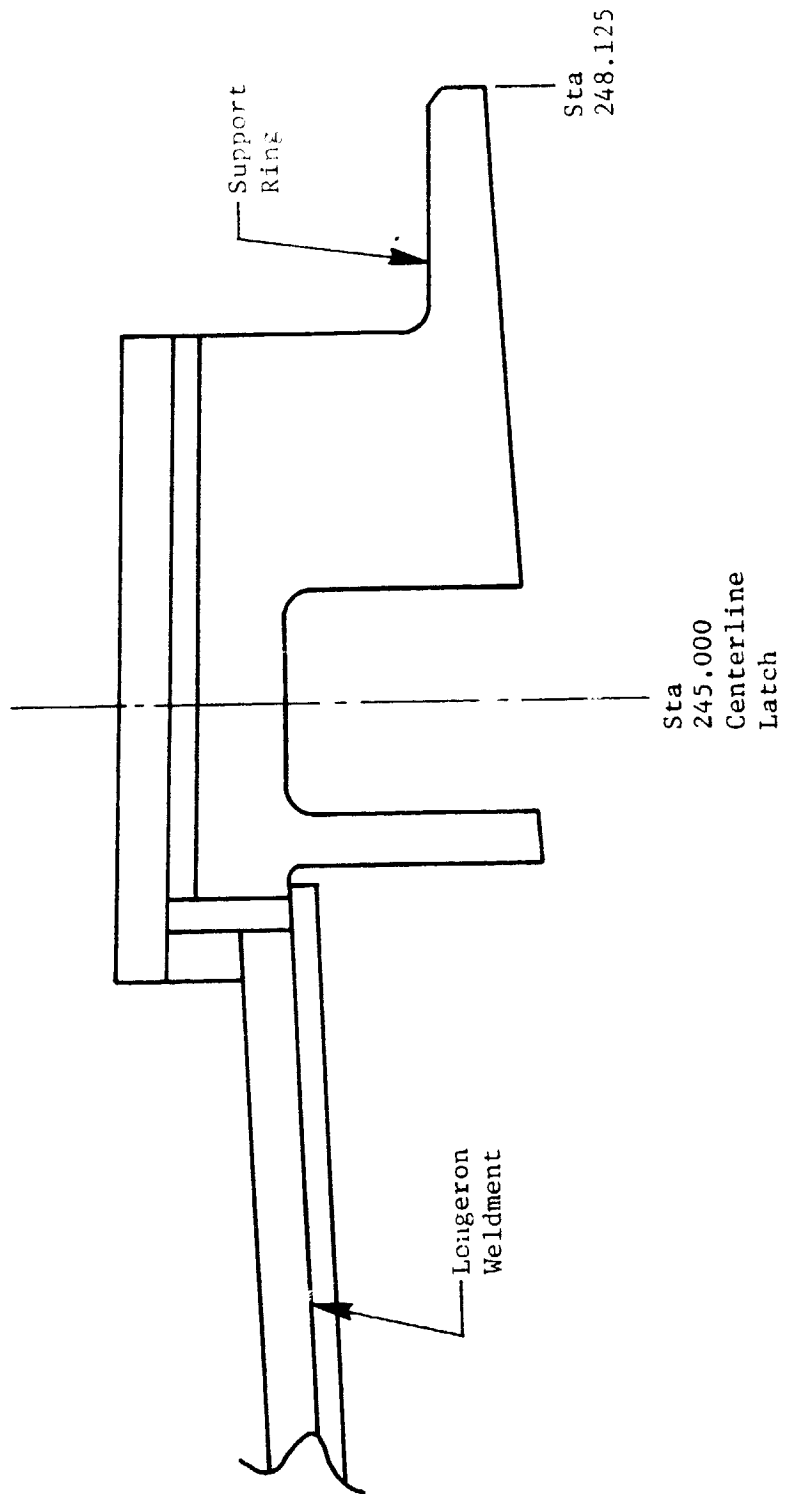


Figure 42. Rear Flange.

ORIGINAL PAGE IS  
OF POOR QUALITY

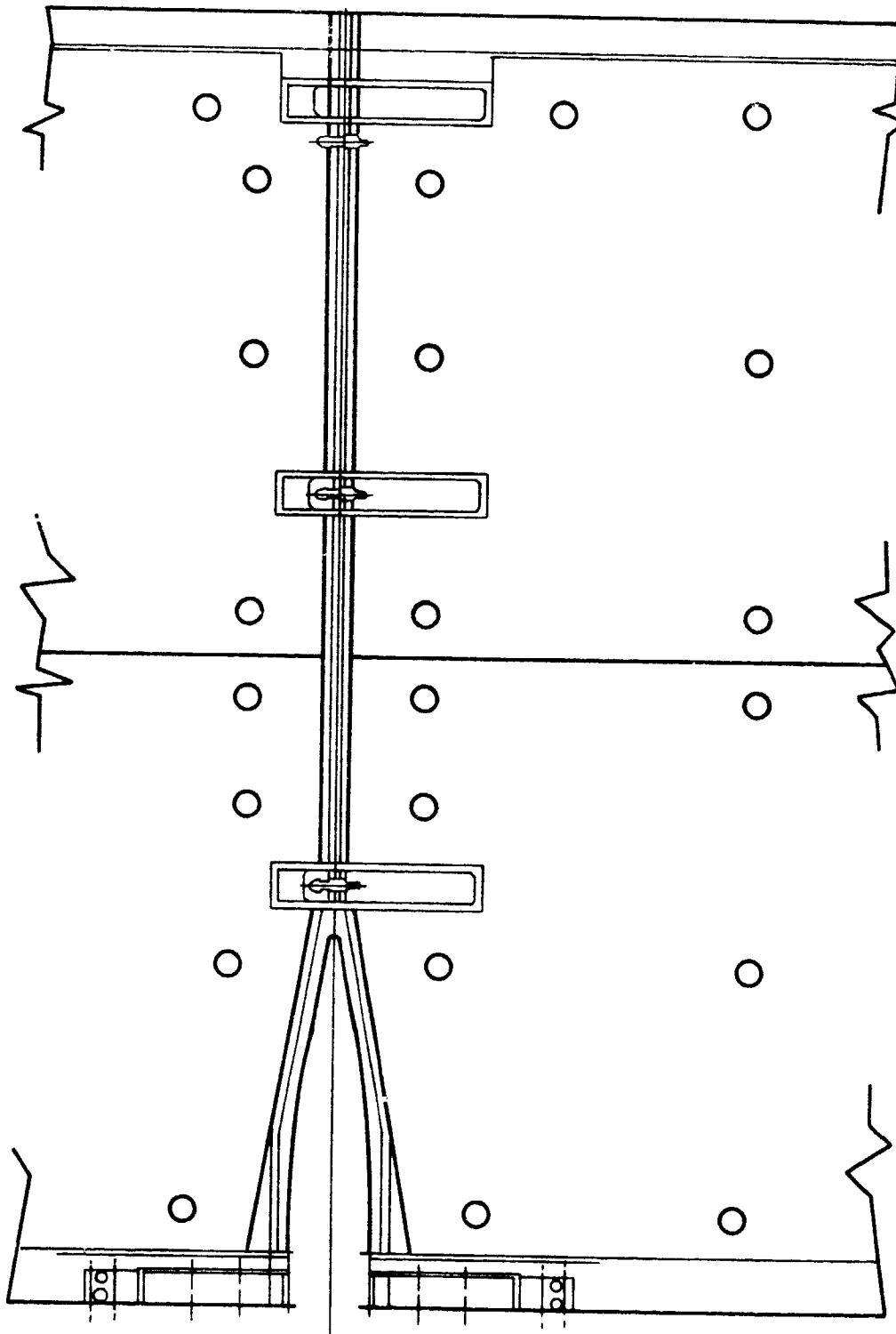


Figure 43. Inner Cowl - Bottom View.

ORIGINAL DRAWING  
OF BEST QUALITY

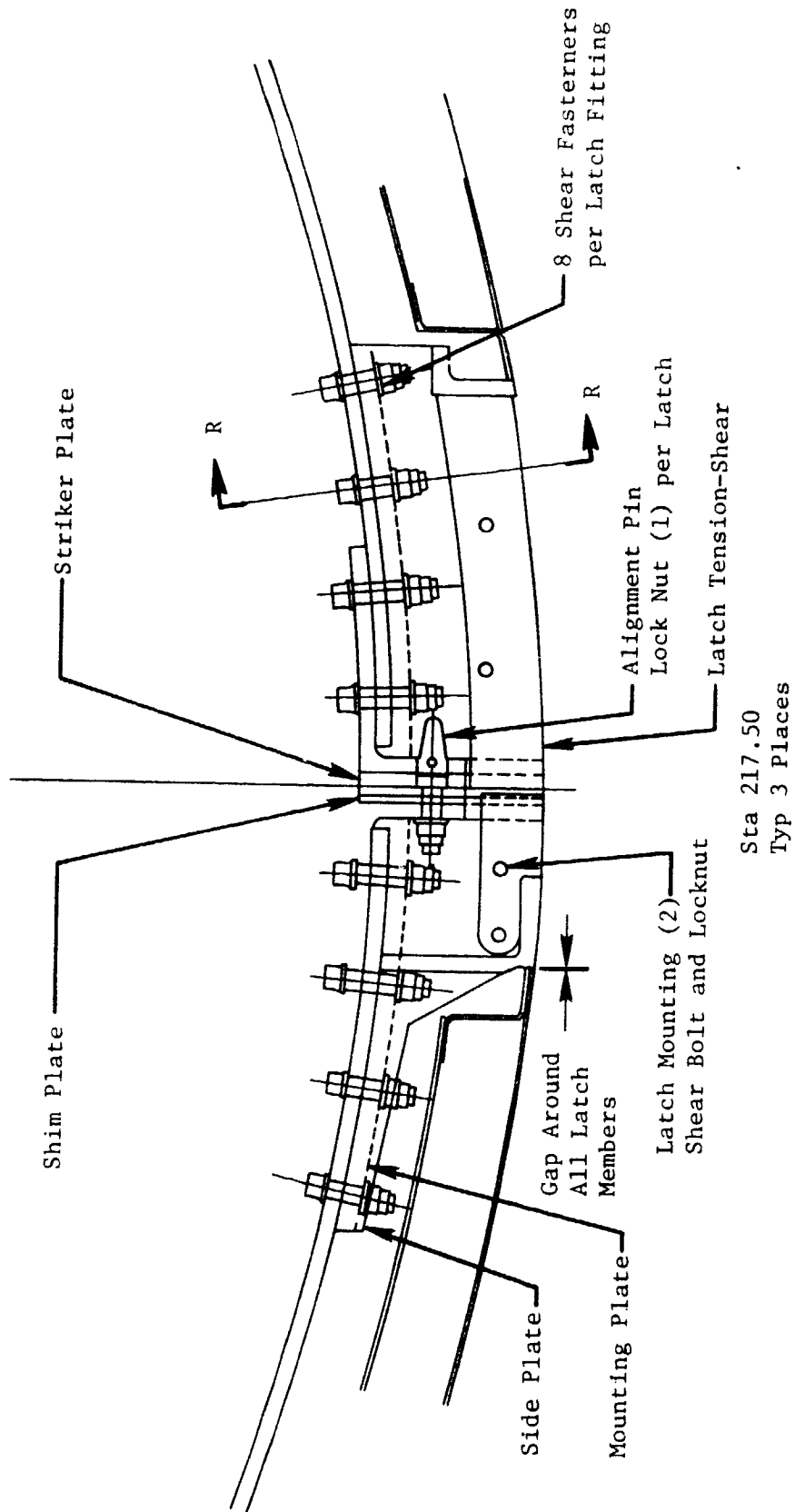


Figure 44. Inner Cowl Doors - Latch Installation.

ORIGINAL PAGE IS  
OF POOR QUALITY

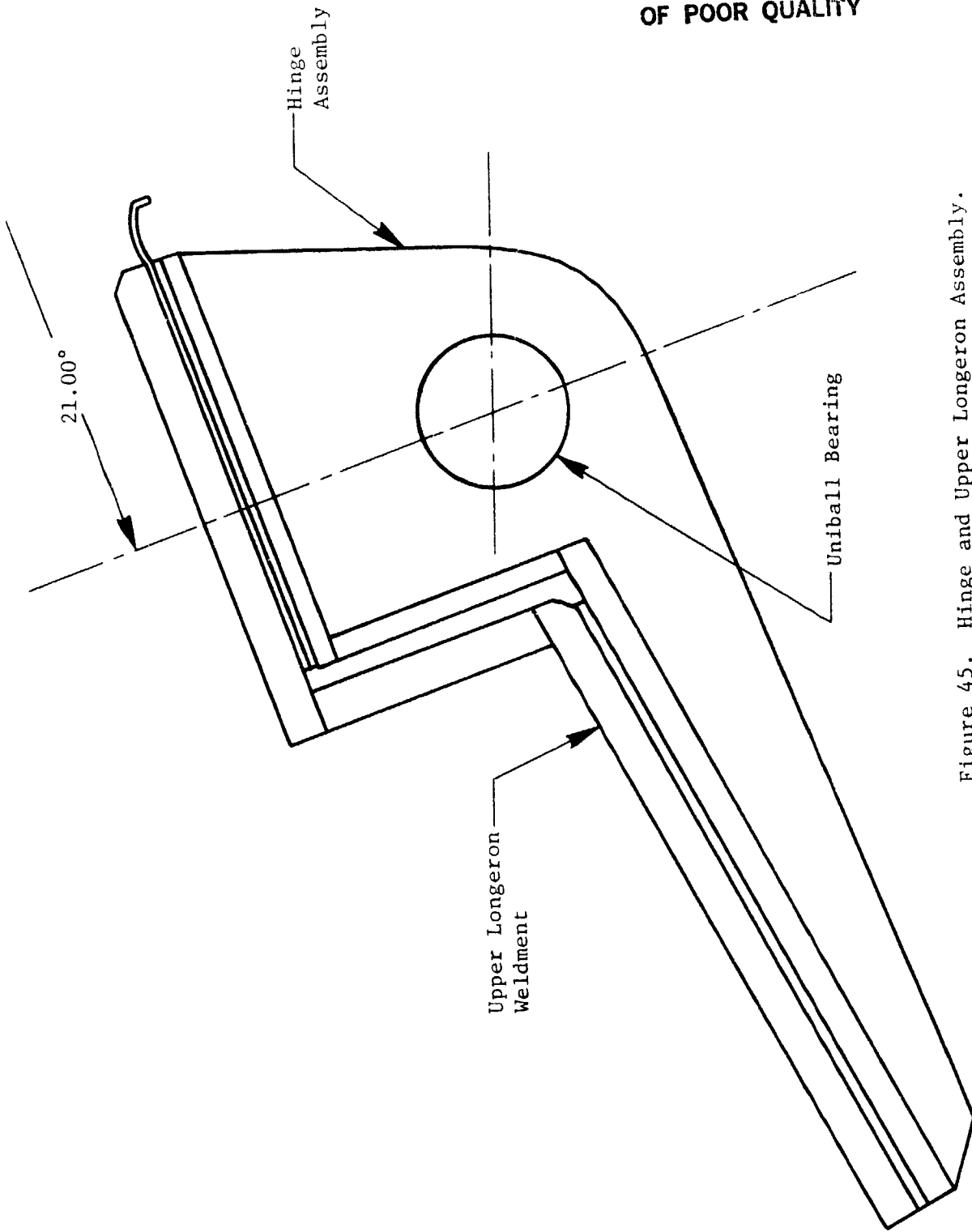


Figure 45. Hinge and Upper Longeron Assembly.



ORIGINAL PAGE IS  
OF POOR QUALITY

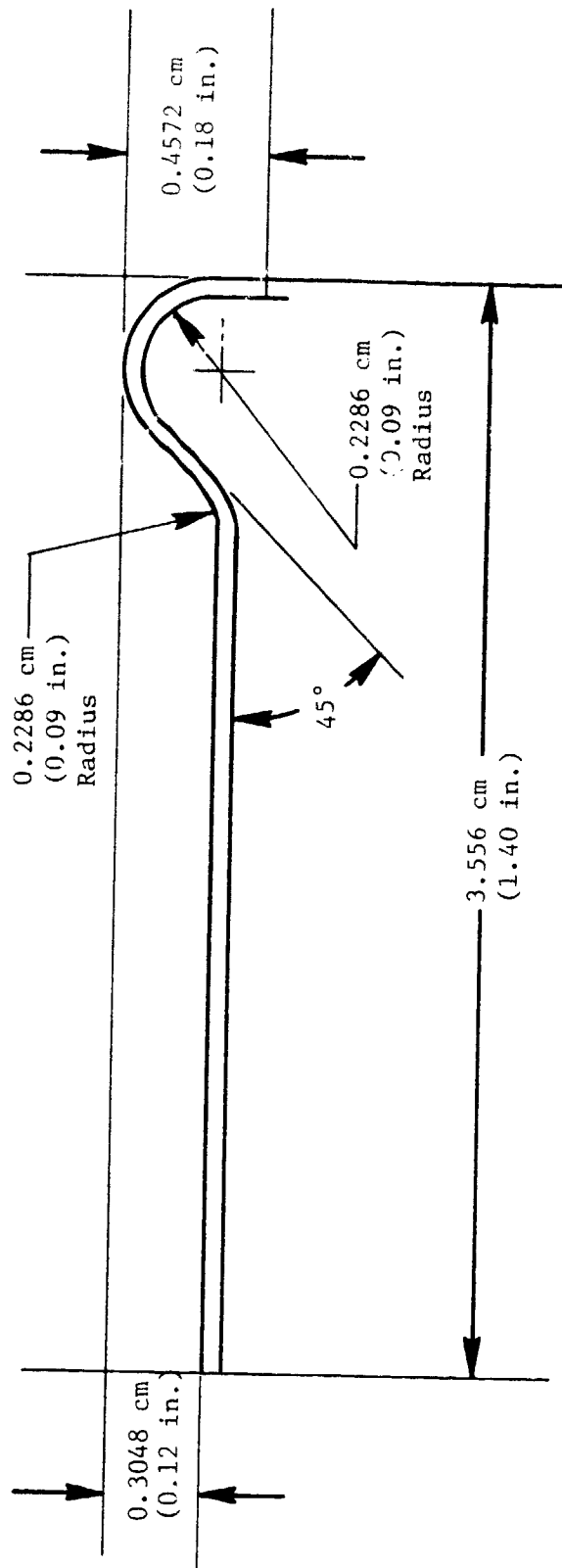


Figure 46. Apron Seal.

ORIGINAL PAGE IS  
OF POOR QUALITY

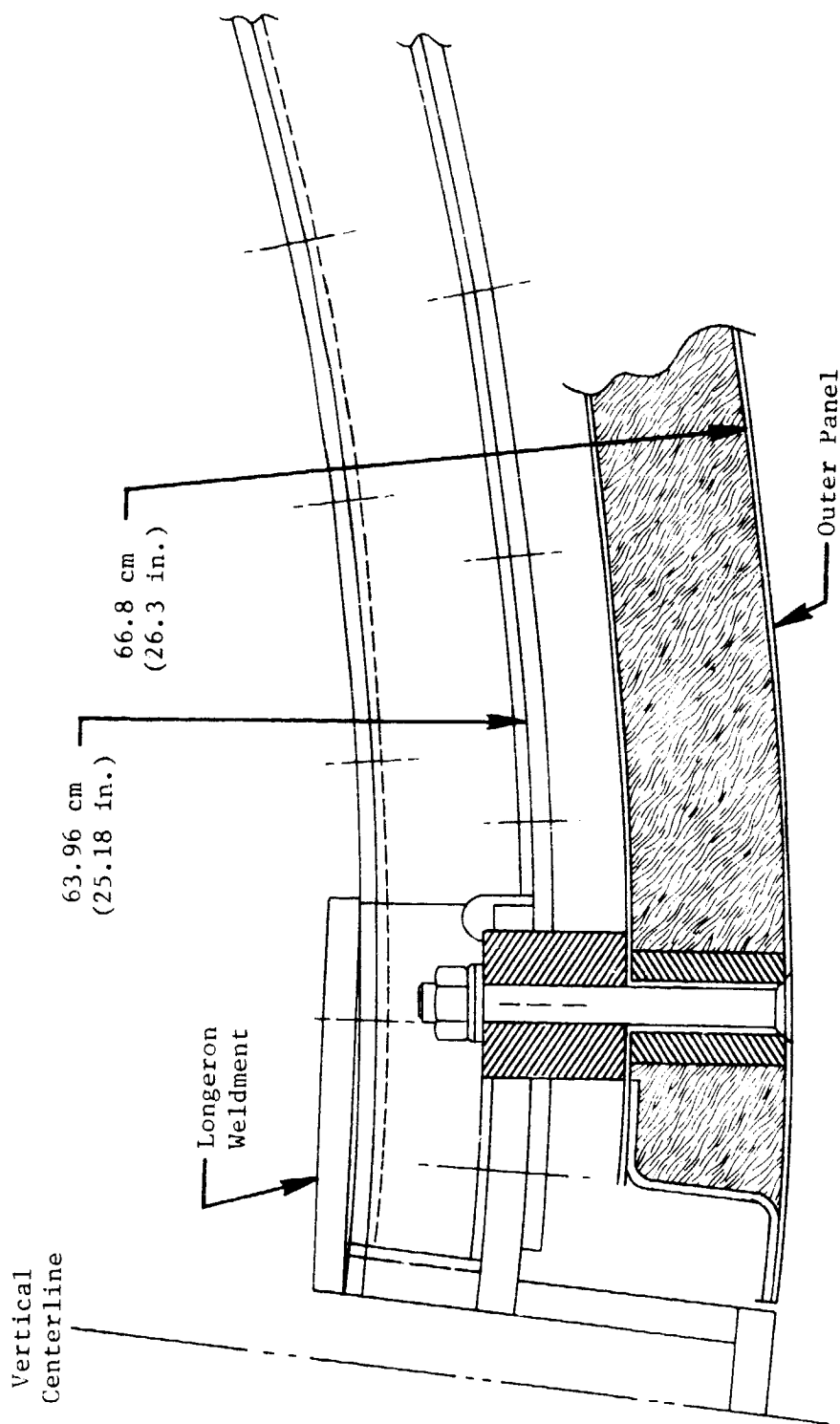


Figure 47. Panel.

ORIGINAL PAGE IS  
OF POOR QUALITY

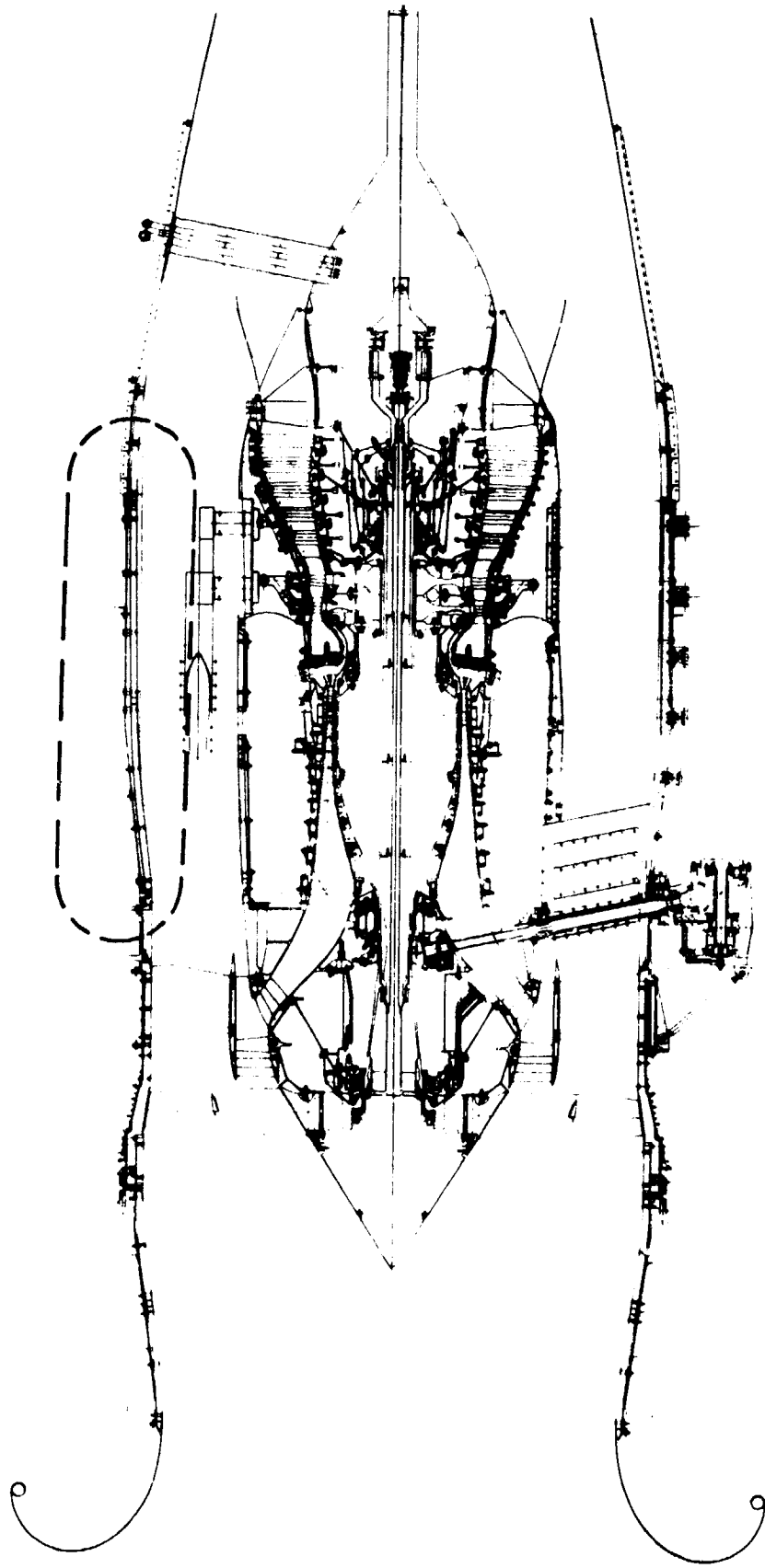


Figure 48. Fan Cowl.

static pressure distribution in the fan stream is shown in Figure 49. The stresses and margins of safety for the doors are shown in Table XVIII. The analysis of the latch and hinge loads is given in Table XIX.

The basic design features of the outer cowl doors and the materials used are listed in Table XX. The forward ring is shown in Figure 50. This ring has a tongue which engages a groove on the aftside of the fan frame. Since the doors are supported from the facility and not the engine, the fit of the tongue into the fan frame groove is very loose so as not to transmit any load through this joint. The aft ring is also a tongue and groove arrangement, as shown in Figure 51, with the tongue fitting into a groove in the mid fan cowl. Since both of these structures are tied to the facility, this is a load carrying joint.

The outer cowl doors are hinged from the facility engine mount beam as shown in Figure 52. The doors are fastened together at the bottom with five latches and a tie bar as depicted in Figure 53. A detail description of a typical latch is shown in Figure 54 and the tie bar arrangement is shown in Figure 55. The tie bar is required to provide structural continuity of the doors in the area of the lower pylon. The acoustic treatment for the doors consists of a set of acoustic panels attached to the structural shell as shown in Figure 56.

D. Aft Outer Exhaust Nozzle - The aft outer exhaust nozzle is located as shown in Figure 57, and is made up of the mid fan cowl, aft fan cowl, and nozzle. The fan stream static pressure distribution is given in Figure 58. Since this structure is supported from the facility rather than the engine, the net axial loading was calculated for use in the engine thrust balance. This load, along with the structural margins of safety, are shown in Table XXI.

The basic design features of the mid fan cowl and the materials used to fabricate this structure are given in Table XXII. The mid fan cowl contains integral acoustic treatment as shown in Figure 59. The structure is made in two halves (Figure 60) to facilitate assembly at the test site. These two halves are bolted together at the bottom and supported from the engine mount beam at the top as shown in Figure 61.

ORIGINAL PAGE IS  
OF POOR QUALITY

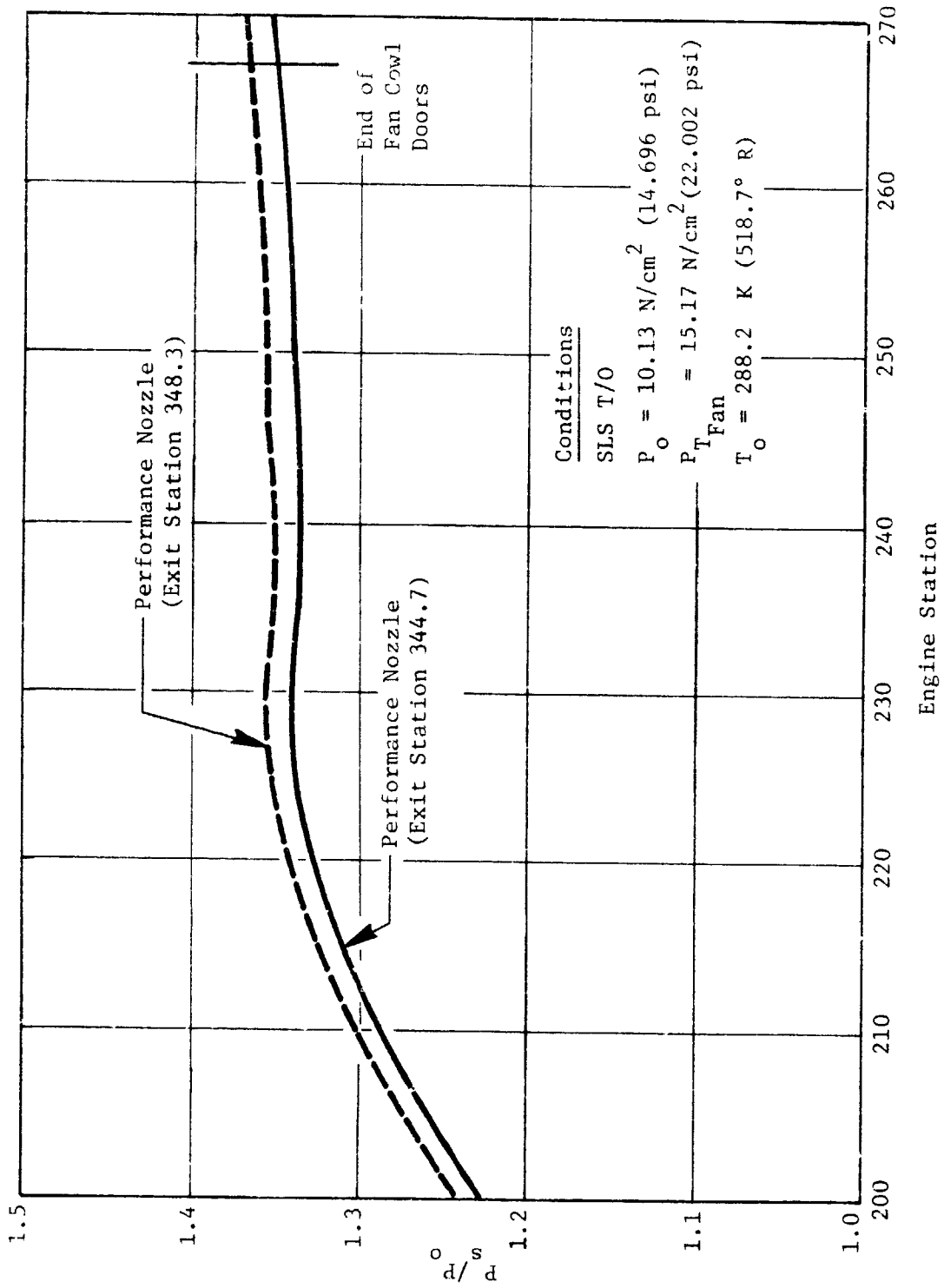


Figure 49. ICLS Fan Cowl Doors - Estimated Static Pressure Distribution.

Table XVIII. Fan Cowl Doors and Outer Apron.

- Max Temperature Environment
  - $T_{max} = 360.8 \text{ K (189.4}^\circ \text{ F)}$   
(SLS Hot Day T/O;  $M_o = 0$ ;  $\Delta T = 35 \text{ K (63}^\circ \text{ F)}$ )
- Loading
  - Max  $\Delta P$  (Internal Loading) Across Structure  
 $\Delta P = 3.79 \text{ N/cm}^2 \text{ (5.5 psi)}$
  - Hoop Stress  
 $\sigma_{Hoop} = 775.6 \text{ N/cm}^2 \text{ (1125 psi); MS = 23.9}$
  - Meridional Stress  
 $\sigma_m = 816.6 \text{ N/cm}^2 \text{ (563 psi); MS = 47.7}$

Table XIX. Latch and Hinge Loads.

- Latch Loads

<u>Latch No.</u>	<u>Max Load N/cm (lbs)</u>	<u>Safety Margin</u>
1 (Tie Rod)	18,642 (4191)	12.9
2	18,375 (4131)	2.2
3	18,869 (2422)	4.5
4	13,549 (3046)	3.3
5	14,011 (1799)	6.4

- Hinge Loads

<u>Hinge No.</u>	<u>Max Load (lbs)</u>	<u>Safety Margin</u>
1	8,669 (1949)	4.2
2	13,069 (2938)	2.5
3	13,202 (2968)	2.4
4	23,820 (3058)	2.3
5	24,287 (3118)	2.3
6	7,788 (1751)	4.8

Table XX. Fan Cowl Doors.

Basic Design Features

Outer Shell

- Monocoque Type Structure
- Supported From Engine Mount Beam by 6 Hinges with Uniballs
- 5 Latches on Lower Split Line, on STA with Hinges

Acoustic Panels

- Solid Back Skin, Perforated Face Sheet 30% Open
- Rolled C Section End Rings
- Formed Solid Longitudinal Ribs
- Panels are 56° Segments with Five Ribs Equally Spaced
- Three Forward and Three Aft Panels Per Door
- Mounted to Outer Shell by Special Inserts in Panels, Bolted to Stand - OFFS That are Welded to Outer Shell

Materials

Outer Shell

- Skin and Stiffeners 6061-T6 Al Alloy
- Machined Rings 6061-T6 Al Alloy
- Hinges 17-4PH Steel, HT-TR H1025
- Latches - (4) AISI Stainless Steel, (1) Forward AISI 4340 Steel and 17-4PH Steel
- Fasteners  
Permanent - NAS Type Steel Huckbolts  
Removable - NAS and MS Type Screws and Bolts
- Seals  
Lower Split Line - Flat Silicone Sponge Rubber  
Upper Split Line - Bulb Type Silicone Rubber (Mounted to Apron)

Acoustic Panels

- Face Sheet, Back Plates, Stiffeners and Ribs 6061-T6 Al Alloy
- Acoustic Treatment - Kevlar 29 Felt
- Fasteners  
Skin Attach MS20426AD and MS20470AD Rivets  
Mount Bolts (9301M44 P02)  
Inserts (9211M62 P01)

ORIGINAL PAGE IS  
OF POOR QUALITY

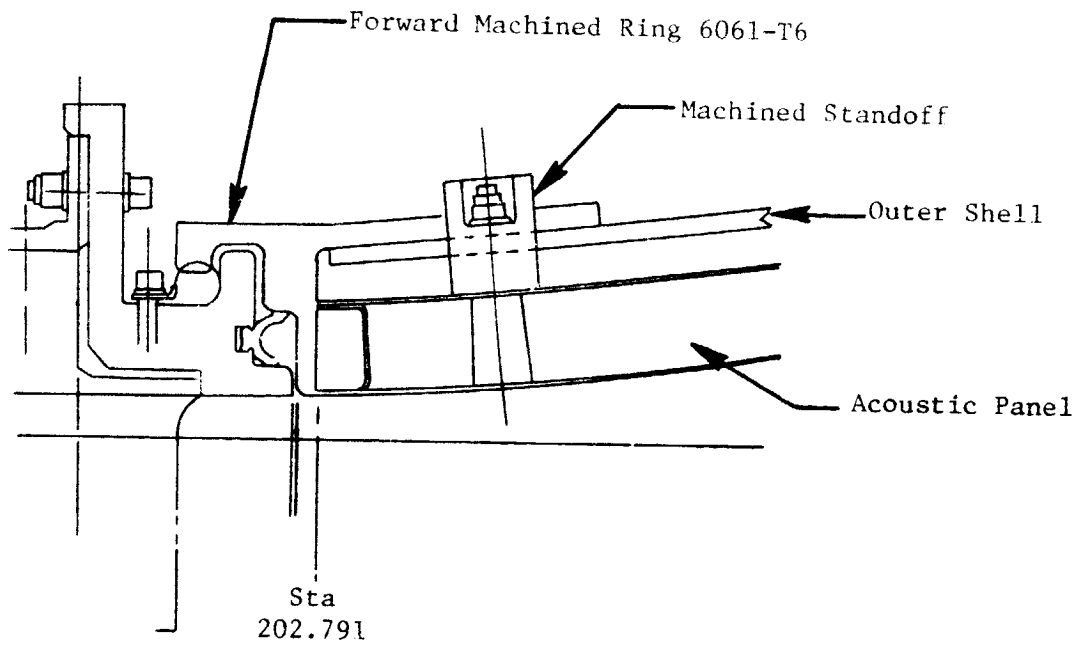


Figure 50. Forward Interface Ring.

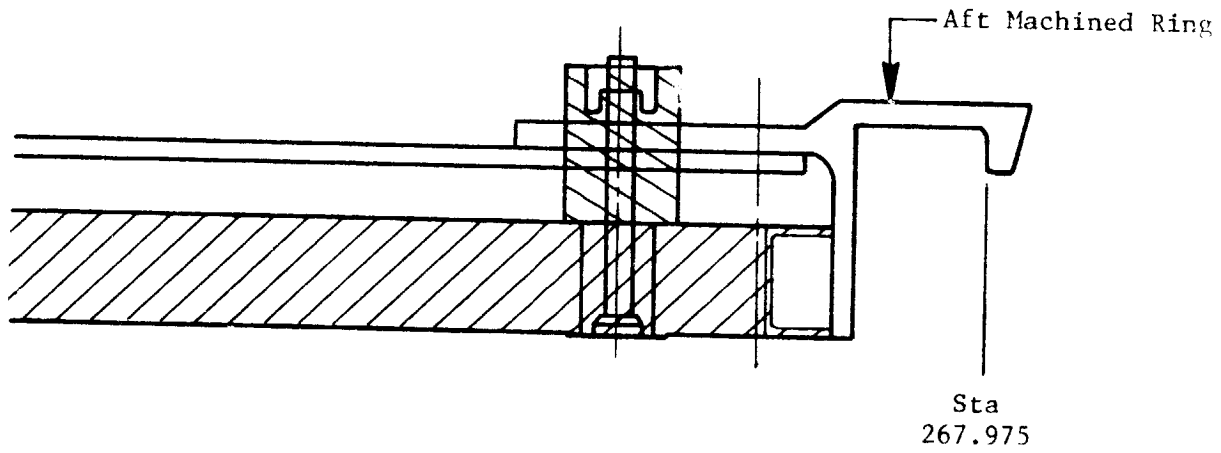


Figure 51. Aft Interface Ring.



ORIGINAL PAGE IS  
OF POOR QUALITY

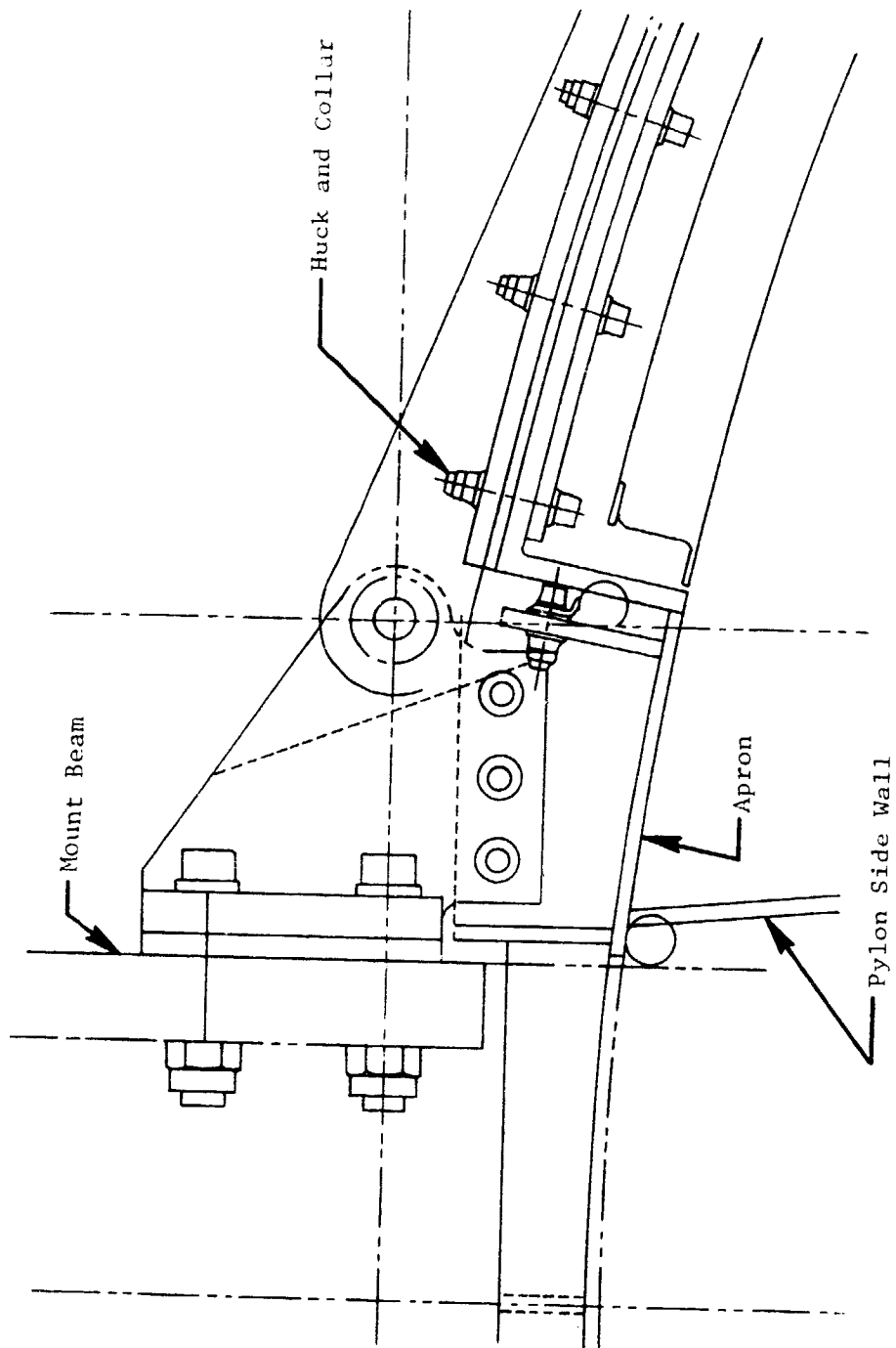


Figure 52. Fan Cowl Hinge (Typical 6 Places).

ORIGINAL PAGE IS  
OF POOR QUALITY

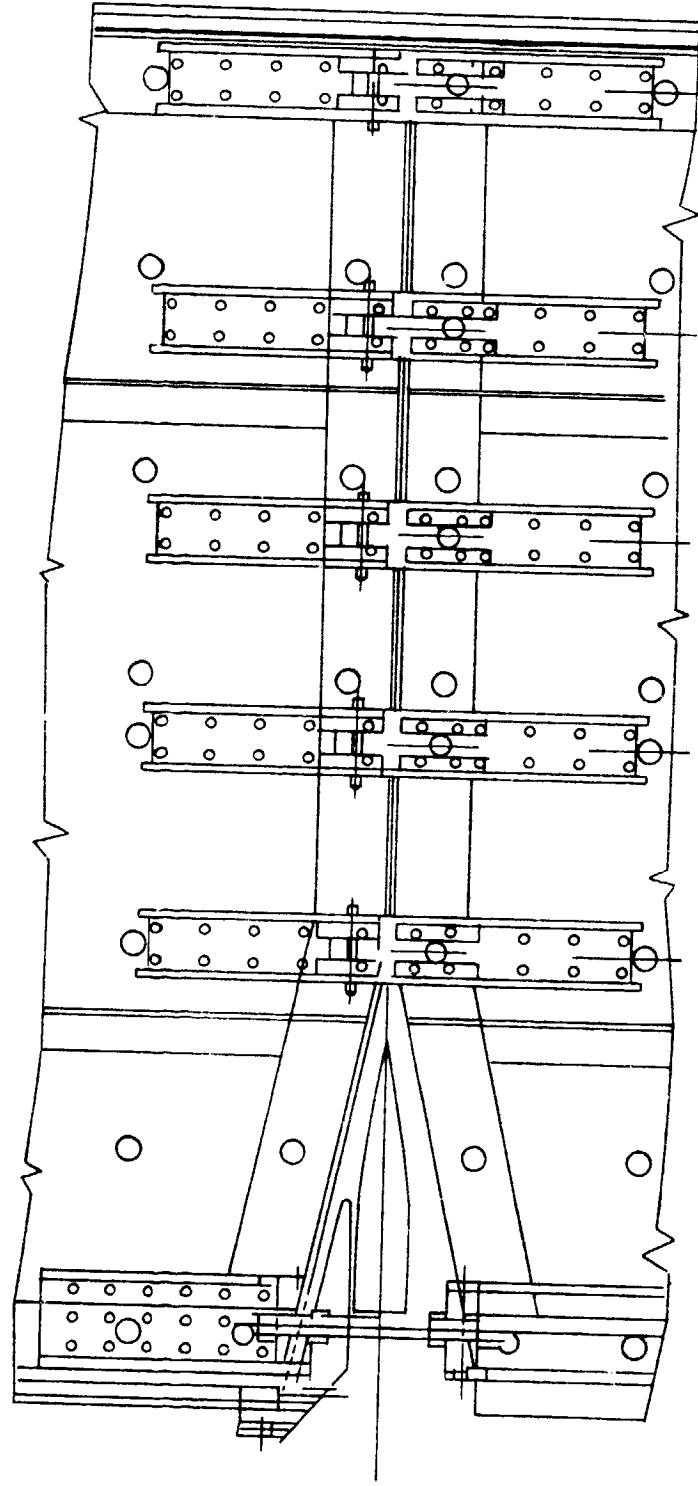
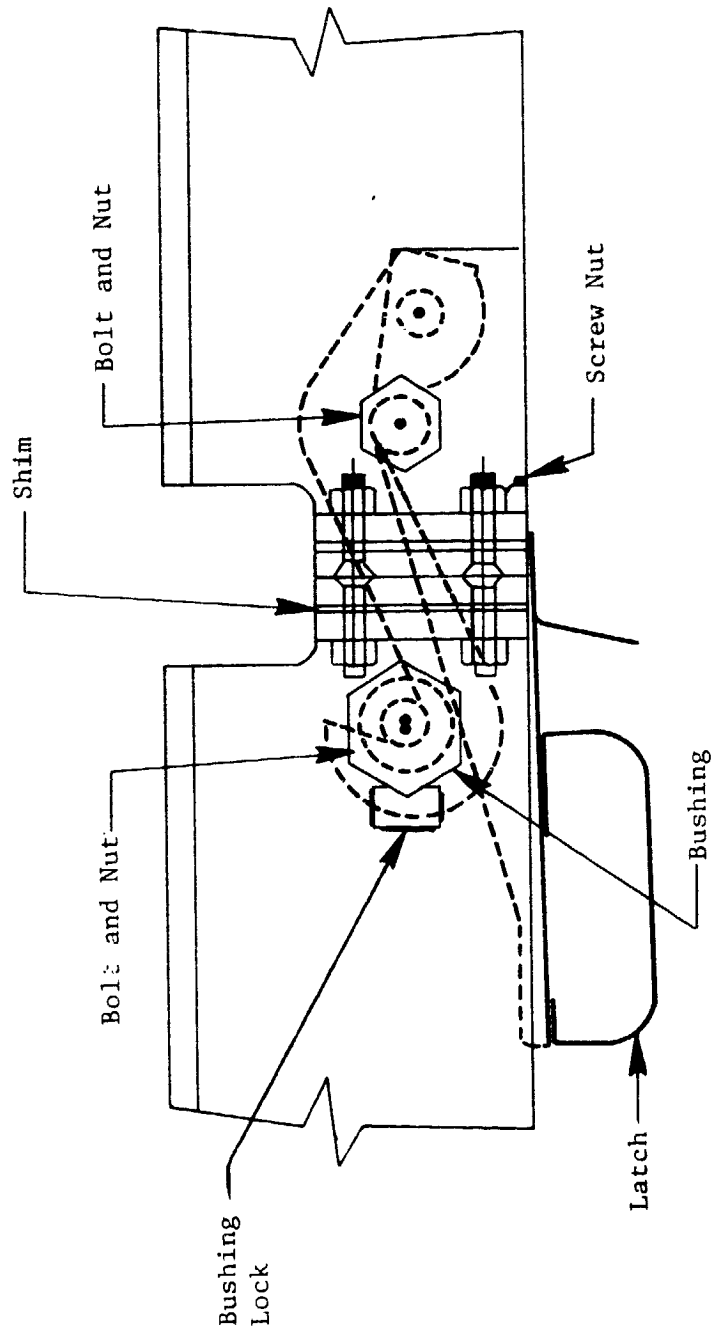


Figure 53. Outer Cowl Doors Bottom Centerline.

CRITICAL DIMENSIONS  
OF POOR QUALITY



(Eccentric Type for Adjustment)

Figure 54. Fan Cowl Latch (Aft 4).

ORIGINAL DRAWING  
OF POOR QUALITY

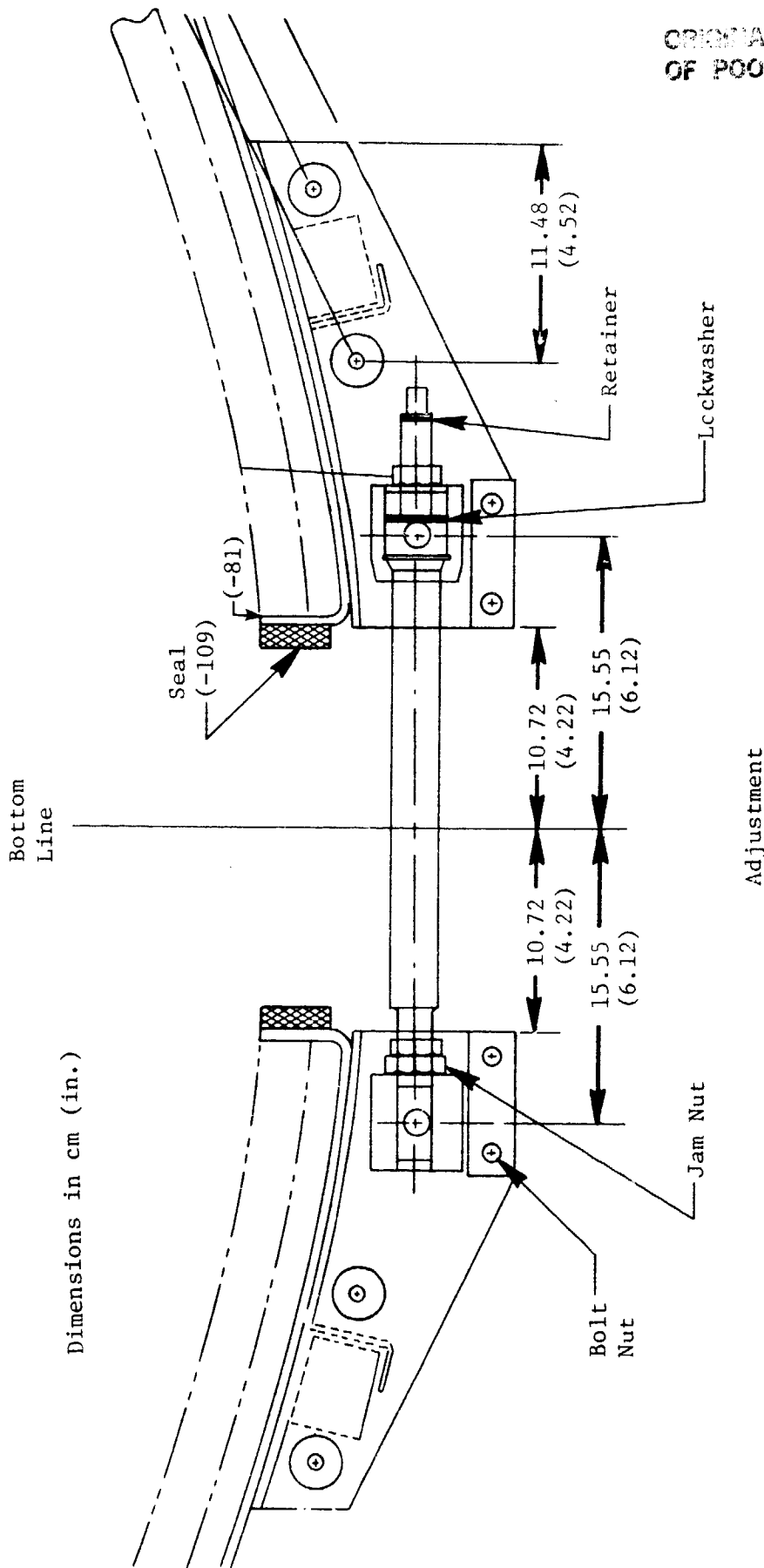


Figure 55. Fan Cowl Latch - Forward Only.

ORIGINAL PAGE IS  
OF POOR QUALITY

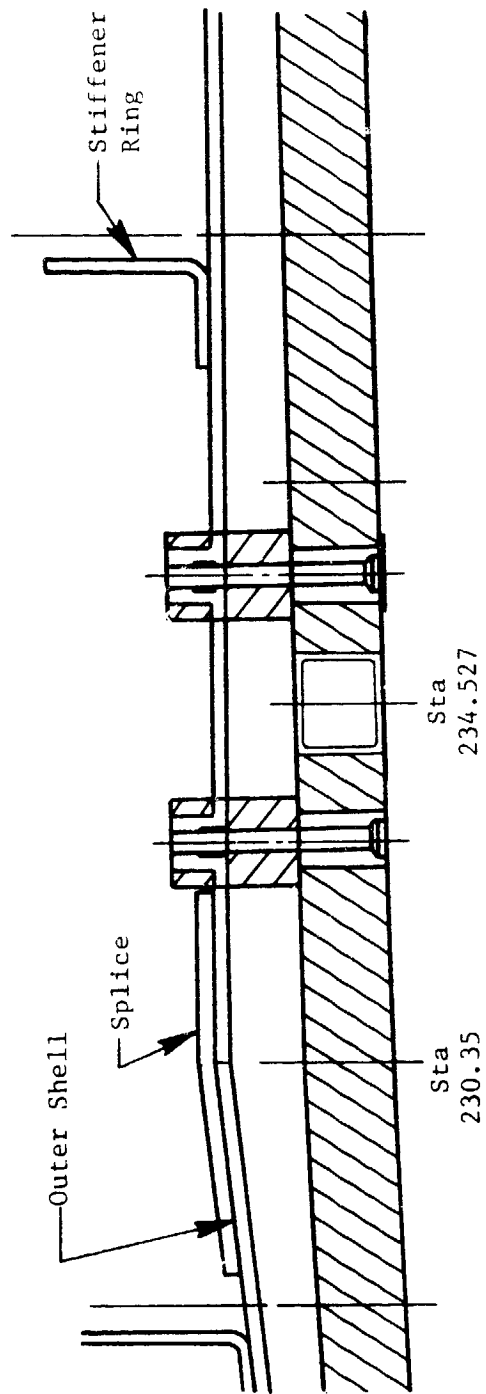


Figure 56. Shell and Acoustic Panels.

ORIGINAL PAGE IV  
OF POOR QUALITY

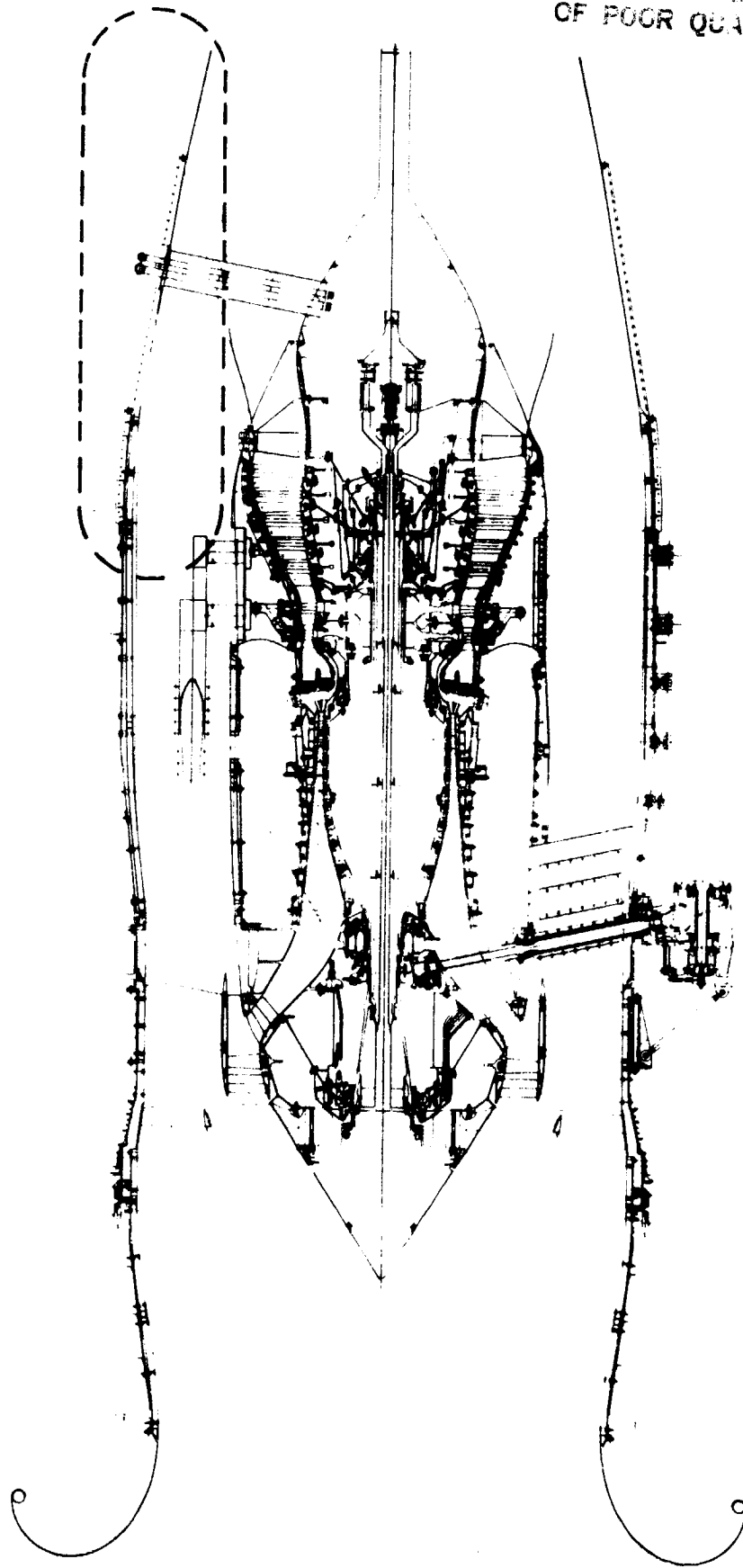


Figure 57. Aft Outer Exhaust Nozzle.

ORIGINAL PAGE IS  
OF POOR QUALITY

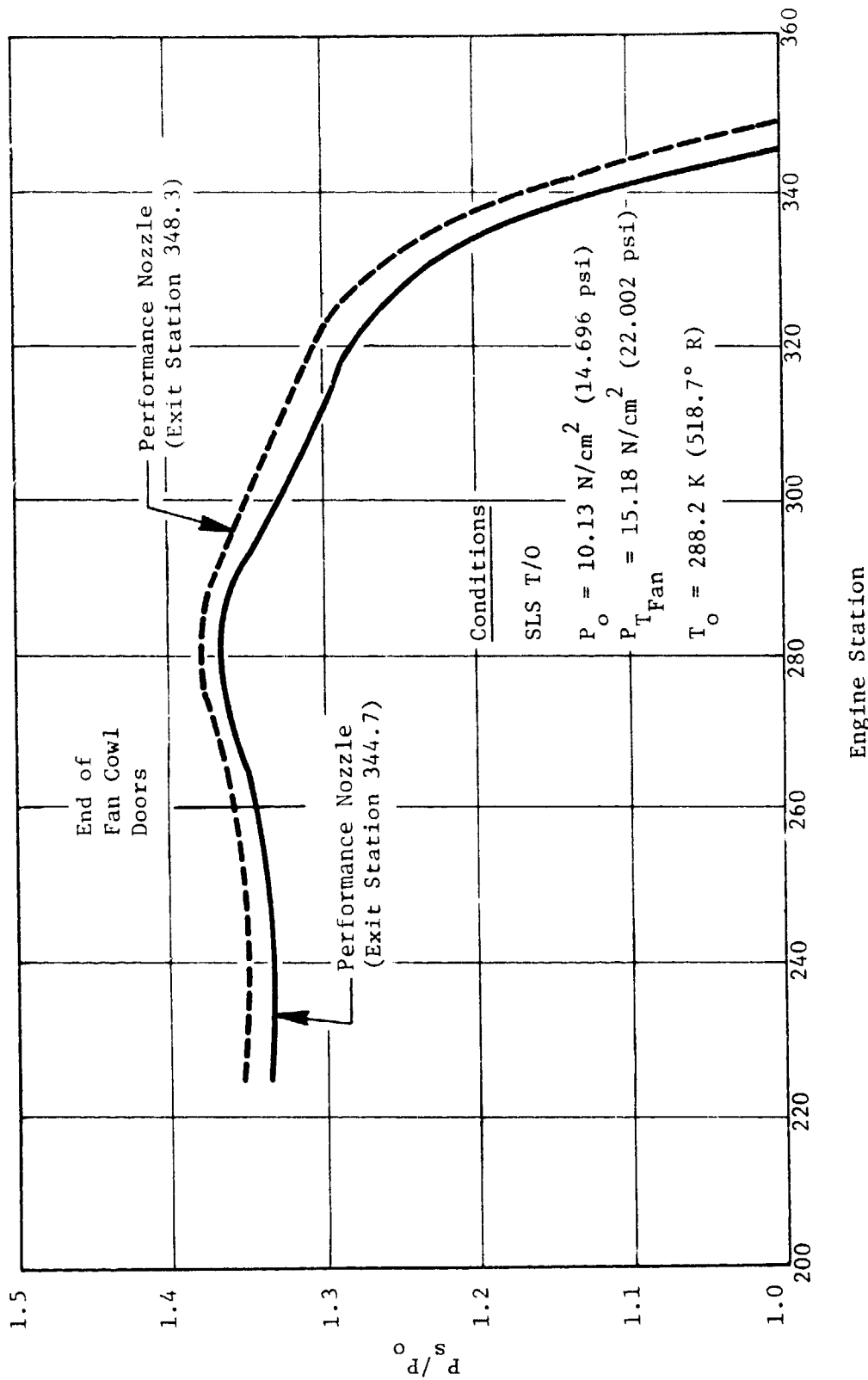
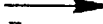



Figure 58. ICLS Aft Outer Exhaust Nozzle - Estimated Static Pressure Distribution.

Table XXI. Aft Outer Exhaust Nozzle Loads.

- Max Temperature Environment
  - $T_{max} = 360.6 \text{ K (189.4}^\circ \text{ F)}$   
(SLS Hot Day T/O;  $M_o = 0$ ;  $\Delta T = 35 \text{ K (-63}^\circ \text{ F)}$ )
- Loading
  - Max  $\Delta P$  (Internal Loading) Across Structure  
 $\Delta P = 3.86 \text{ N/cm}^2 \text{ (5.6 psi)}$
  - Hoop Stress  
 $\sigma_{Hoop} = 791.5 \text{ N/cm}^2 \text{ (1148 psi); MS} = 66.9$
  - Meridional Stress  
 $\sigma_M = 395.8 \text{ N/cm}^2 \text{ (574 psi); MS} = 134$
  - Net Axial Loading  
(+)  
  
 $F_{Axial} = \Delta P_{max} (\Delta A)$   
Net
  - (+)  
  
 $F_{Axial} = 72,105 \text{ N (16,210 lb)}$   
Net

Max Resulting Moment

$$M = 7,313,077 \text{ N/cm (647,265 in./lb)}$$

- Critical Bolt Loading  
 $P = 10,408 \text{ N (2340 lb); MS} = 0.13 \text{ Crit}$   
Crit



Table XXII. Midfan Cowl.

Basic Design Features

- Integral Structure and Acoustic Panel
- Stretch Formed Outer Skin Structure Attaches to Rolled "Z" Rings at Each End
- Rolled Z Rings Attach to Machined Interface Rings at Each End
- Forward Machined Interface Ring Incorporates Tongue and Groove Joint Along With a Chevron Seal
- Aft Machined Interface Ring Bolts to Midcowl
- Cowl Splits at Lower Centerline; Belted Together Through Axial Flange
- Upper End of Cowl Attaches to Engine Mount Beam by Longitudinal Angle.

Materials

- Rings, Back Skin, Longerons, Face Sheet and Splices - 6061-T6 Al Alloy
- Acoustic Treatment - Kevlar 29 Felt
- Chevron Seal - 9012M36, Silicone Rubber
- Fasteners

ΔPermanent: MS24694C Flush Screws and NAS Lockbolts

ΔRemoveable: AN4 Bolts



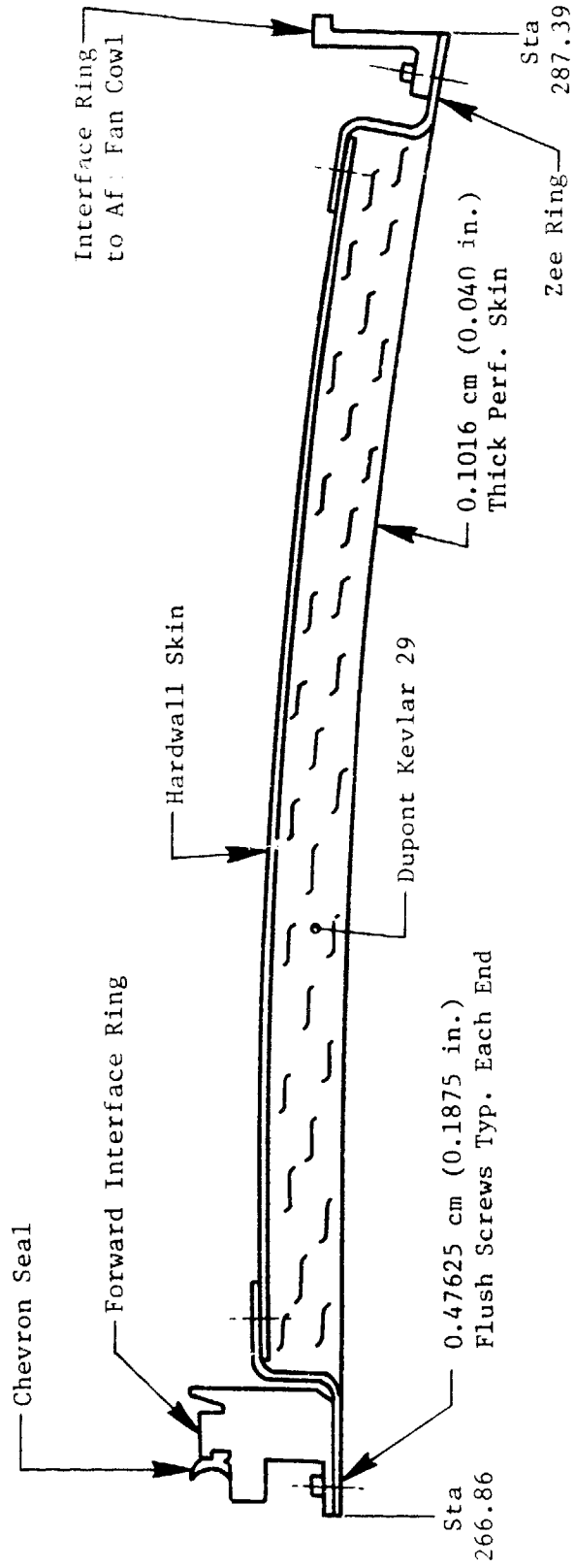
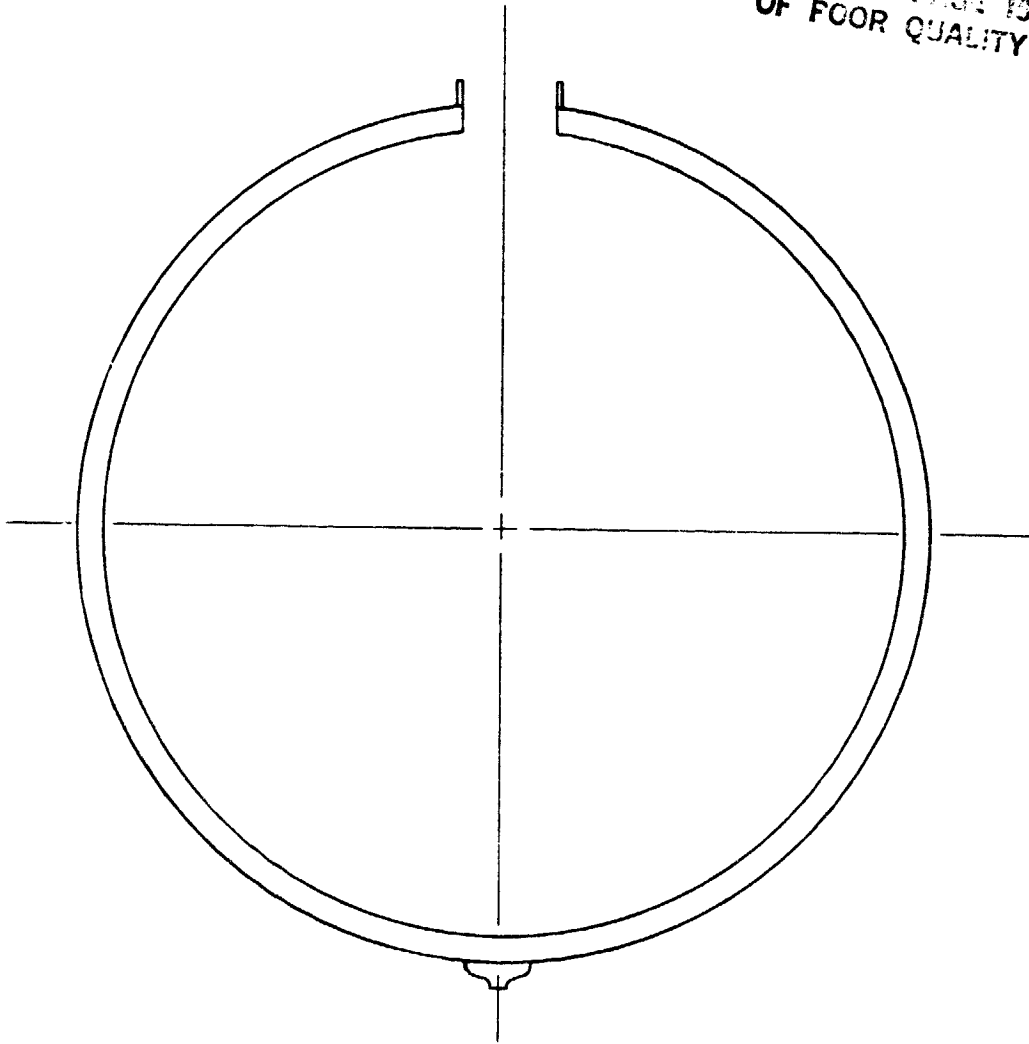


Figure 59. Typical Cross Section of Midfan Cowl.

2-2

Top Vertical  
Centerline

ORIGINAL PAGE IS  
OF POOR QUALITY



View Aft Looking Forward

Figure 60. Orientation Midfan Cowl Assembly.

ORIGINAL PAGE IS  
OF POOR QUALITY

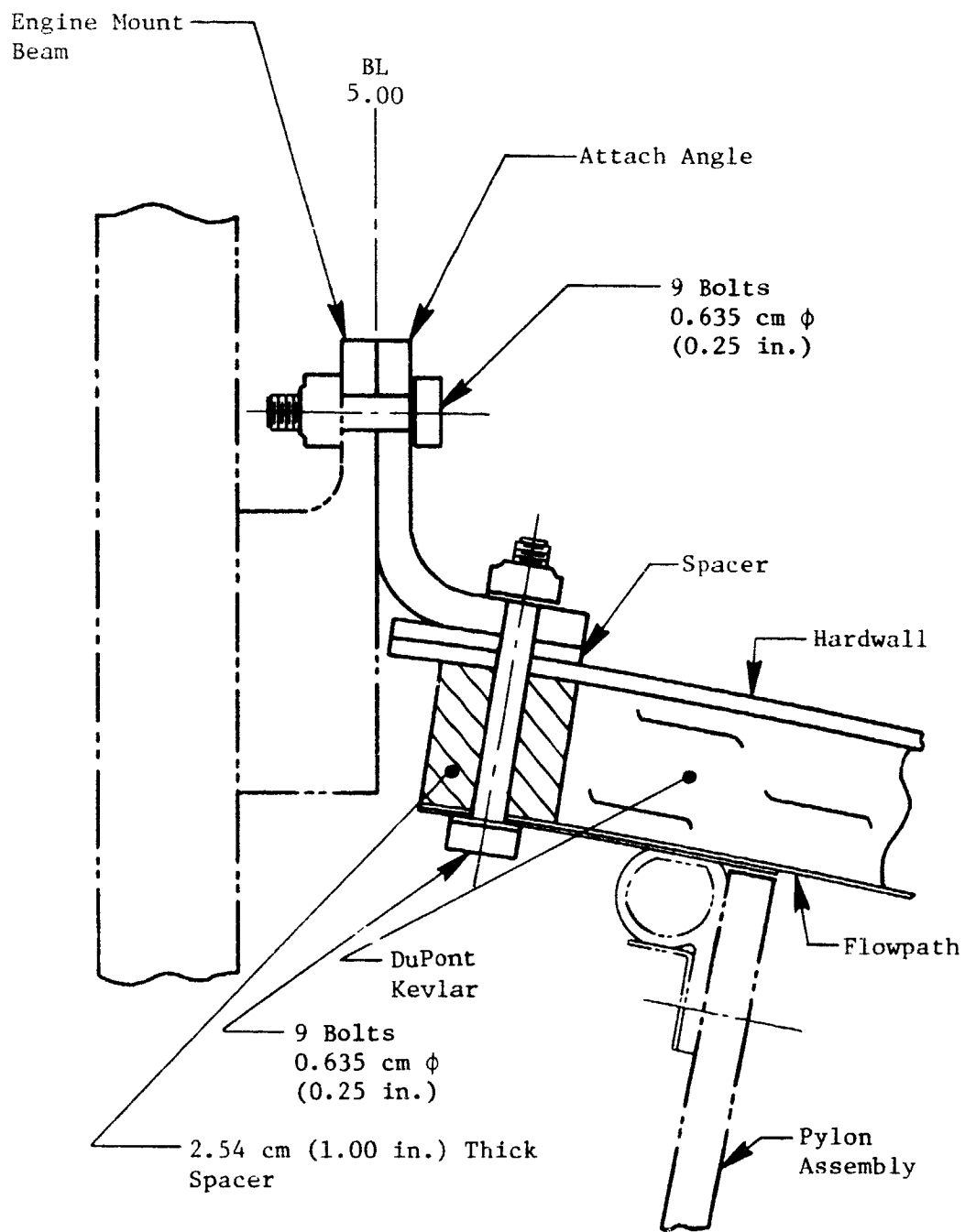


Figure 61. Midfan Cowl Upper Attachment to Mount Beam.

The basic design features of the aft fan cowl, along with a list of materials used in its fabrication, are shown in Table XXIII. The structure contains no acoustic treatment. It is made in two halves and is attached to the mount beam at the top centerline and to itself at the bottom as shown in Figure 62. There are two manufacturing splices on the horizontal centerline. The forward ring, Figure 63, attaches to the mid fan cowl and the aft ring, Figure 64, supports the nozzle. The method of joining the two halves together is shown in Figure 65.

The ICLS vehicle will utilize a conical nozzle rather than the converging/diverging nozzle designed for the FPS. The basic design features and materials are shown in Table XIV. Two nozzles will be built (Figure 66). The performance nozzle will be used when determining basic engine performance while the survey nozzle will be used to evaluate mixer effectiveness. The survey nozzle is slightly larger to account for the blockage of the instrumentation rakes mounted behind the nozzle for this evaluation. The nozzles are bolted to the rear of the aft fan cowl through the interface ring (Figure 67). The nozzles will be made in two halves and spliced together as shown in Figure 68.

E. Pylon - The pylon structure is located as shown in Figure 69 and is used to house the mount structure, various aircraft services, and the scoop and plenum serving the active clearance control system. The loading and margins of safety for the pylon sidewalls are shown in Table XXV. The basic design features of the pylon and the materials used are listed in Table XXVI. The overall scoop and plenum structure is shown (side view and top view) in Figures 70 and 71. Since the system must serve two separate valves, the scoop is divided into two halves (Figure 72) to provide air to a dual plenum arrangement.

The pylon leading edge (Figure 73) is a fabricated structure bolted to the forward edge of the mount beam. The sidewalls consisted of a number of separate panels attached through bulk heads to the side of the mount beam. A number of these panels are removable for access to the mount structure and the clearance control system. The type of fastening used for these panels is

Table XXIII. Aft Fan Cowl.

Basic Design Features

- Stretch Formed Conical Skin, 90° Segments
- Machined Interface Rings at Both Ends
- Splits at Upper and Lower  $\epsilon$  for Installation/Removal of Cowl
- Back to Back Angle Splice at Upper and Lower  $\epsilon$
- Cantilever Attachment to Mount Beam by Longitudinal Member at Upper Angle Splice
- Permanent Strap Splice at 90° and 270°
- Can be Installed/Removed in 360° Section
- No Acoustic Treatment

Materials

- Rings, Skins and Splices - 6061-T6 Al Alloy
- Fasteners
  - Permanent - NAS Lockbolts
  - Removable - AN4 Bolts

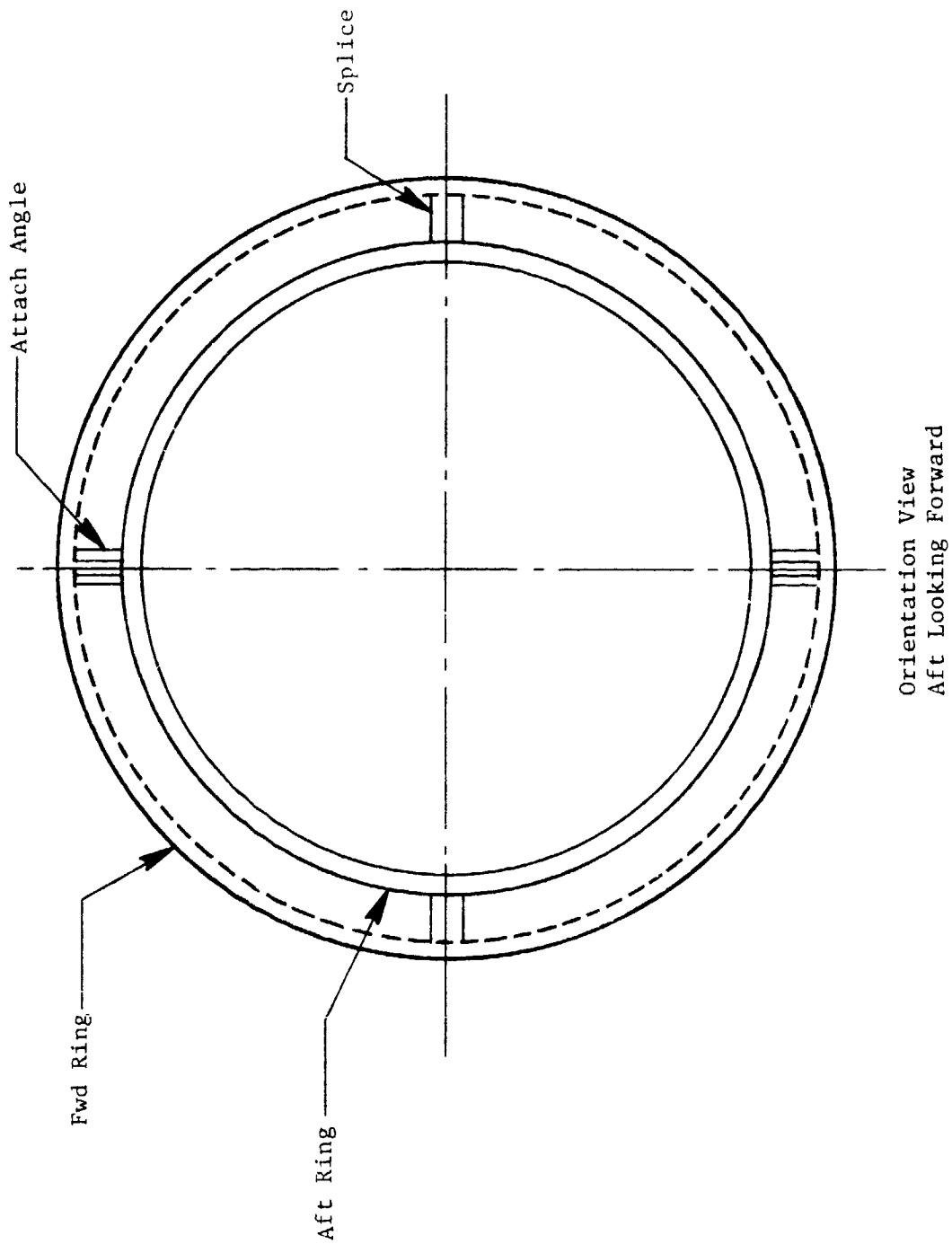
Table XXIV. Nozzle Assemblies.

Basic Design Features

- Machined Interface Rings
- Rolled Conical Skins
- Skin Fastened to Ring with Lockbolts, Staggered Pattern

Materials

- Rings and Skin - AlSi 321 Stainless Steel
- Lockbolts - NAS1456



Orientation View  
Aft Looking Forward  
Figure 62. Aft Fan Cowl.

Sta  
287.392

**ORIGINAL PAGE IS  
OF POOR QUALITY**

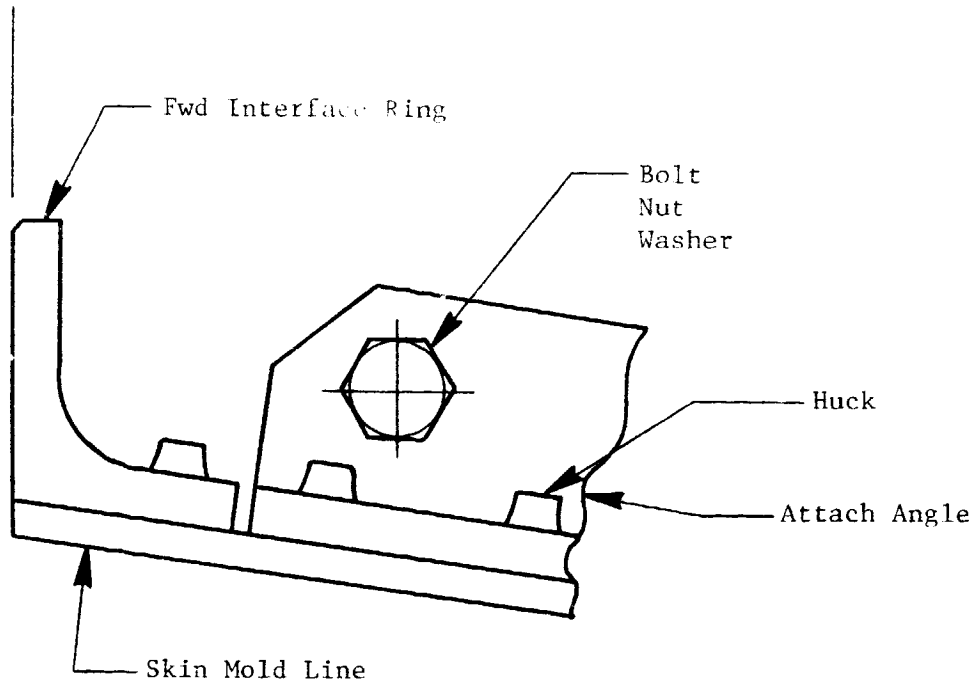


Figure 63. Forward Interface Aft Fan Cowl.

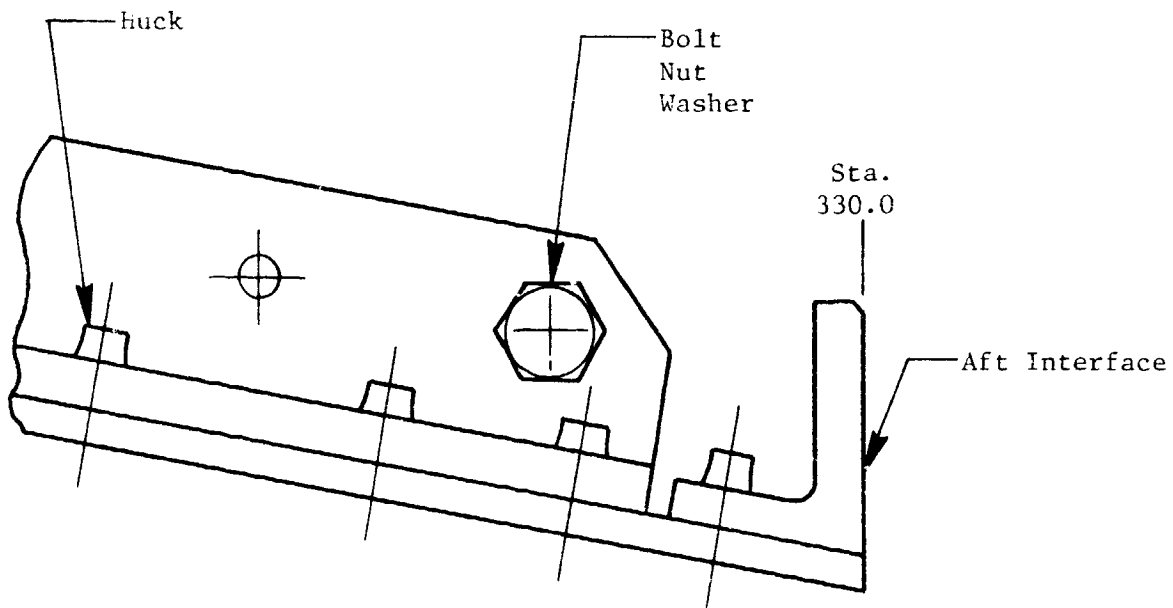
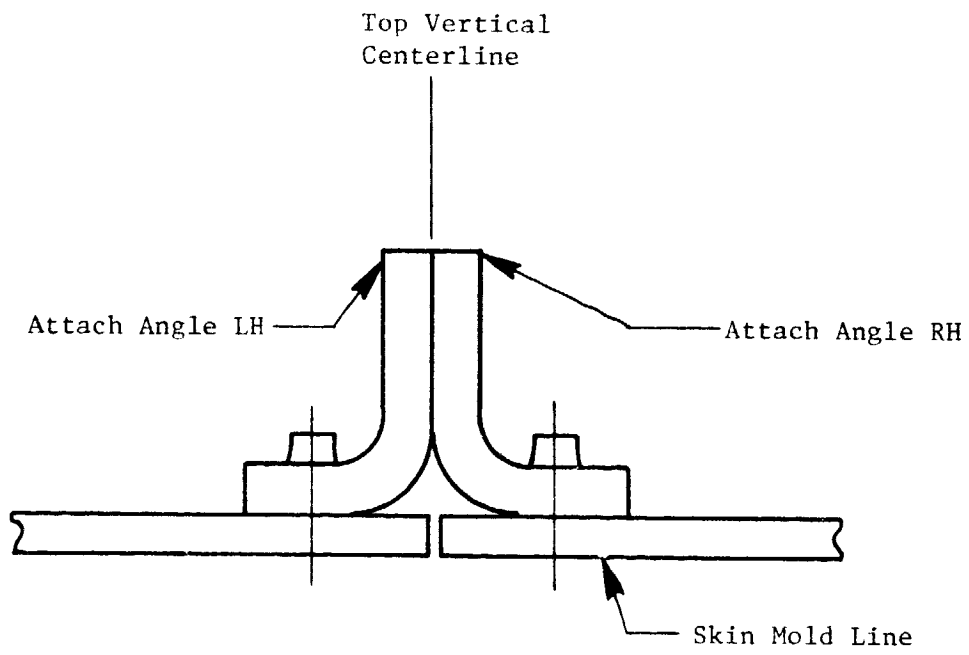


Figure 64. Aft Interface Aft Fan Cowl.





Typical Top and Bottom

Figure 65. Station Cut of Aft Fan Cowl.

ORIGINAL PAGE IS  
OF POOR QUALITY

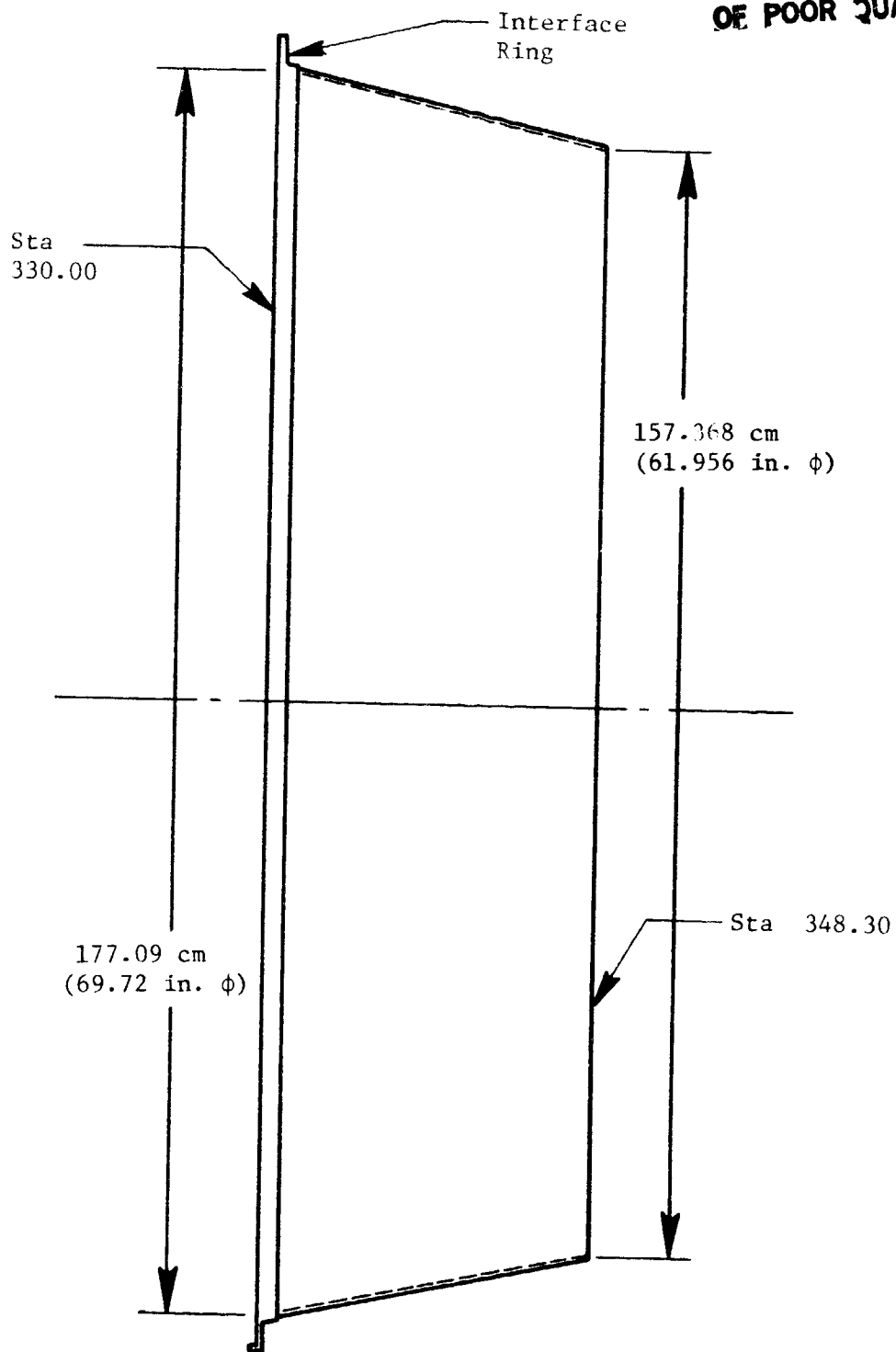


Figure 66. Nozzle Assembly Version No. 1 and Version No. 2.

ORIGINAL PAGE IS  
OF POOR QUALITY

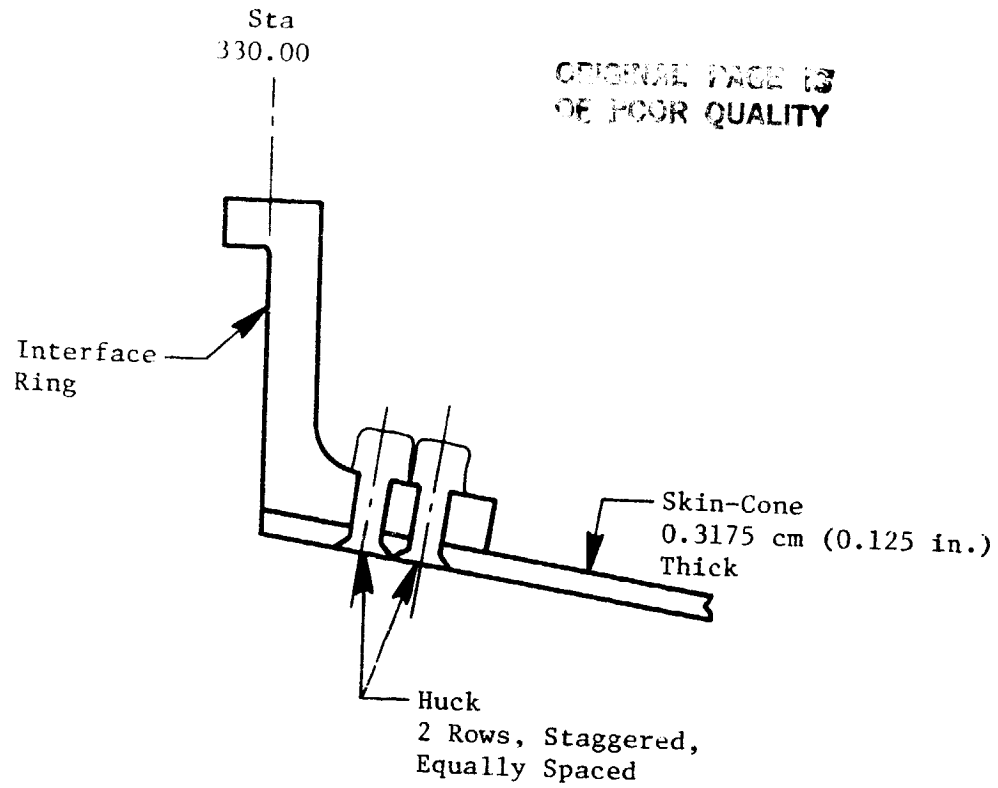


Figure 67. Interface Ring.

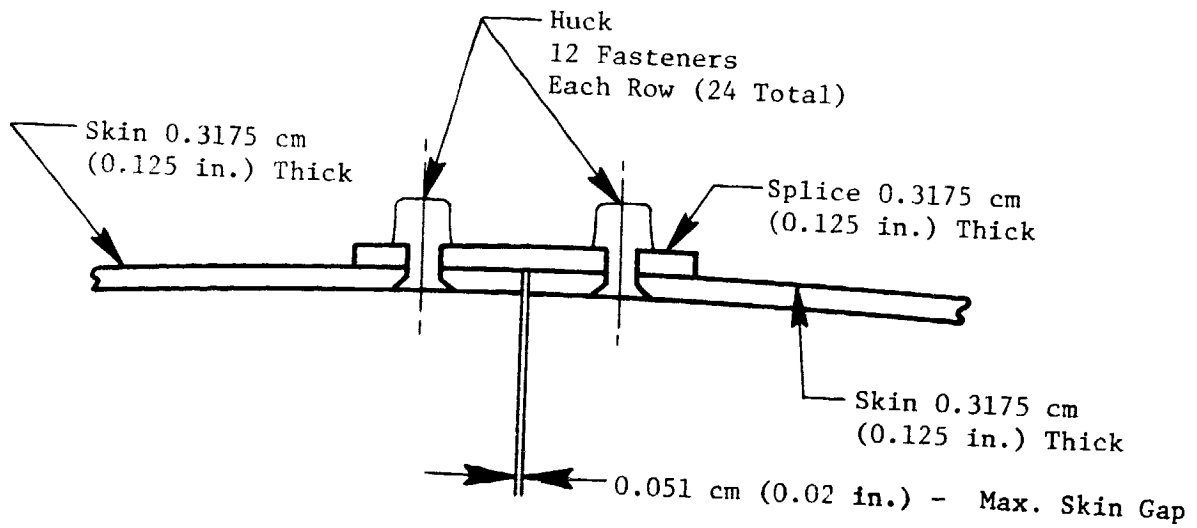


Figure 68. Typical Top and Bottom Vertical  
Centerline Splice.

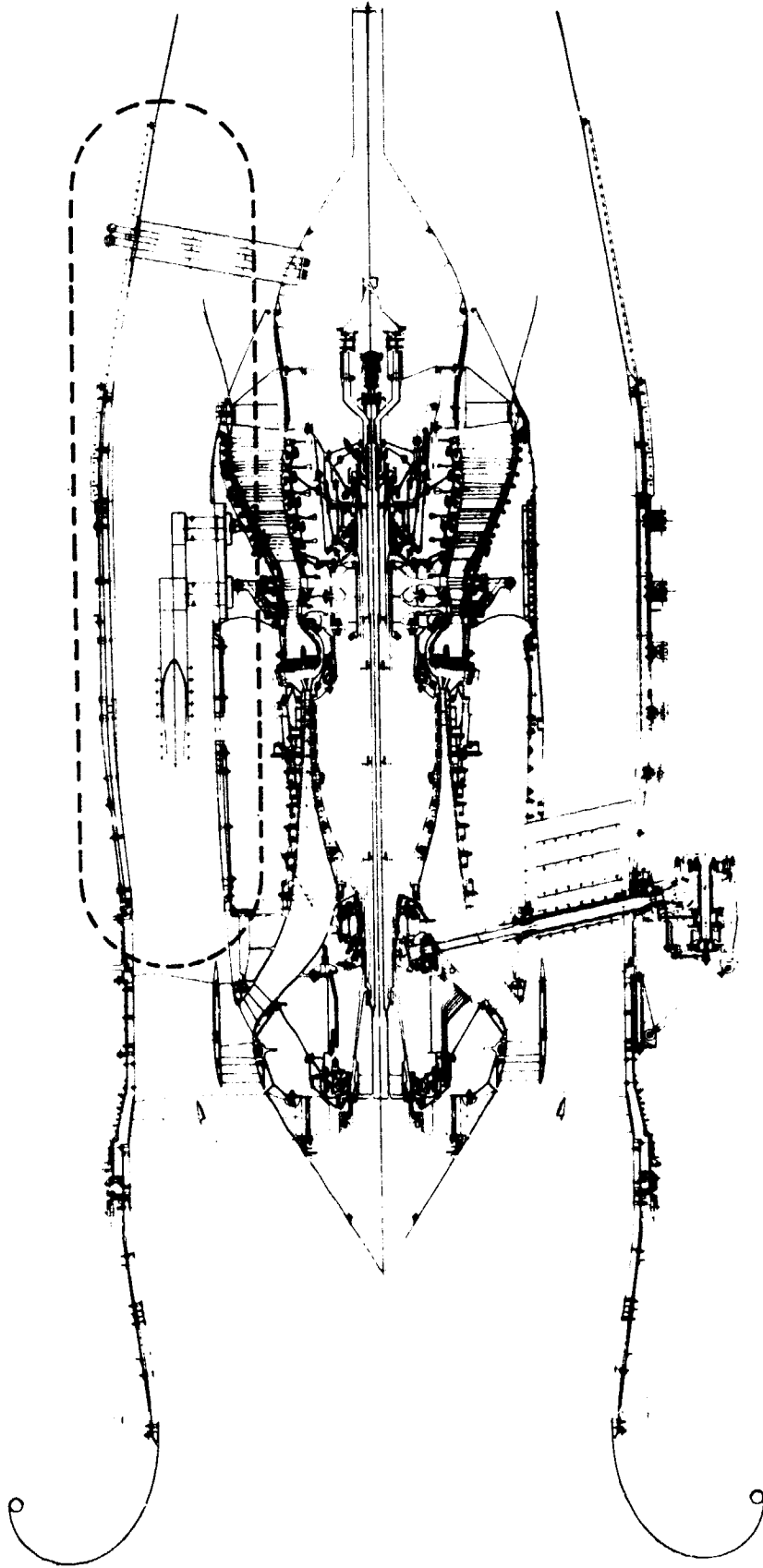


Figure 69. Pylon.

Table XXV. Pylon Loads.

- Max Temperature Environment
  - $T_{\max} = 360.6 \text{ K} (189.4^\circ \text{ F})$  in Boattail Region  
(SLS Hot Day T/O;  $M_0 = 0$ ;  $\Delta T = 35 \text{ K} (-63^\circ \text{ F})$ )
- Loading
  - Max Load Across Pylon Skins  
 $\Delta P_{\max} = 5.03 \text{ N/cm}^2 (7.3 \text{ psi})$
  - Max Stress in Typical Panel  
 $\sigma_{\max} = 9774.7 \text{ N/cm}^2 (14,177 \text{ psi}); MS = 0.98$  (For Al)  
 $= 5.3$  (For Steel)

Table XXVI. Pylon.

Basic Design Features

- Monocoque Type Structure
- Supported from Engine Mount Beam
- Separable 3 Piece Assembly
  - Leading Edge Noise Section
  - Forward Section
  - Aft Section
- Split Plenum Chamber Housed in Forward Section
- Airscoop Mounted on L.H. Forward Section
- No Acoustic Treatment

Materials

- Leading Edge Segments and Forward Section - 6061-T6 Al Alloy
- Aft Section AISI 321 Stainless Steel
- Fasteners
  - Permanent:
    - NAS Type Steel Huck Bolts
    - MS20427 Monel Rivets
    - MS20426 Al Alloy Rivets
  - Removable.
    - NAS1102E4 Screws With NAS21060C4 Nutplates
- Seals
  - Dacron Covered Silicone Rubber
  - Bulb Type With Silicone Sponge Core
- Air Scoop - F161 PrePreg Fiber Glass
- Plenum - 6061-T6 Al Alloy

ORIGINAL PAGE IS  
OF POOR QUALITY

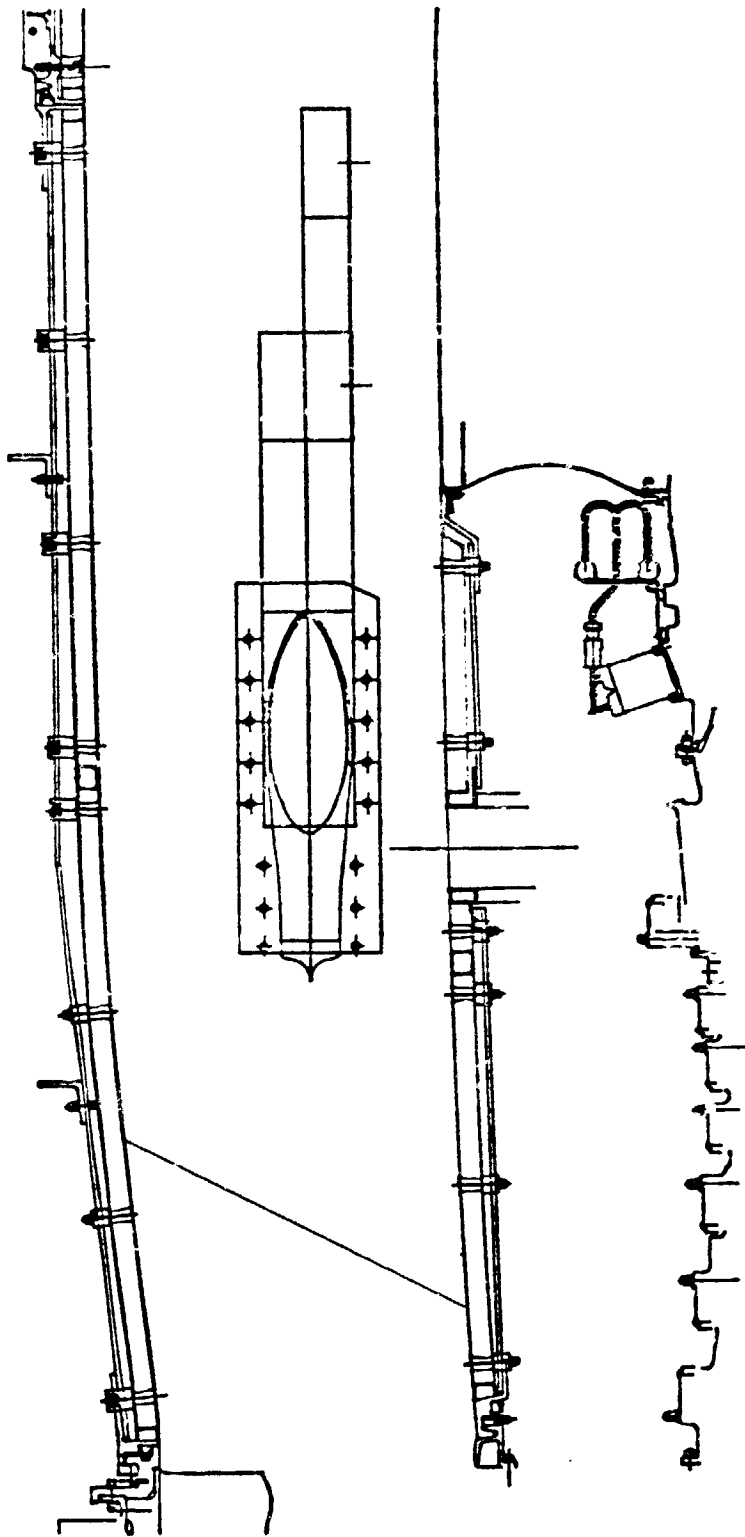


Figure 70. Scoop and Plenum.

ORIGINAL PAGE IS  
OF POOR QUALITY

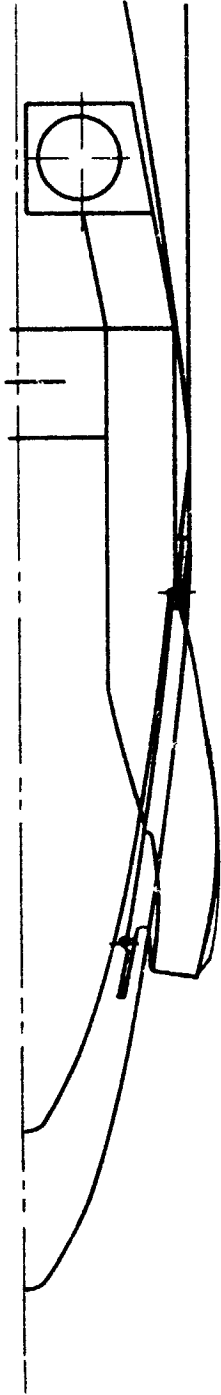


Figure 71. Scoop - Top View.



ORIGINAL PAGE IS  
OF POOR QUALITY

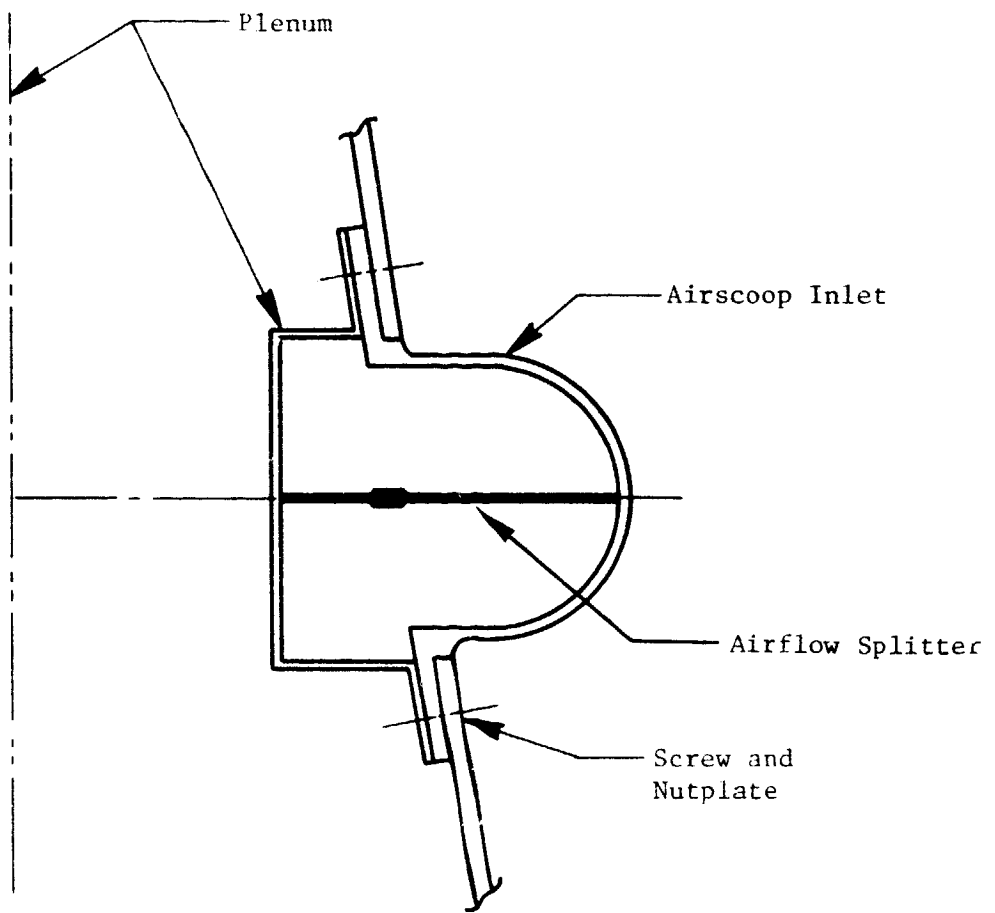


Figure 72. Pylon Plenum Chamber and Airscoop Inlet.

ORIGINAL PART IS  
OF POOR QUALITY

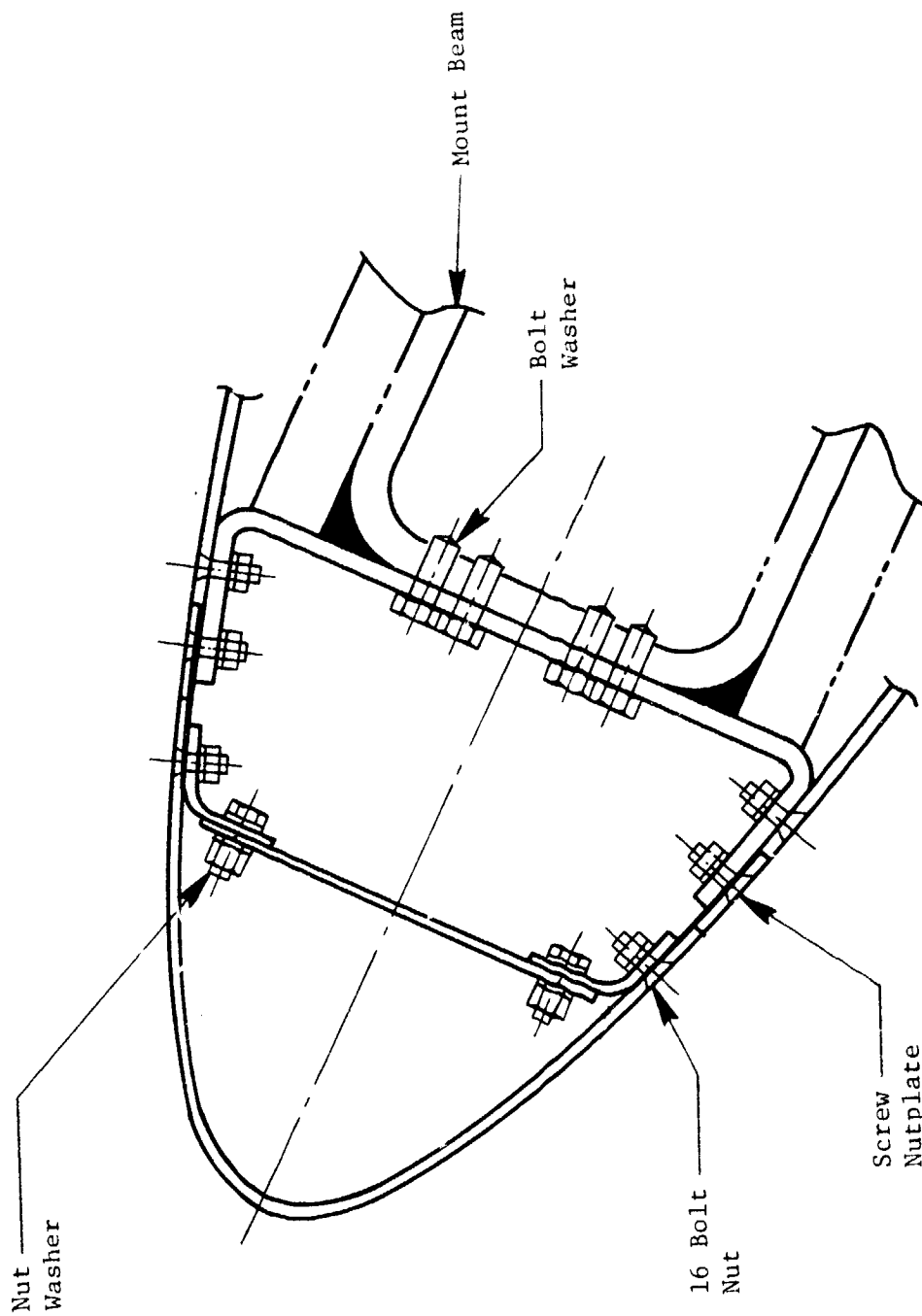


Figure 73. Pylon Leading Edge Section.

shown in Figure 74 with the removable panels utilizing the screw/nut plate arrangement. The pylon sidewalls are sealed against the core cowl apron as shown in Figure 75. The method of closing out the trailing edge of the pylon is depicted in Figure 76 and the attachment of the sidewalls to the mount beam is shown in Figure 77. The aft mount links penetrate the sidewalls and extend into the fan flow stream. The openings in the sidewall for these links are sealed as shown in Figure 78.

ORIGINAL PROJECT  
OF POOR QUALITY

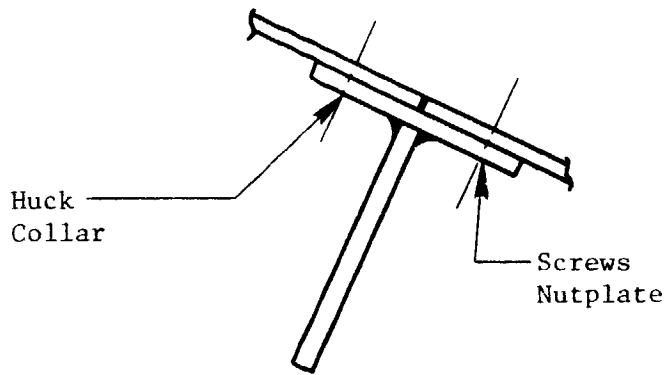


Figure 74. Sidewall Panels - Removable Section.

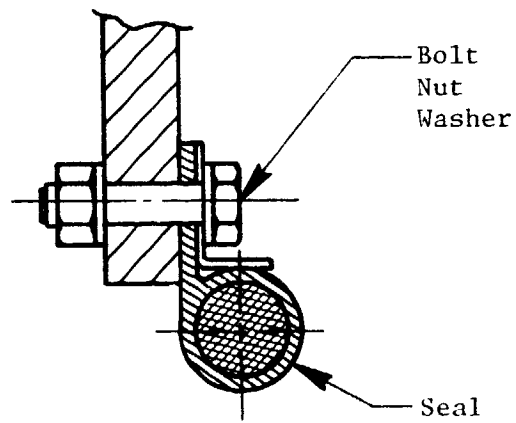


Figure 75. Pylon - Seal Cross Section.

ORIGINAL PAGE IS  
OF POOR QUALITY

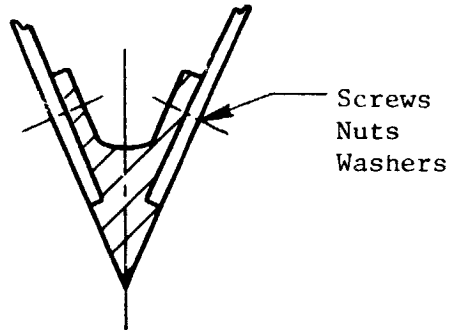


Figure 76. Pylon - Trailing  
Edge Section.

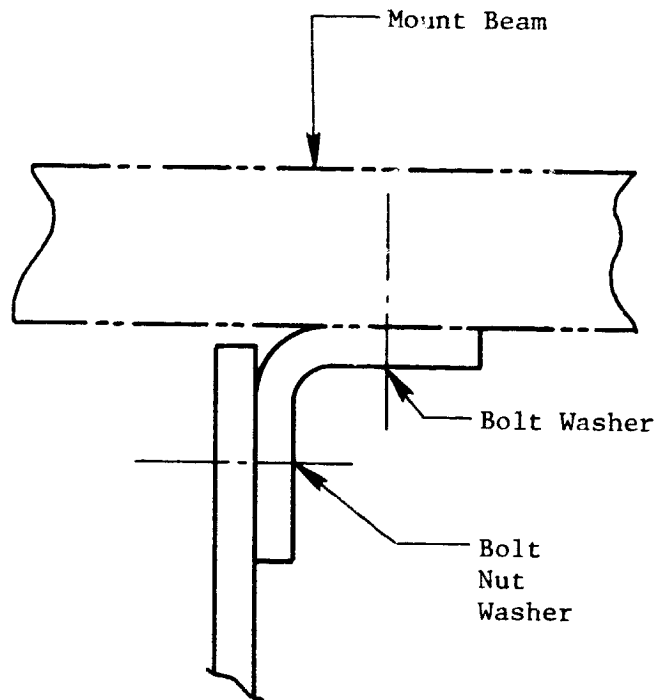


Figure 77. Pylon - Typical Pylon to Beam Support.

ORIGINAL PAGE IS  
OF POOR QUALITY

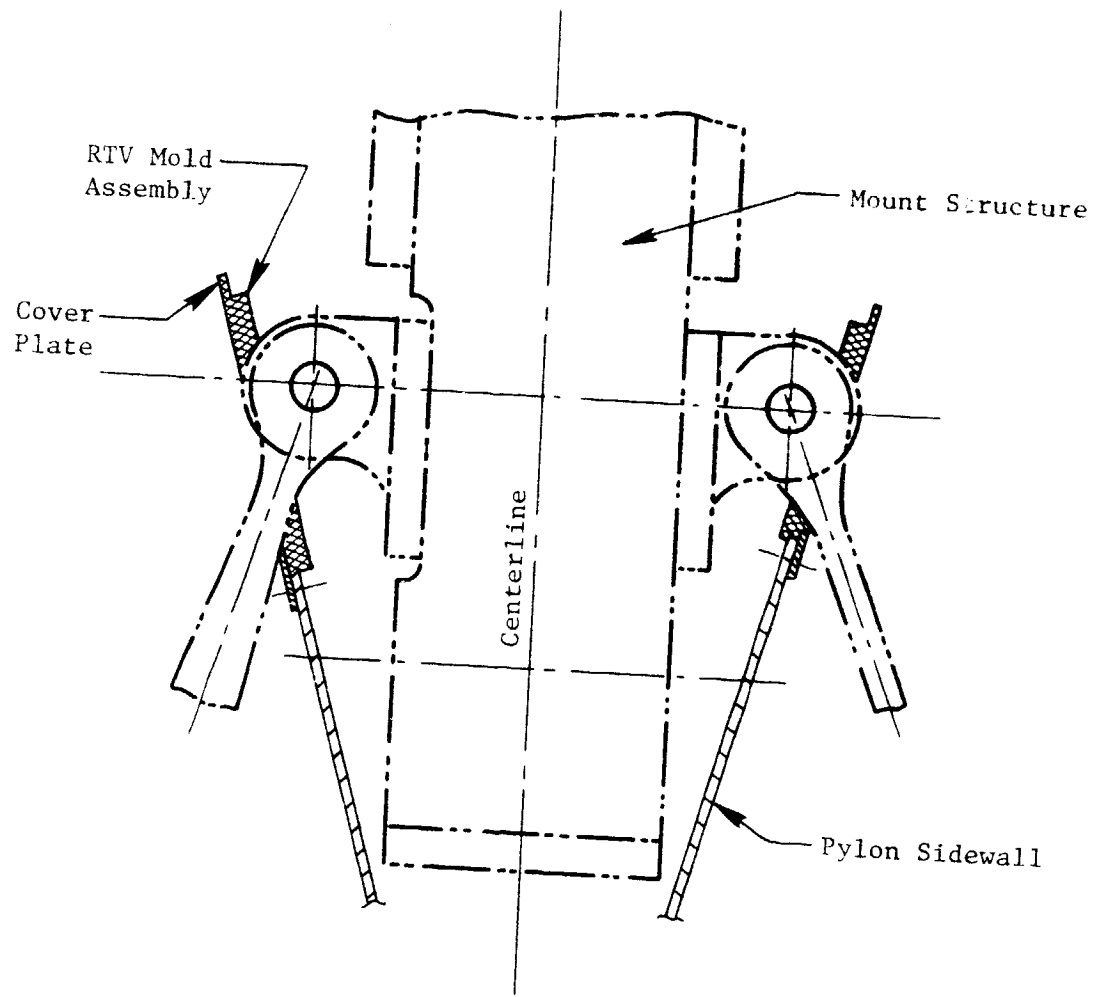


Figure 78. Aft Mount Link Penetration.

## V ASSEMBLY AND TRIAL FIT

To ease the problems of assembly at the test site, a trial fit of all the nacelle structure, excluding the inlet, to the mount beam and aft fan frame rings will be conducted at Mojave. The dummy engine and mount structure shown in Figure 79 will be shipped to Mojave and all the nacelle components will be assembled to this structure. Some of the interfacing hardware, such as hinges and attach angles will be line drilled at this time to assure proper positioning.

ORIGINAL PAGE IS  
OF POOR QUALITY

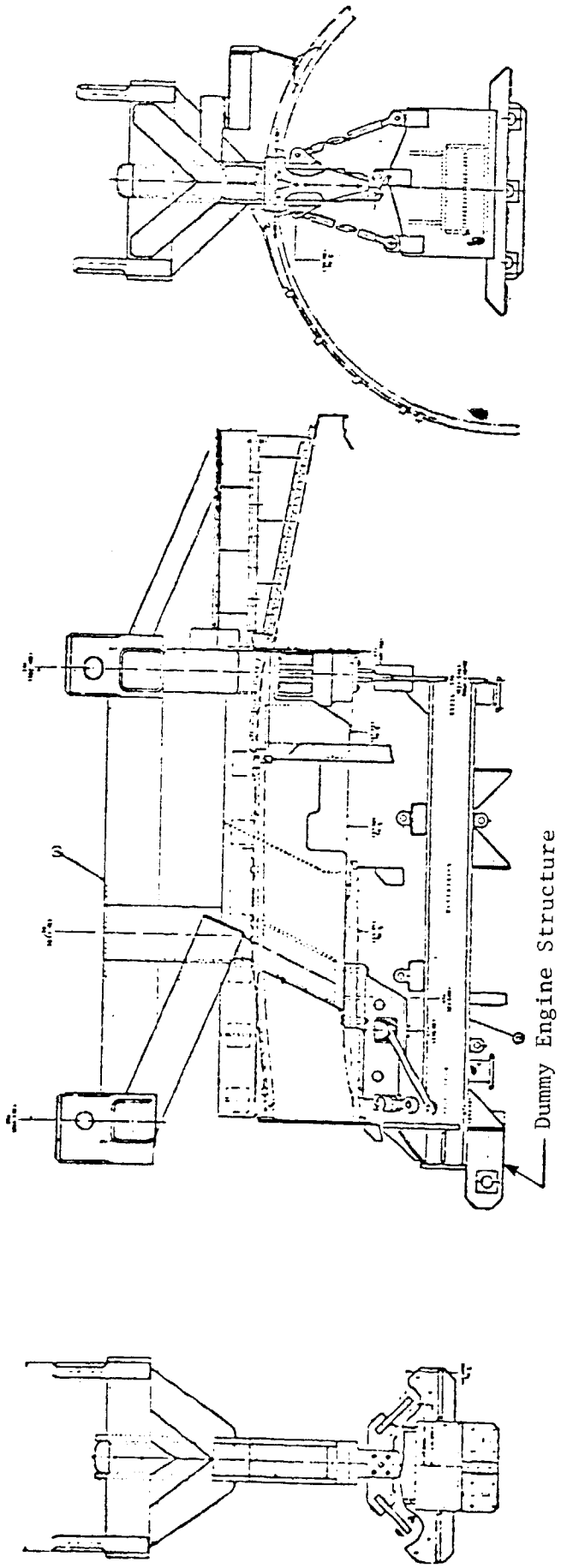


Figure 79. Mount Structure - Assembly and Trial Fit.



## VI INSTRUMENTATION

Since the ICLS vehicle is intended to investigate the performance of the E<sup>3</sup> engine, an extensive amount of instrumentation is required. The instrumentation that must be installed in the nacelle structure is listed for each component in Table XXVII. In addition to providing support for all of this instrumentation, blank-off pads must be provided for all instrumentation that penetrates the flowpath and is not installed for all tests.

Table XXVII. Instrumentation.

Inlet

- 46 Wall Static Pressure Taps
- 1 T2 Sensor
- 2 Acoustic Pressure Transducers  
(Additional Transducer Mounted in Fan Casing)
- 3 Linear Potentiometers  
(Mounted at Fan Casing Interface)

Core Cowl Doors

- 1 Radial Pt/Tt Rake
- 13 Wall Static Pressure Taps
- 12 Skin Thermocouples (Under Cowl)
- Aft Sump Pressurization Lead (at Idle)
- Instrumentation Bundle (Routed Through Cover  
Plates for 5th Stage and CDP Piping)
- Y Fitting For Shop Cooling Air/Argon for Fire Protection

Fan Cowl Doors

- 1 T25 Hydromechanical Sensor
- 7 Wall Static Pressure Taps
- 1 Acoustic Traverse Probe
- 7 Pt/Tt Arc/Radial Rakes

Aft Outer Exhaust Nozzle

- 6 Wall Static Pressure Taps
- 1 Acoustic Traverse Probe
- 10 Skin Thermocouples Secured on Surface
- Provisions for Supporting Instrumentation Strut

## VII SUMMARY

The design and fabrication of the ICLS nacelle structure is proceeding according to plan. The status of the program, as of the date of the nacelle DDR, is shown in Table XXVIII. The program is on schedule and is being conducted within the funding allocated to this effort. An ICLS Nacelle cross section is shown in Figure 80.

Table XXVIII. Summary.

Design - Complete  
Detail Drawing - 75 Drawings Issued - 97% Complete  
Tool Design - 100% Complete  
Tool Fabrication - 100% Complete  
Material - 100% Received  
Fabrication - 100% Complete  
Assembly - 95% Complete

Planned Delivery 6/1/82

ORIGINAL PAGE IS  
OF POOR QUALITY

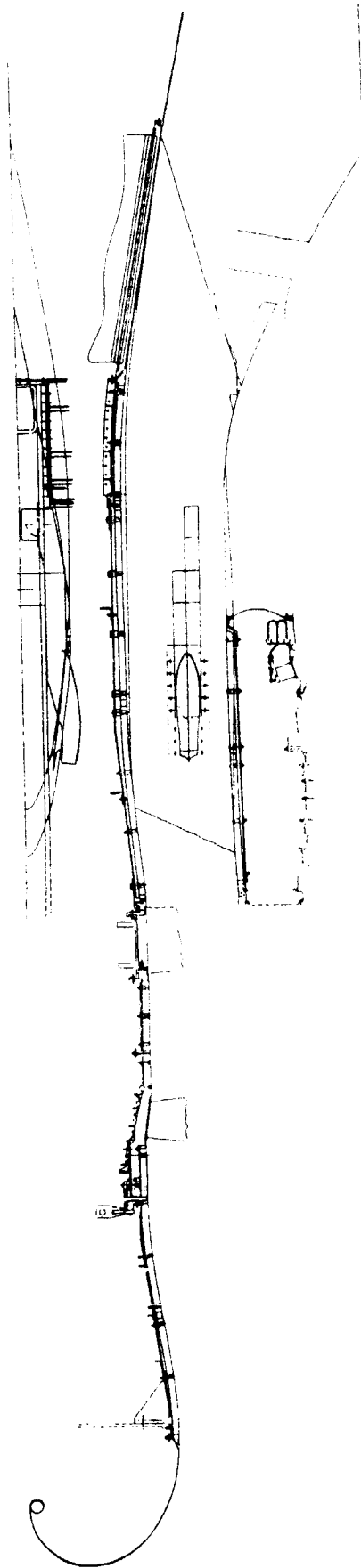


Figure 80. ICLS Nacelle Cross Section

VIII REFERENCES

1. Kuchar, A.P. and Stotler, C.L., "Energy Efficient Engine Nacelle Preliminary Analysis and Design Report," NAS3-20643, R80AEG474, August 1980.

**END**

**DATE**

**FILMED**

**JAN 8 1985**